6-1-1977

Mathematical Models of Little Creek Harbor and the Lynnhaven Bay System

Gaines C. Ho
Virginia Institute of Marine Science

Albert Y. Kuo
Virginia Institute of Marine Science

Bruce J. Neilson
Virginia Institute of Marine Science

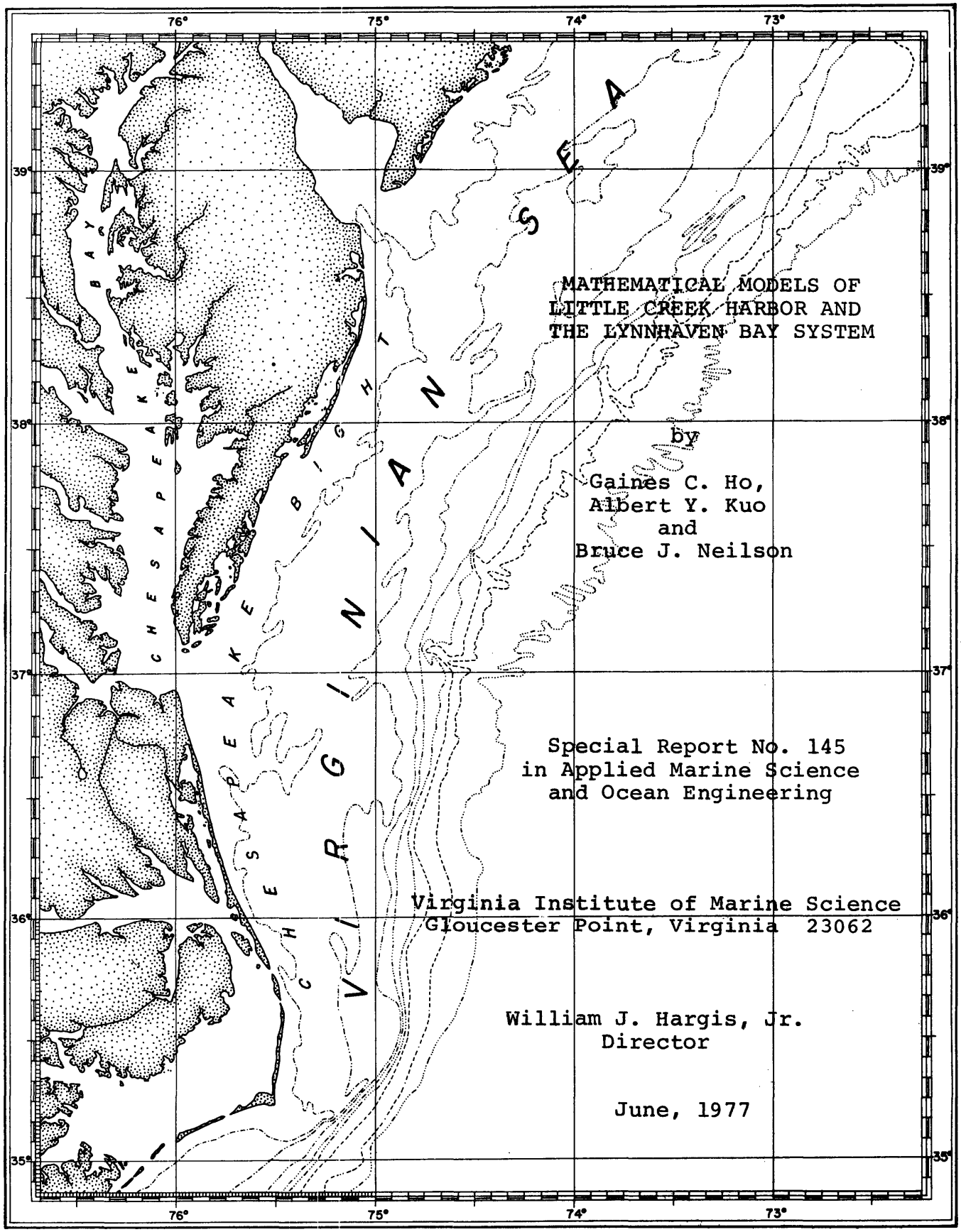

MATHEMATICAL MODELS OF LITTLE CREEK HARBOR AND THE LYNNHAVEN BAY SYSTEM

by

Gaines C. Ho,
Albert Y. Kuo
and
Bruce J. Neilson

Special Report No. 145
in Applied Marine Science
and Ocean Engineering

Virginia Institute of Marine Science
Gloucester Point, Virginia 23062

William J. Hargis, Jr.
Director

June, 1977

MATHEMATICAL MODELS OF LITTLE CREEK HARBOR AND THE LYNNHAVEN BAY SYSTEM

by

Gaines C. Ho,
Albert Y. Kuo
and
Bruce J. Neilson

A Report for the Hampton Roads Water Quality Agency

Special Report No. 145
in Applied Marine Science
and Ocean Engineering

The preparation of this report was financed through a grant from the U. S. Environmental Protection Agency under Section 208 of the Federal Water Pollution Control Act Amendments of 1972.

Virginia Institute of Marine Science
Gloucester Point, Virginia 23062

William J. Hargis, Jr.
Director

June, 1977

TABLE OF CONTENTS

LIST OF FIGURES

LIST OF TABLES

ACKNOWLEDGEMENTS

The work described in this report was financed through a grant from the U. S. Environmental Protection Agency under Section 208 of the Federal Water Pollution Control Act Amendments of 1972.

Numerous persons have assisted in the preparation and review of this report. In particular, the efforts of the following persons are hereby noted with appreciation:

Ms. Angela D'Amico for data analyses and reduction;

Ms. Susan Sturm for preparing the drawings;

Remote Sensing Section of VIMS for mapping; and

Ms. Cathy Garrett for her patient typing of this report.

I. INTRODUCTION

The Small Coastal Basins of the "Hampton Roads 208 Study Area" (shown in Figure 1) include the Back and Poquoson Rivers on the Virginia Peninsula and Little Creek Harbor and the Lynnhaven Bay System on the southern shore of Chesapeake Bay. This report deals with the water quality models which have been applied to Lynnhaven Bay and Little Creek.

The Lynnhaven Bay and Little Creek drainage basins lie within the Hampton Roads metropolitan area, but are somewhat removed from the urban centers. They are experiencing a rapid rate of development and some problems are encountered with this urbanization. In general, water quality problems for these two basins arise from non-point sources of pollution rather than point discharges of treated sewage. The major contribution of non-point source pollutants in the Lynnhaven Bay System appears to be from residential developments. A major non-point source of pollutants in Little Creek Harbor is the fleet of large navy vessels using the harbor.

When the 208 Study began, comprehensive and synoptic surveys of water quality in these two basins were not available. For this reason the Hampton Roads Water Quality Agency contracted the Virginia Institute of Marine Science to conduct a field sampling program which had two elements: intensive surveys and slack water surveys. Data from the intensive surveys were used to calibrate mathematical models of water quality in these estuaries. Slack survey data were used to verify these models. The field program and water quality conditions

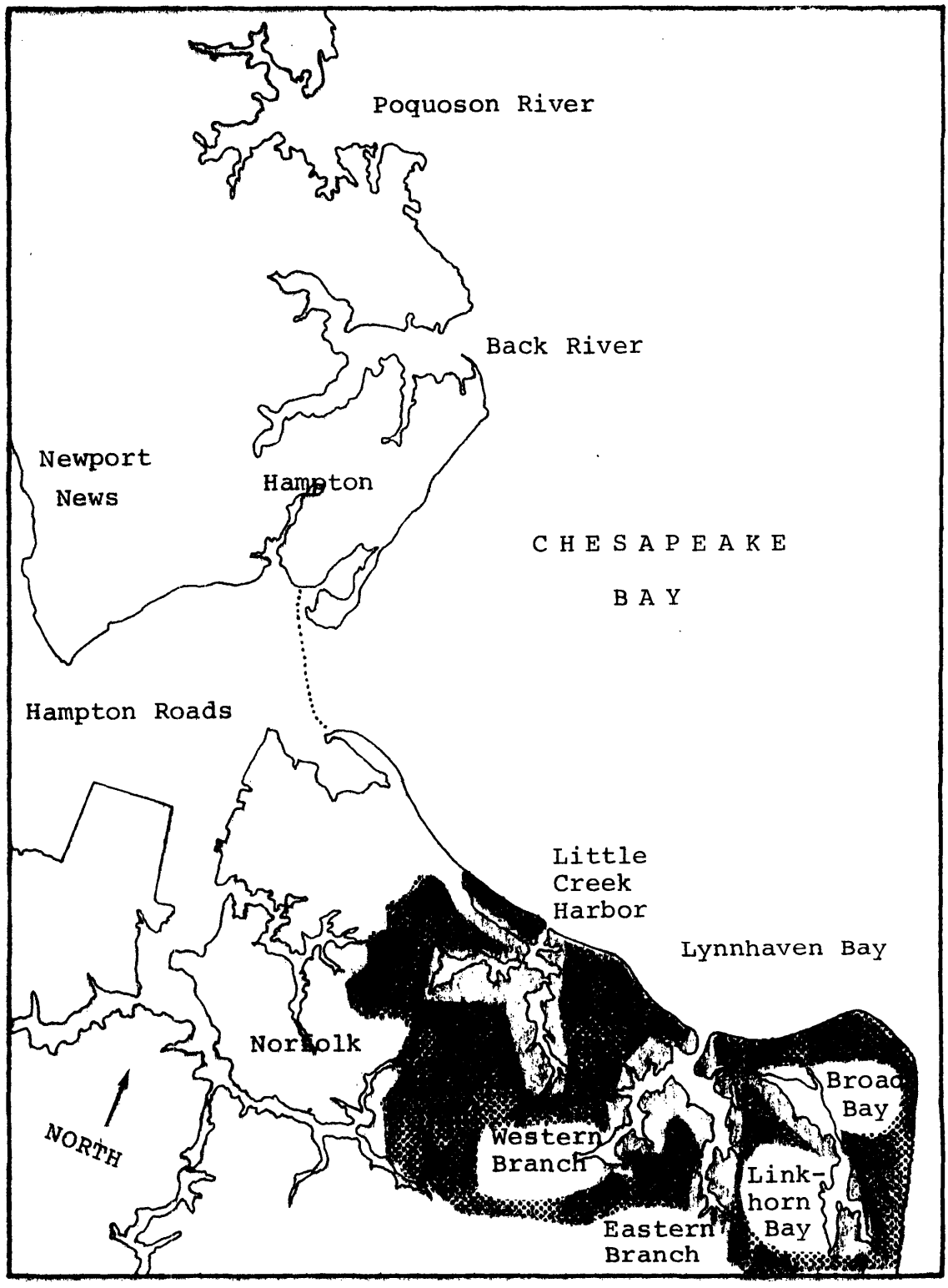

Figure 1. Small Coastal Basins.

have been presented in an earlier report (Neilson, 1976).

This report is devoted to a description of the water quality model, the procedures by which the model was calibrated to simulate the behavior of each estuary, and comparisons of field data and model predictions. The model used for this study, a tidal flushing model, is based on tidal prism theory. It is convenient to use since it requires a minimum amount of input data: the tidal range, freshwater flow, basin topography, add pollutant loads. The parameters modelled include salinity, dissolved oxygen, carbonaceous biochemical oxygen demand, ammonia nitrogen, nitrate- and nitrite-nitrogen, organic nitrogen, inorganic phosphorus, organic phosphorus, chlorophyll "a", and fecal coliforms.

II. DESCRIPTION OF THE STUDY AREA

The Lynnhaven Bay System, shown in Figure 2a, has several segments: the Eastern and the Western Branches of Lynnhaven Bay, Long Creek, Broad Bay, and Linkhorn Bay. The entire system is shallow with maximum depths of around 3 meters, except near the Inlet. The drainage area of this system is small, about 156 sq. km. (60 sq. miles). The whole basin lies entirely within the geological Coastal Plain Province, the lowlying area between the fall line and the Atlantic Ocean. Due to slight topographic relief and small drainage area, this basin does not contain any large free flowing tributaries.

Little Creek Harbor is a small coastal basin to the west of Lynnhaven Bay on the southern shore of the Chesapeake Bay (see Figure 1). The naval base at Little Creek is a major training facility for the U. S. Navy amphibious assault forces. Little Creek Reservoir, Lake Whitehurst, Lake Lawson and Lake Smith, former tributaries in the Little Creek Basin, have been dammed for water supply by the City of Norfolk (see Figure 2b). Only during times of heavy rainfall will there be any flow over the spillways into Little Creek Harbor. The basin has a very small drainage area, 63 sq. km. (24 sq. miles). Only slight longitudinal salinity variations have been observed, although saltier sea water is able to enter the harbor because of its greater depth (40-45 feet).

The forcing function for the tides within both systems is the tide range in the Chesapeake Bay. Tidal flushing

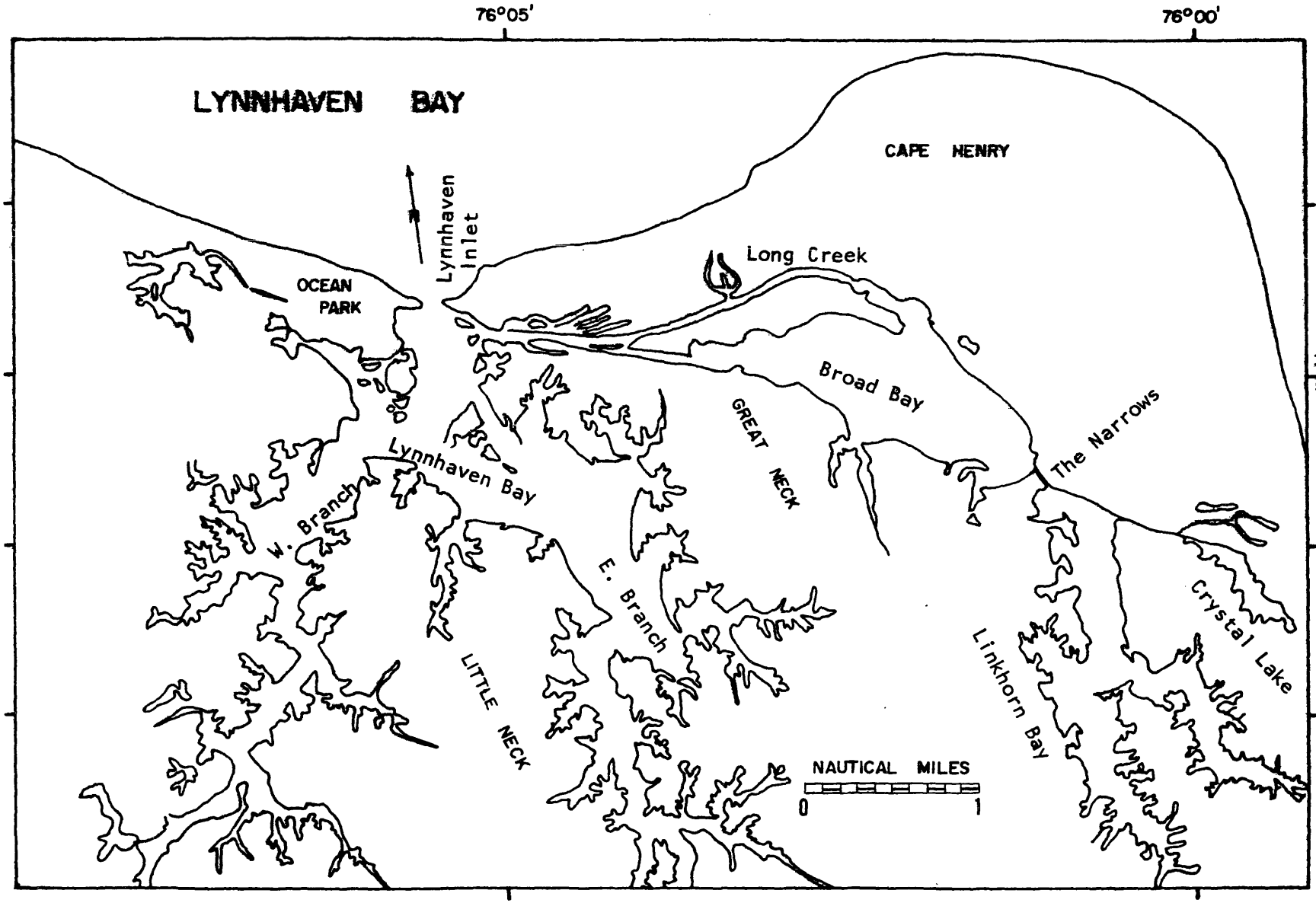

Figure 2a. The Lynnhaven Bay System.

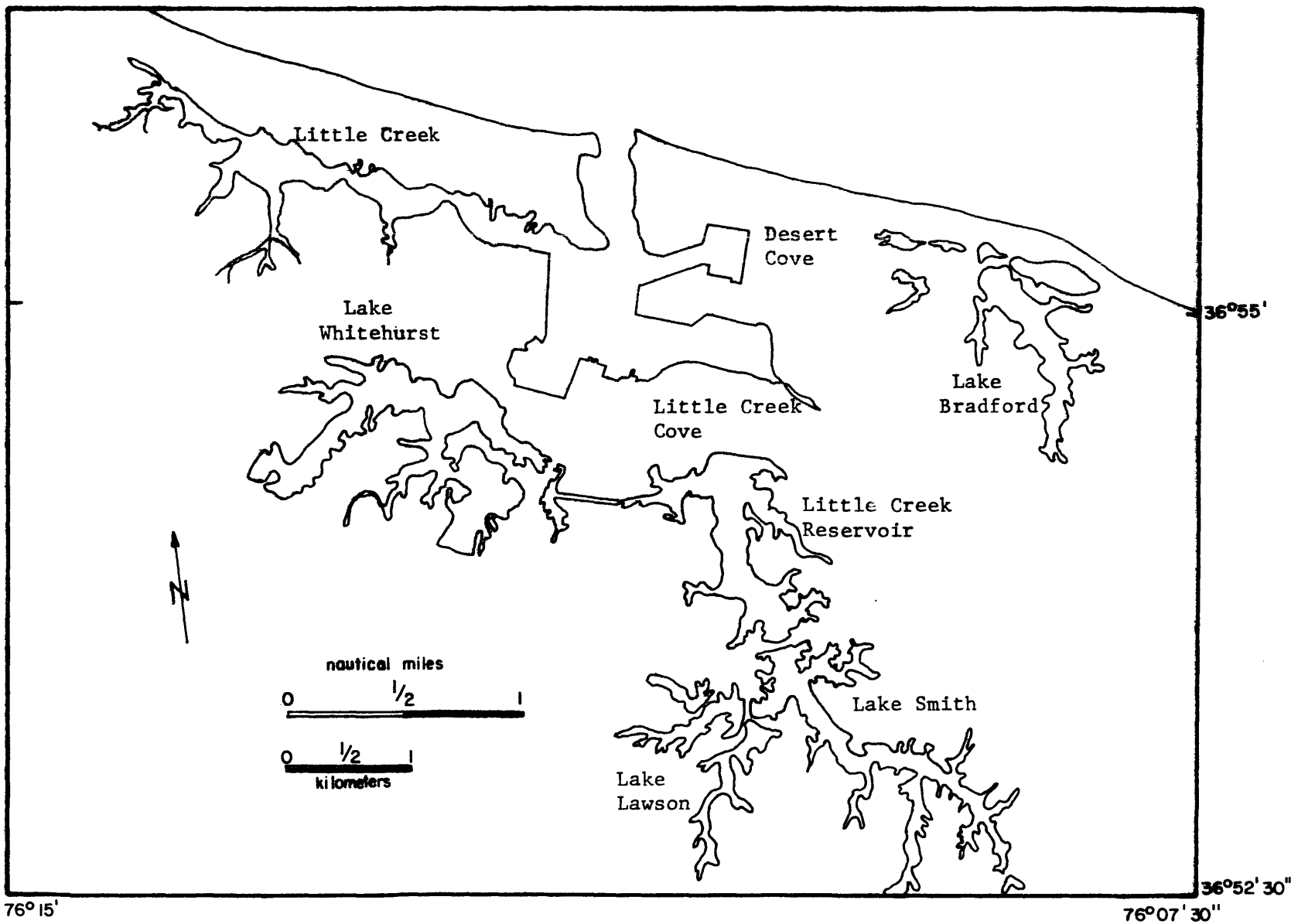

Figure 2b. The Little Creek.

predominates since the freshwater flows are small. The Eastern and Western Branches of the Lynnhaven Bay show mild, longitudinal salinity gradients. Board Bay has a more pronounced longitudinal salinity gradient since the north-western portion is influenced by the comparatively salty water flowing through Long Creek. The tide range in Linkhorn Bay is about one half that which occurs in Lynnhaven Inlet. This implies that the exchange of waters between Linkhorn Bay and Chesapeake Bay is not great. The longitudinal salinity gradient in Little Creek is mild due to tidal mixing and the short length of the basin.

III. WATER QUALITY SURVEY AND HYDROGRAPHIC STUDY

In September, 1975, the Virginia Institute of Marine Science conducted intensive surveys of water quality in Lynnhaven Bay and Little Creek. The data from these surveys have been used to calibrate the mathematical models.

Other necessary inputs to the models are low tide and high tide water volumes and the local intertidal volume (the fraction of the total tidal prism in each part of the estuary). In order to characterize basin geometry, 40 and 23 bathymetric profiles were made in the Lynnhaven Bay and Little Creek respectively. These were used to obtain average depths at low water. The locations of these transects and profiles are on file at VIMS.

The VIMS Remote Sensing Section also conducted a survey to map the surface area of these estuaries as a function of tidal phase. Areas were calculated from black and white infrared film which can be used with conventional mapping equipment to make water surface maps at various tidal stages. Lynnhaven Bay and Little Creek were overflown five times on October 5, 1975. Then a map of each estuary was constructed as a basis for calculating the water area at high tide. The estuaries were divided into segments of relatively uniform topography. Within each estuary, the segments were further subdivided whenever necessary to increase mapping accuracy. Enlarged base maps of the segments were obtained from the imagery as a function of tidal phase, and then planimetered using an electronic coordinate digitizer at

NASA Langley Research Center. Numerical integration was performed by computer to calculate the area of each segment. The area of marsh islands within each segment wes measured and subtracted from the segment area to arrive at the high tide water area. The low tide area was then calculated by drawing in the exposed mud flats, shoals, and beaches on the base maps and subtracting these from the high tide area. The methods, the locations of the segments, and the results including surface area measurements have been published (Munday, et al., 1976), and are on file at VIMS.

Tide gages were installed at five and three stations in the Lynnhaven Bay and the Little Creek respectively. Tidal height at the Lynnhaven Bay stations was measured from September 12 through September 18, 1975, but that of the Little Creek was measured from September 19 through September 26, 1975. The location of tide gages and tidal measurements for these two estuaries also are on file at VIMS.

IV. MATHEMATICAL MODEL

The waste assimilation capacity of an estuary results from the interaction of complex chemical, biological and hydrodynamic factors. The best way to determine the maximum allowable amounts of pollutants from varying sources is the formulation and application of a mathematical model of water quality in the estuarine system. The existence of such a model enables the planner to assess the impact of waste discharges and non-point source pollution and to compare alternative management policies.

1. Model Development

For this study a tidal flushing model based on tidal prism theory was used. The tidal prism is defined as the intertidal volume, or the difference between the volumes of water in an estuary at high and low tides. The rise and fall of the tide at the mouth of an estuary or coastal creek causes an exchange of water masses through the entrance. This results in a temporary storage of large amounts of sea water in the estuary during flood tide and the drainage of this water during ebb tide. Since the water brought into the estuary on flood tide mixes with 'polluted' estuarine water, a portion of the pollutant mass in the estuary will be flushed out of the estuary on ebb tide. This kind of flushing mechanism due to the rise and fall of the tide is called tidal flushing.

The classical tidal prism theory was an early attempt to describe transport processes in an estuary. The theory

assumes that mixing is complete throughout the entire estuary at high tide. Ketchum (1951) modified this tidal prism theory by dividing the estuary into segments, in each of which complete mixing is assumed at high tide. The length of each segment is defined by the tidal excursion, or the average distance travelled by a water particle on the flood tide, since this is the maximum length over which complete mixing can be assumed.

Some of the assumptions used by Ketchum are retained in this model. It is assumed that the estuary or coastal creek is in hydrodynamic equilibrium. That is, the freshwater inflow is constant and the net seaward transport of freshwater over a tidal cycle equals the volume of freshwater introduced by surface runoff during the same period. There is no net exchange of salt over a tidal cycle. This implies a balance between the inflow and outflow of sea water. The assumption that complete mixing is achieved within each segment having a length equal to or less than a tidal excursion also is retained.

(a) Segmentation of Water Bodies

In the original (Ketchum's) approach, the segmentation of the estuary is started at the head of the estuary by defining the first segment as the one above which the tidal prism equals the river flow over a tidal cycle. This approach fails in the singular case of no freshwater inflow. A new approach which accomodates this singular case by starting the segmentation from the mouth of the estuary was developed under the Cooperative State Agencies Program (Kuo, 1976).

The water body outside of the mouth is assumed to be the first segment (figure 3). The first segment within the estuary is indexed as the segment number two, bounded by transects one and two. The first transect is across the mouth, the second transect is chosen such that a water particle will move from the first to the second transect over flood tide. Therefore, the tidal prism, or intertidal volume, upstream of the second transect must be big enough to accommodate the volume of water in segment two at low tide plus the total volume of freshwater inflow over flood tide, i.e.

$$P_2 = V_2 + R_2,$$

or

$$V_2 = P_2 - R_2$$

where V_2 is the low tide volume of the second segment, P_2 is the tidal prism upstream of the second transect and R_2 is the volume of river water entering the estuary upstream of the second transect during half a tidal cycle. In general, a water particle at the (n-1)th transect at the beginning of flood tide should move to the nth transect at the end of flood tide. Thus,

$$P_n = V_n + R_n \tag{1}$$

or

$$\begin{aligned} V_n &= P_n - R_n \\ &= P_{n+1} + \rho_{n+1} - (R_{n+1} + r_{n+1}) \end{aligned} \tag{2}$$

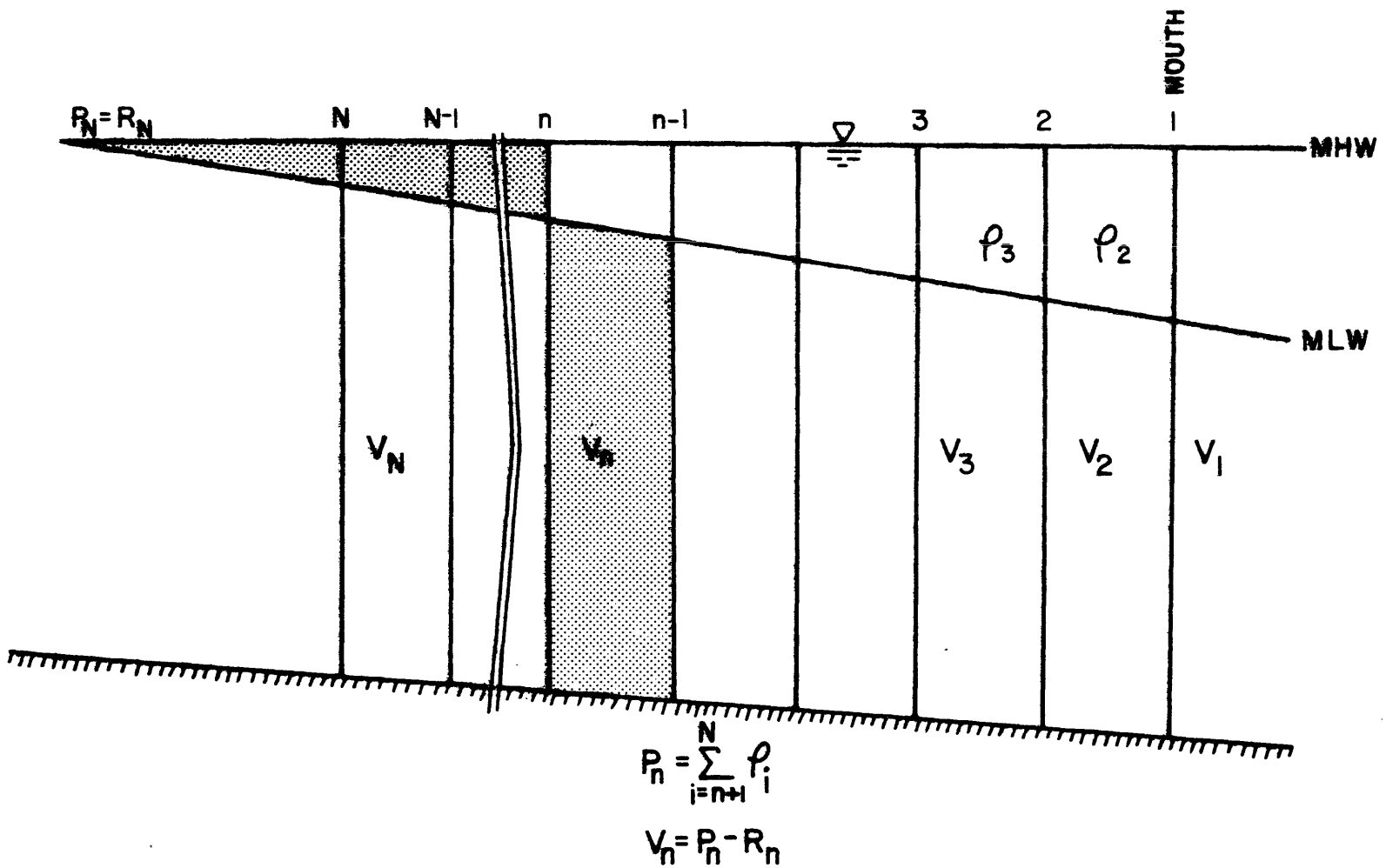

Figure 3. Segmentation of an estuary.

or

$$V_n = V_{n+1} + \rho_{n+1} - r_{n+1} \qquad (3)$$

where

V_n = low tide volume of the nth segment

P_n = tidal prism upstream of the nth transect

R_n = total freshwater discharge above the nth transect over half a tidal cycle

ρ_n = local tidal prism of the nth segment

r_n = lateral freshwater input into the nth segment over half a tidal cycle

Equation (3) states that the low tide volume of a segment equals to the high tide volume of its immediate landward segment minus the lateral freshwater input into that segment. In the special case of no lateral freshwater input, this is the same criterion Ketchum (1951) used for segmenting the estuary. It is seen from equation (2) that V_n tends to zero as P_n decreases toward the head of the estuary. Therefore, there is an infinite number of segments. This is in agreement with the fact that the tidal excursion tends toward zero at the head of the estuary. Mixing is never completed over any finite segment at this landward end since the tidal excursion is greatly reduced.

Segmentation is continued until $P_{n+1} < 3R_{n+1}$. This condition is described in section C of this chapter (see equation 5). Therefore, for all segments, $P_{n+1} \geq 3R_{n+1}$. Once this constraint does not hold, the remainder of the estuary is combined into one single segment, the Nth segment,

as shown in figure 1. The prism upstream of the Nth transect equals the upstream freshwater discharge, that is $P_n = R_n$. If there is no river flow, this method of segmentation is still valid. In this case, segmentation can be continued as long as one wishes. The last one includes the remainder of the tidal creek or estuary.

The length of the Nth segment so determined is larger than the local tidal excursion and complete mixing cannot be achieved within this segment. However, the concentration predicted by the model for this segment still represents the average value for the segment.

(b) Determination of Segment Lengths

Figure 4 shows for a hypothetical estuary the accumulated low tide volume, V(x), and the difference between the tidal prism and the river flow upstream of a point, $(P(x) - R(x))$, plotted as a function of x, the distance from the mouth. V(x) is defined as the accumulated low tide volume from the mouth to some transect located at a distance x from the mouth. P(x) is defined as the inter-tidal volume upstream of a transect located at x. R(x) is defined as the freshwater input during a half tidal cycle, also upstream of a transect located at x. The values for V(x) and $(P(x) - R(x))$ can be tabulated and graphed as shown in figure 4.

Since the segment length equals the tidal excursion, the low tide volume of the first segment within the estuary should equal the inter-tidal volume minus the river flow over a half tidal cycle upstream of the segment's landward boundary.

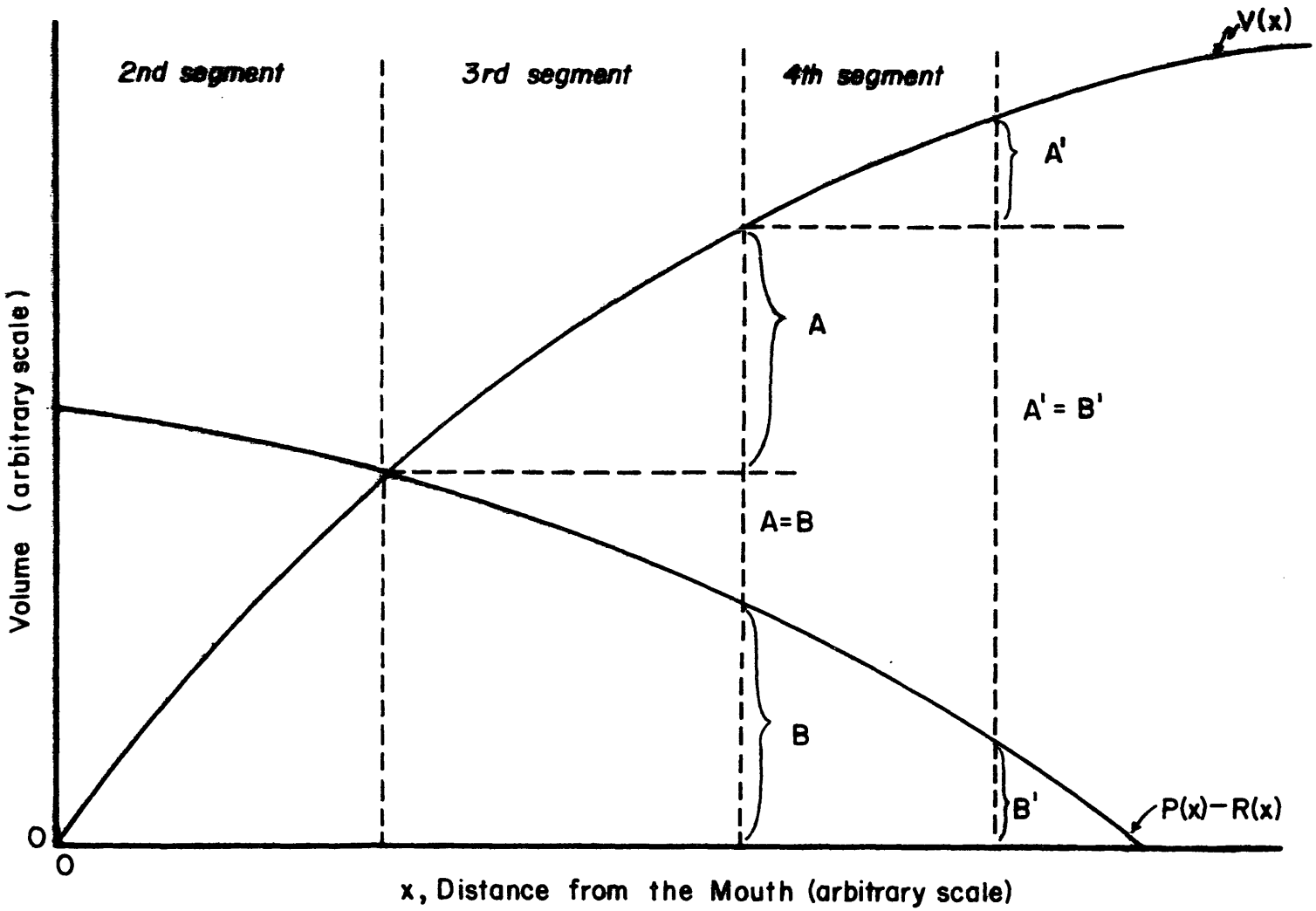

Figure 4. Graphical method of segmentation of an estuary.

This point, where $V(2) = (P(2) - R(2))$ can be determined graphically. The volume P_1 represents the entire intertidal volume of the estuary. Similarly, the volume R_1 represents the entire freshwater input into the estuary, including lateral inflow. These values are not used directly in the calculation, since the first low tide volume considered is V_2. V_1 is meaningless, as it is located outside the mouth. The initial segment, therefore, is indexed as segment two. Once the initial segment is determined, successive segments are determined graphically, as shown in figure 4. Segmentation continues until the boundary constraint previously mentioned is violated.

For an estuary with tributaries, P(x) is similarly defined, only now it includes the intertidal volume of the tributaries. R(x) is defined such that the freshwater input from the tributaries is included. The value V(x) remains as the low tide volume along the main stem. These volumes are shown graphically in figure 5. Once again, the initial segment is determined such that the low tide volume V_2 equals the intertidal volume minus the river flow upstream of that point. In a segment where a tributary comes in, the local low tide volume equals the tidal prism landward of it plus the prism minus the river flow of the branch. Each of the tributaries may be segmented in the same way as that of the main stem.

(c) Calculation of the Concentrations of Conservative Substances

As the tide propagates upstream from the mouth, the

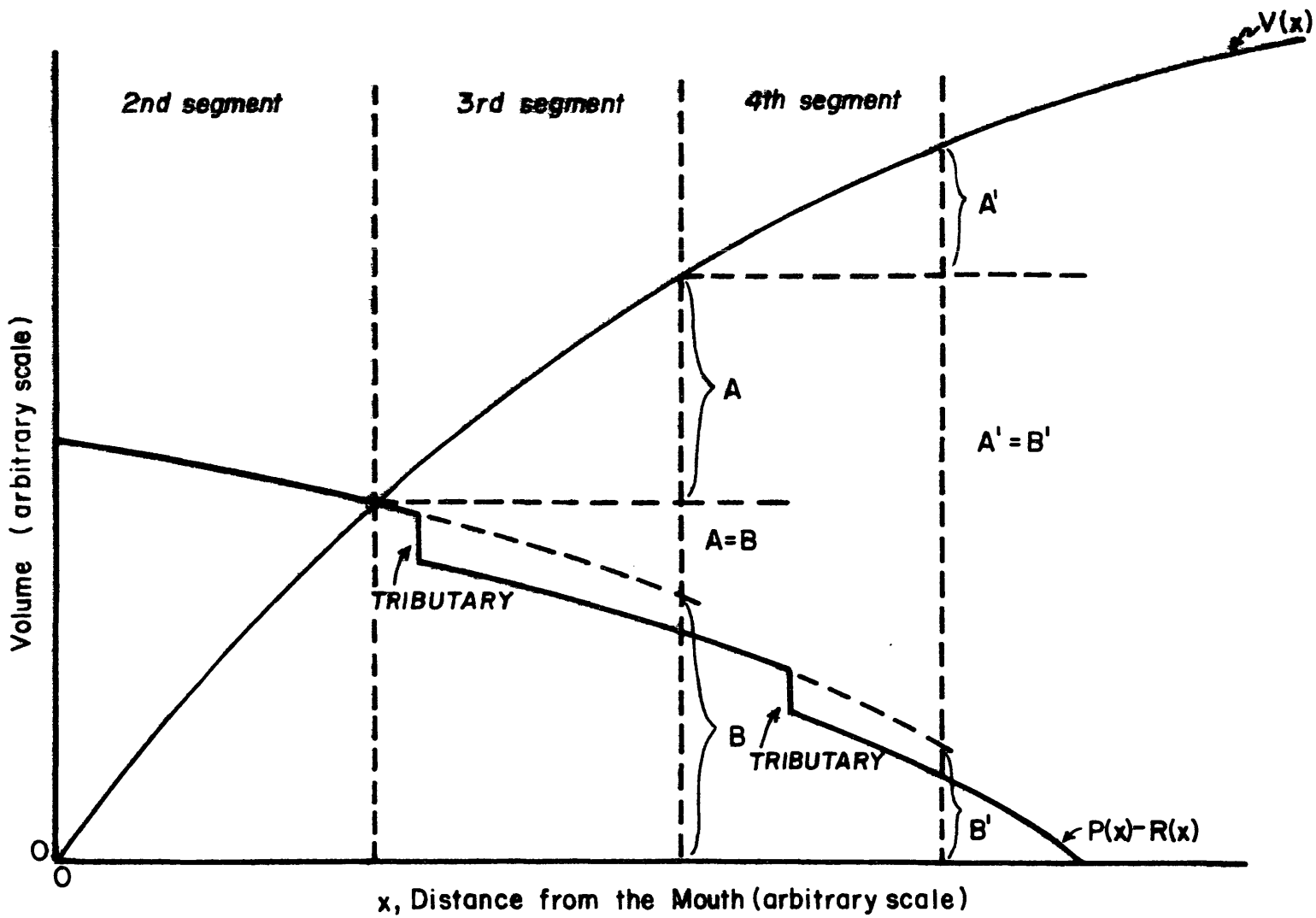

Figure 5. Graphical method of segmentation of a tributary.

volume of water ($P_{n-1} - R_{n-1}$) moves upstream across the (n-1)th transect and mixes with the water V_n present in the nth segment at low tide. Of this mixed water, the portion ($P_n - R_n$) moves upstream across the nth transect and is mixed with V_{n+1} and so forth. At the ebbing tide, the volume of water ($P_n + R_n$) moves downstream across the nth transect, pushing a volume ($P_{n-1} + R_{n-1}$) across the (n-1)th transect, and so forth, thus completing tidal flushing.

The flow across the transects bounding the nth segment is shown in the following sketch.

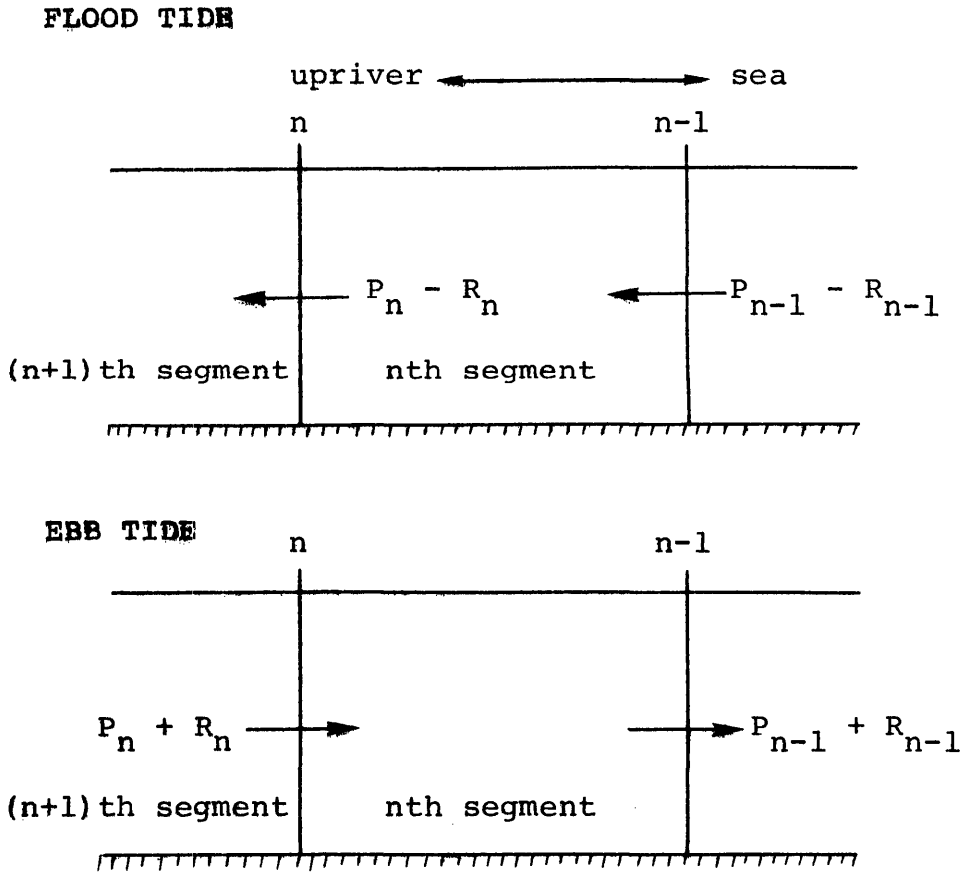

The flow across the transects bounding the nth segment.

At ebb tide, the water volume moving across the nth transect, $(P_n + R_n)$, may be separated into two parts, except for the last transect of the estuary. The first part is the water in the (n+1)th segment at high tide. This is

$$V_{n+1} + \rho_{n+1} = P_{n+1} - R_{n+1} + \rho_{n+1}$$

$$= P_n - R_{n+1}$$

This volume has concentration Cl_{n+1} where Cl_{n+1} is the high tide concentration in the (n+1)th segment at the beginning of tidal cycle. The remainder of the water can be represented as

$$(P_n + R_n) - (V_{n+1} + \rho_{n+1})$$

$$= P_n + R_n - (P_n - R_{n+1})$$

$$= R_n + R_{n+1}$$

This volume, $R_n + R_{n+1}$, has the concentration Cl_{n+2} if

$$R_n + R_{n+1} < V_{n+2} + \rho_{n+2}$$

$$= P_{n+2} - R_{n+2} + \rho_{n+2} \qquad (4)$$

$$= P_{n+1} - R_{n+2}$$

or $$P_{n+1} > R_n + R_{n+1} + R_{n+2}$$

or approximately

$$P_{n+1} \geq 3R_{n+1} \qquad (5)$$

The segmentation should be stopped before the inequality is violated. If violated, the volume of water $R_n + R_{n+1}$ will have a concentration that depends on Cl_{n+3} as well as Cl_{n+2}. The mass transport into and out of the nth segment during ebb tide may now be expressed as

$$\text{mass in} = ETP_n = \text{Ebb Tide Transport into the nth Segment}$$

$$= (P_n - R_{n+1})\ Cl_{n+1} + (R_n + R_{n+1})\ Cl_{n+2} \qquad (6)$$

$$\text{mass out} = ETP_{n-1} = \text{Ebb Tide Transport out of the nth Segment}$$

$$= (P_{n-1} - R_n)\ Cl_n + (R_{n-1} + R_n)\ Cl_{n+1} \qquad (7)$$

The last, Nth segment has a volume larger than that set by the criteria of segmentation. Therefore, the volume of water moving through the Nth segment must be considered separately. The volume moving into the Nth segment equals $2R_N$ or the river flow over a tidal cycle. This volume has concentration Cl_{N+1}. The volume leaving the segment equals $P_{N-1} + R_{N-1}$ which would have concentration Cl_N. The mass transport into and out of the Nth segment during ebb tide may be expressed as

$$\text{mass in} = ETP_N = \text{Ebb Tide Transport into the Nth Segment}$$

$$= 2R_N\ Cl_{N+1} \qquad (8)$$

$$\text{mass out} = ETP_{N-1} = \text{Ebb Tide Transport out of the Nth Segment}$$

$$= (P_{N-1} + R_{N-1})\ Cl_N \tag{9}$$

These values are calculated separately in the computer program.

Some of the water that leaves a segment during ebb tide might return during the following flood tide. Ketchum did not account for this fact in the original model. A returning ratio, α_n, is defined such that $100\alpha_n$ is the percentage of old water reentering through the nth transect at flood tide. The fraction of new water entering through the nth transect at flood tide may be expressed as $(1-\alpha_n)$.

At flood tide, the volume $(P_n - R_n)$ flowing through the nth transect has the concentration

$$\alpha_n\ Cl_{n+1} + (1 - \alpha_n)\ C2_n$$

where $C2_n$ equals the high tide concentration at the end of tidal cycle. The mass transport into and out of the nth segment during flood tide may be expressed as

$$\text{mass in} = FTP_{n-1} = \text{Flood Tide Transport into the nth Segment}$$

$$\{\alpha_{n-1}\ Cl_n + (1 - \alpha_{n-1})\ C2_{n-1}\}\ (P_{n-1} - R_{n-1}) \tag{10}$$

$$\text{mass out} = FTP_n = \text{Flood Tide Transport out of the nth Segment}$$

$$\{\alpha_n\ Cl_{n+1} + (1 - \alpha_n)\ C2_n\}\ (P_n - R_n) \tag{11}$$

The change of mass, Δm, with respect to time is

$$\Delta m/\Delta t = \text{sources} + (\text{mass in}) - (\text{mass out}) \tag{12}$$

In the present development, the change of mass in the nth segment over the entire tidal cycle can be represented as

$$(C2_n - C1_n)\ (V_n + \rho_n) = \text{sources} + ETP_n - ETP_{n-1} + FTP_{n-1} - FTP_n \tag{13}$$

or

$$(C2_n - C1_n)\ (V_n + \rho_n) = \text{sources} + ETP_n - ETP_{n-1} + \{\alpha_{n-1}\ C1_n + (1 - \alpha_{n-1})\ C2_{n-1}\}\ (P_{n-1} - R_{n-1}) - \{\alpha_n\ C1_{n+1} + (1 - \alpha_n)\ C2_n\}\ (P_n - R_n) \tag{14}$$

Letting $VH_n = V_n + \rho_n$, $PRF_n = P_n - R_n$ and separating the contribution of mass by lateral inflow from source term, the equation can then be solved for $C2_n$.

$$C2_n = \left[C1_n + \frac{\text{sources}}{VH_n} + \frac{ETP_n - ETP_{n-1}}{VH_n} + \frac{PRF_{n-1}}{VH_n}\{\alpha_{n-1}\ C1_n + (1 - \alpha_{n-1})\ C2_{n-1}\} + \frac{PRF_n}{VH_n}(\alpha_n\ C1_{n+1}) + \frac{2r_n BC_n}{VH_n}\right] \Big/ \left\{1 + \frac{PRF_n}{VH_n}(1 - \alpha_n)\right\} \tag{15}$$

where 'sources' represents the addition of mass due to man-made sources and $2r_n \cdot BC_n$ represent that from lateral inflow of fresh water, BC_n is the concentration in the lateral inflow.

If N is the total number of segments, (N-1) equations will be obtained by writing equation (15) for n=2 to N. The (N-1) equations may be solved for the (N-1) unknowns, $C2_n$, if the initial concentrations, $C1_n$ and two boundary conditions, $C2_1$ and $C1_{N+1}$ are specified. The principal operation of the numerical computation is then to compute the concentrations in each segment at the first tidal cycle with a given or assumed initial concentration field at the zeroth tidal cycle. The computed concentration field at the first tidal cycle will then be used as the initial condition to compute the concentration field at the second tidal cycle, and so forth. Each computation cycle will advance time by the increment of one tidal cycle until a specified tidal cycle or equilibrium concentration field is reached. Within each computation cycle, the (N-1) equations are solved by successive substitution, since $C2_{n-1}$ is the only unknown upon which $C2_n$ depends.

(d) Calculation of the Concentrations of Nonconservative Substances

Equation (12) represents the rate of the change of mass within a segment due to external sources and physical transport. For nonconservative substances, additional terms are required to simulate the chemical and biological processes which may cause an increase or decrease of a particular substance within a segment. In general,

equation (12) may be rewritten as

$$\Delta m/\Delta t = \text{sources} + (\text{mass in}) - (\text{mass out}) + B \qquad (12a)$$

where B represents all the chemical and biological processes. In the present model, B is expressed explicitly in terms of concentrations of related substances at the beginning of time step increment. Therefore, it does not introduce additional unknowns in equation (15).

The nonconservative substances considered in the present study include fecal coliforms, organic nitrogen, ammonia nitrogen, nitrite-nitrate nitrogen, organic phosphorus, inorganic phosphorus, chlorophyll "a" as phytoplankton, carbonaceous biochemical oxygen demand and dissolved oxygen. With the exception of fecal coliforms, the above parameters form an inter-dependent system. The interaction of the physical, chemical and biological processes among the parameters is shown in figure 6. In this model, all chemical and biological processes are simulated with as zero or first order reactions, and act independently of the physical transport processes.

With the concentration fields specified or calculated at the beginning of tidal cycle (high water slack) the calculation of the concentration fields at the end of tidal cycle is separated into two steps. First, the concentration fields are calculated assuming only the physical transport processes in action. Second, the calculated concentration

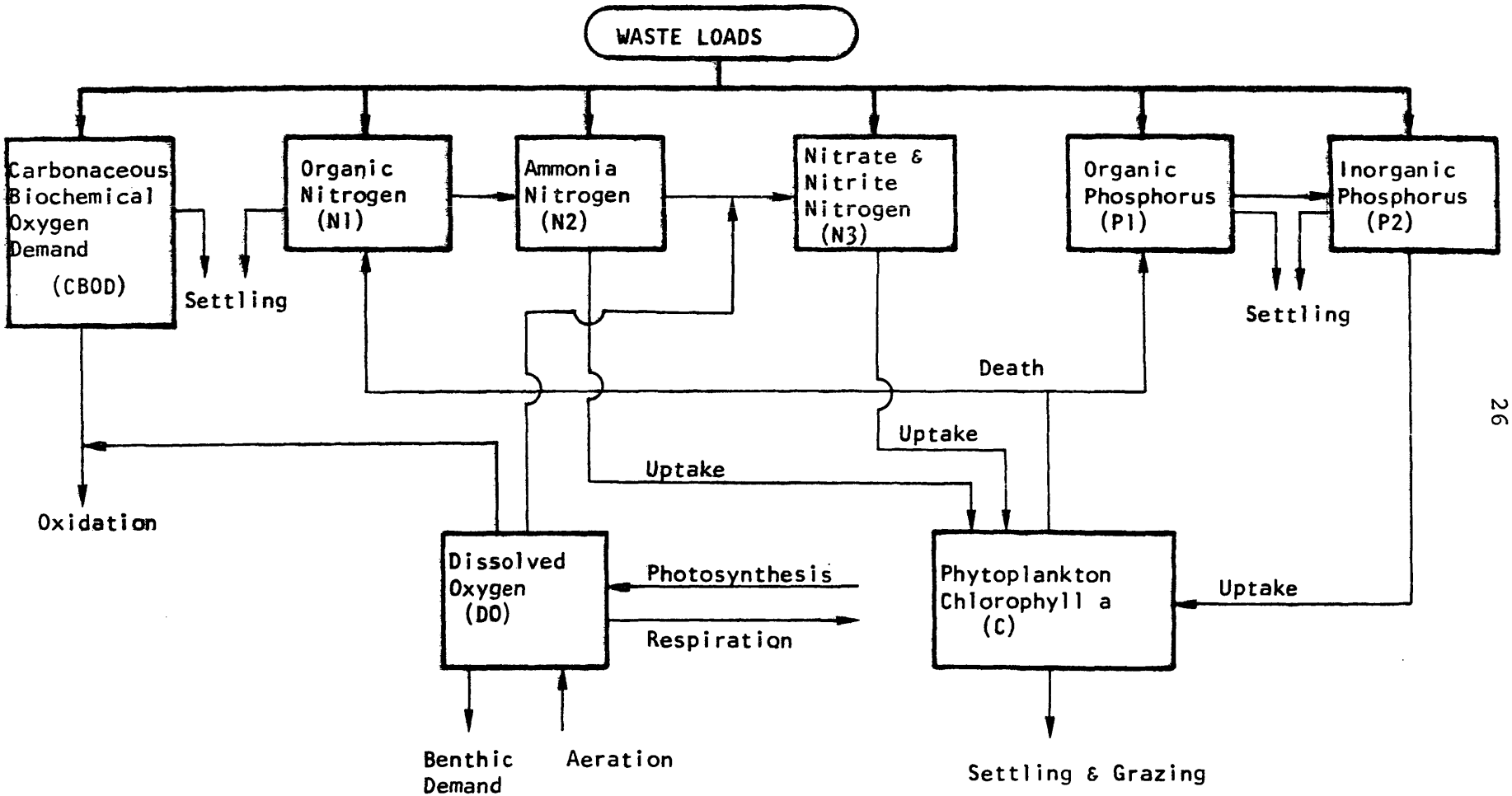

Figure 6. Schematic Diagram of Interaction of Ecosystem Model

field are adjusted for the chemical and biological processes. The first step of calculation is the same as that of conservative substance described in the previous section. The second step of calculation is the addition and/or subtraction of terms obtained through the integration, over time interval Δt, of the terms representing the chemical and biological processes. The adjustment for each parameter is described in the following. In the discussion below, the 'starred' variables designate the concentrations after adjustment for the chemical and biological processes, the unstarred variables designate those calculated with physical transport processes alone in action. All pertinent variables are functions of segment location but the subscripts for segment number have been omitted for brevity.

(1) Coliform Bacteria, C

$$C^* = C \cdot \exp(-k_b \cdot \Delta t) \tag{17}$$

where

k_b is the die off rate,

Δt is time increment.

(2) Organic Nitrogen, N1

$$N1^* = N1 \cdot \exp\{-(k_{n11} + K_{n12})\Delta t\} + a_n \cdot \{1.0 - \exp(-R_s \cdot \Delta t)\} \cdot CH$$

$$+ a_n \cdot 0.4 \cdot \{1.0 - \exp(-k_g \cdot \Delta t)\} \cdot CH \tag{18}$$

where

k_{n11} is the settling rate,

k_{n12} is the organic-N to NH_3 hydrolysis rate,

a_n is the nitrogen-chlorophyll ratio,

R_s is the phytoplankton endogenous respiration rate,

CH is the chlorophyll concentration,

kg is the zooplankton grazing rate.

(3) Ammonia Nitrogen, N2

$$N2^* = N2 \cdot \exp(-k_{n23} \cdot \Delta t) + \{1.0 - \exp(-k_{n12} \cdot \Delta t\} \cdot N1 - a_n \cdot P_r \cdot \{\exp(G_c \cdot \Delta t) - 1.0\} \cdot CH \quad (19)$$

where

k_{n23} is the NH_3 to NO_3 nitrification rate,

G_c is the phytoplankton growth rate,

P_r is the ammonia preference by phytoplankton, and is given by

$$P_r = \frac{N2}{N2 + K_{mn}}$$

K_{mn} is the Michaelis constant for nitrogen.

(4) Nitrite-Nitrate Nitrogen, N3

$$N3^* = N3 \cdot \exp(-k_{n33} \cdot \Delta t) + \{1.0 - \exp(-k_{n23} \cdot \Delta t)\} \cdot N2 - a_n(1.0 - P_r) \cdot \{\exp(G_c \cdot \Delta t) - 1.0\} \cdot CH \quad (20)$$

where

k_{n33} is the nitrate nitrogen escaping rate.

(5) Organic Phosphorus, P1

$$P1^* = P1 \cdot \exp\{-(k_{p11} + k_{p12})\Delta t\} + a_p\{1.0 - \exp(-R_s \cdot \Delta t)\} \cdot CH + a_p \cdot 0.4 \cdot \{1.0 - \exp(-k_g \cdot \Delta t)\} \cdot CH \quad (21)$$

where

k_{p11} is the settling rate,

k_{p12} is the organic P to inorganic P conversion rate,

a_p is the phosphorus - chlorophyll ratio.

(6) Inorganic Phosphorus, P2

$$P2^* = P2 \cdot \exp(-k_{p22} \cdot \Delta t) + \{1.0 - \exp(-k_{p12} \cdot \Delta t)\} \cdot P1 - a_p \cdot \{\exp(G_c \cdot \Delta t) - 1.0\} \cdot CH \quad (22)$$

where

k_{p22} is the settling rate.

(7) Carbonaceous Oxygen Demand, CBOD

$$CBOD^* = CBOD \cdot \exp\{-(k_1 + k_s) \cdot \Delta t\} + 2.67 \cdot a_c \cdot 0.4\{1-\exp(-k_g \cdot \Delta t)\} \cdot CH \quad (23)$$

where

k_1 is the oxidation rate of CBOD,

k_s is the settling rate,

a_c is the carbon-chlorophyll ratio,

(8) Dissolved Oxygen, DO

$$DO^* = DO - \{1.0-\exp(-k_1 \cdot \Delta t)\} \cdot CBOD - 4.57\{1.0-\exp(-k_{n23} \cdot \Delta t)\} \cdot N2 - BEN \cdot \Delta t + \{1.0-\exp(-k_2 \cdot \Delta t)\}(DO_s - DO) + a_d \cdot \{\exp(G_c \cdot \Delta t)-1.0\}CH - a_r\{1.0-\exp(-R_s \cdot \Delta t)\} \cdot CH \quad (24)$$

where

k_1 is the oxidation rate of CBOD,

BEN is the benthic oxygen demand,

k_2 is the reaeration rate,

DO_s is the saturated oxygen concentration,

a_d or a_r is the amount of oxygen produced (or consumed) per unit chlorophyll synthesized (or destroyed) in the photosynthesis (or respiration) process

(9) Chlorophyll 'a', CH

$$CH^* = CH \cdot \exp\{(G_c - k_{cs} - R_s - k_g) \cdot \Delta t\} \quad (25)$$

where

k_{cs} is the phytoplankton settling rate,

(e) Evaluation of Rate Constants

(1) Coliform bacteria die off rate, k_b

$$k_b = (k_b)_{20} \cdot 1.040^{T-20}$$

where $(k_b)_{20}$ is the die off rate at 20°C and T is temperature in degree centigrade. The normal range of $(k_b)_{20}$ is 0.5-4.0/day.

(2) Settling rate of organic nitrogen, k_{n11}

k_{n11} is of the order of 0.1/day

(3) Organic N to NH_3 hydrolysis rate, k_{n12}

$$k_{n12} = aT$$

where a is of the order of 0.007/day/degree

(4) NH_3 to NO_3 nitrification rate, k_{n23}

$$k_{n23} = aT$$

where a is of the order of 0.01/day/degree

(5) NO_3 escaping rate, k_{n33}

k_{n33} is usually negligible

(6) Organic phosphorus settling rate, k_{p11}

k_{p11} is of the order of 0.1/day

(7) Organic P to inorganic P conversion rate, k_{p12}

$$k_{p12} = aT$$

where a is of the order of 0.007/day/degree

(8) Inorganic phosphorus settling rate, k_{p22}

k_{p22} is of the order of 0.1/day

(9) CBOD decay rate, k_1

$$k_1 = (k_1)_{20} \cdot 1.047^{(T-20)}$$

where $(k_1)_{20}$ is the decay rate at 20°C, whose normal range is 0.1 - 0.5/day.

(10) CBOD settling rate, k_s

k_s is usually negligible

(11) Reaeration rate, k_2

$$k_2 = (k_2)_{20} \cdot 1.024^{(T-20)}$$

where $(k_2)_{20}$ is the reaeration rate at 20°C. $(k_2)_{20}$ is calculated with O'Connor-Dobbins formula

$$(k_2)_{20} = \frac{(D_c U)^{1/2}}{h^{3/2}}$$

where D_c is the molecular diffusivity of oxygen in water, U and h are the mean water velocity and depth respectively.

(12) Saturated oxygen concentration, DO_s

The saturation concentration of dissolved oxygen depends on temperature and salinity. From tables of saturation concentration (Carritt and Green, 1967) a polynomial equation was determined by a least-squares method.

$$DO_s = 14.6244 - 0.367134T + 0.0044972T^2 - 0.0966S + 0.00205TS + 0.0002739S^2$$

where S is salinity in parts per thousand and DO_s is in mg/liter.

(13) Benthic oxygen demand, BEN

The bottom sediment of an estuary may vary from deep deposits of sewage or industrial waste origin to relatively shallow deposits of natural material of plant origin and finally to clean rock and sand. The oxygen consumption rate of the bottom deposits must be determined with field measurements. Field data were used when available. A value of 1.0 $gm/m^2/day$ at 20^oC is typical for most estuaries. The temperature effect was simulated by (Thomann, 1972):

$$BEN = (BEN)_{20} \cdot 1.065^{(T-20)}$$

where $(BEN)_{20}$ is the benthic demand at 20^oC.

(14) Nitrogen-chlorophyll ratio, a_n

a_n is of the order of 0.01 mg N/µg CH

(15) Phosphorus-chlorophyll ratio, a_p

a_p is of the order of 0.001 mg P/µg CH

(16) Carbon-chlorophyll ratio, a_c

a_c is of the order of 0.05 mg carbon/µg CH

(17) Oxygen produced per unit of chlorophyll growth, a_d

$$a_d = 2.67 \cdot a_c \cdot PQ$$

where PQ is photosynthesis quotient, PQ = 1.0 ~ 1.4.

(18) Oxygen consumed per unit of chlorophyll "a" respired, a_r

$$a_r = 2.67\ a_c/RQ$$

where RQ is respiration quotient.

(19) Phytoplankton settling rate, k_{cs}

$$k_{cs} = S_\ell/h$$

where S_ℓ is settling velocity, whose normal range is 0.5 to 5 ft/day.

(20) Zooplankton grazing rate, kg

In reality, kg should depend on the concentration of herbivorous zooplankton biomass. Since zooplankton are not included in this model, kg is assumed to be zero, and the grazing effect is accounted for by settling.

(21) Endogenous respiration rate, R_s

$$R_s = aT$$

where a is of the order of 0.005/day/degree.

(22) Growth rate, G_c

The growth rate expression is that developed by Di-Toro, O'Connor and Thomann (1971) and as used in this model is given by

$$G_c = \underbrace{k_{gr}T}_{\text{temperature effect}} \cdot \underbrace{I\ (I_a,\ I_s,\ k_e,\ CH,\ h)}_{\text{light effect}} \cdot \underbrace{N(N2,N3,P2)}_{\text{nutrient effect}}$$

where k_{gr} is the optimum growth rate of the order of 0.1/day/degree. The functional form, I, for the light effect incorporates vertical extinction of solar radiation and self-shading effect. The form is

$$I = \frac{2.718f}{k_e h} (e^{-\alpha_1} - e^{-\alpha_o})$$

$$k_e = k_e' + 0.0088 \cdot CH + 0.054 \cdot CH^{0.66}$$

$$\alpha_1 = \frac{I_a}{I_s} e^{-k_e h}$$

$$\alpha_o = \frac{I_a}{I_s}$$

k_e' is the light extinction coefficient at zero chlorophyll, k_e is the overall light extinction coefficient, f is the photoperiod, I_a is the average incoming solar radiation and I_s is the optimum light intensity, about 300 langleys per day. The nutrient effect makes use of product Michaelis - Mention kinetics and is given by

$$N = \frac{N2 + N3}{K_{mn} + N2 + N3} \cdot \frac{P2}{K_{mp} + P2}$$

where K_{mn} is the half saturation concentration for total inorganic nitrogen and K_{mp} is the half saturation concentration for phorphorus. K_{mn} and K_{mp} have been reported to be about 0.03-0.04 and 0.003-0.005 mg/l respectively.

2. Model Application

Examination of the salinity distributions reveals that at times during the summer the Lynnhaven Bay System and Little Creek Harbor are well mixed and the freshwater inflow is almost zero (Neilson, 1976). These conditions make the tidal prism model applicable.

In order to apply the model to a water body, the system must be divided into segments each having a length equal to the local tidal excursion. Segmentation of these two estuaries was done by the graphical method described in Section IV-1-b. The data required were cross-sectional profiles, surface area and tide ranges, all of which are on file at VIMS. The resulting segmentation is shown in Figure 7. For convenience, the Lynnhaven Bay system was treated as two subsystems: Lynnhaven Bay and Broad Bay. The Lynnhaven Bay subsystem was then divided into one main stem and one branch, as was the Broad Bay subsystem. The Little Creek System was divided into one main stem and three branches. The main stem and the branch of Lynnhaven Bay subsystem were divided into 5 and 5 segments respectively, with the branch entering the main stem in segment 2. The main stem and the branch of Broad Bay subsystem were divided into 8 and 3 segments respectively, with the branch entering the main stem in segment 7. The main stem and branches of the Little Creek system were divided into 5 and 4 segments respectively, with branches 1 and 2 entering the main stem in segment 3, and branch 3 entering at segment 5.

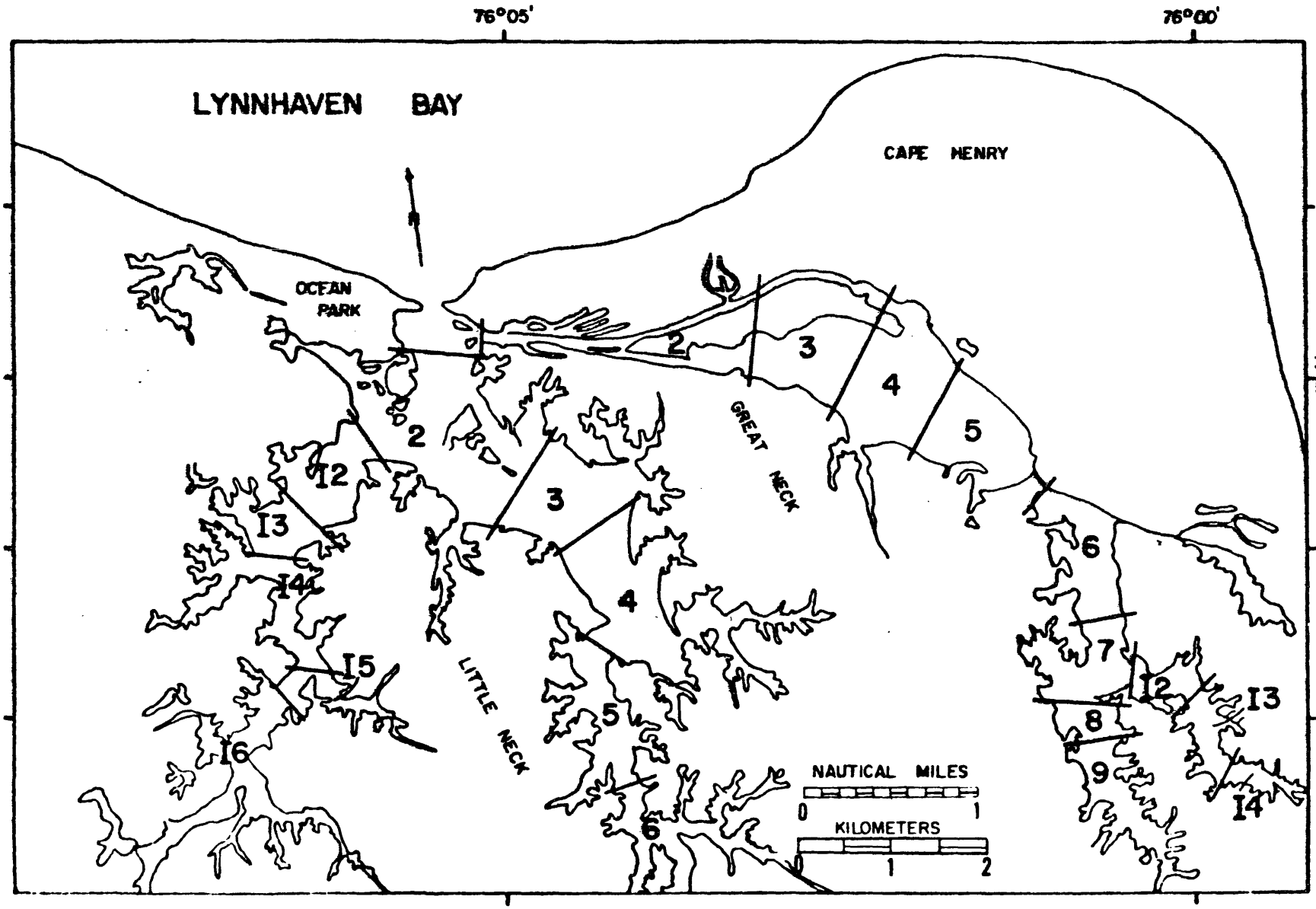

Figure 7a. Segmentations of Lynnhaven Bay System.

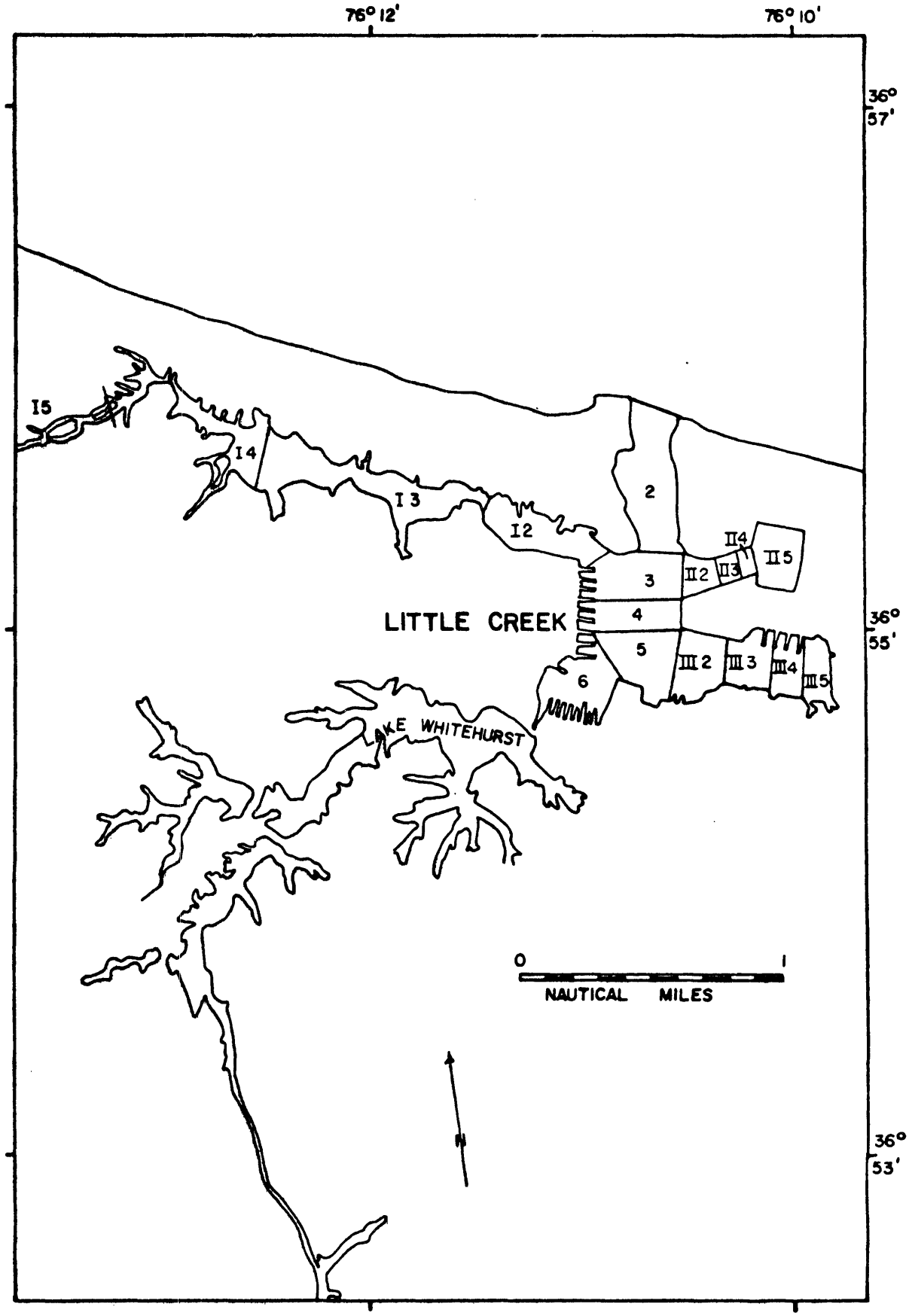

Figure 7b. Segmentation of Little Creek System.

3. Model Calibration and Verification

Before being put into practical usage, a mathematical model must be calibrated and verified. That is, the model must be adjusted so that it reproduces the behavior observed in the prototype. Therefore, a complete set of field data must be acquired. Measurements of both independent and interdependent variables must be made over a period of time at selected locations throughout the area of concern.

Independent variables are those factors which are not modelled but are included in the model as known constants. Some of these factors, such as temperature and solar radiation, can be measured directly. Those factors which can not be measured directly must be estimated using literature values or they may be derived from field observation (phytoplankton growth rate, for example). A list of the observed independent variables used as inputs to model is given in Table 1.

Interdependent variables are those factors which are modelled and are related. For example, nitrification reduces the amount of ammonia nitrogen, and the decay of oxygen demanding materials reduces the amount of dissolved oxygen. The matrix shown in Table 2 indicates the interdependence among variables, in the sense of the existence of a direct mathematical relationship. Obviously, the fecal coliform and salinity submodels may be calibrated independently, but the remaining eight components must be calibrated simultaneously.

The field data used in the calibration step were collected in September, 1975. A description of the field study

TABLE 1. Model Inputs Derived from Observation

Input	Source
River Channel Geometry	VIMS Bathymetry and Remote Sensing Surveys
Tidal Range	VIMS Tidal Height Survey and NOAA Data
Fresh Water Inflow	Malcolm Pirnie Engineers, Inc.
Incident Solar Radiation	Concurrent Pyroheliometer Data taken by VIMS
Bottom Oxygen Demand	VIMS Surveys, September, 1975
Non-point Source Pollutants	VIMS Stormwater Surveys, 1976 and Malcolm Pirnie Engineers, Inc., 1977
Point Source Pollutants	Virginia State Water Control Board, and Betz Engineers
Temperature	VIMS Surveys, September, 1975

Table 2.

Ecosystem Component Interdependence Matrix

Depends On / Component	Salinity	Organic Nitrogen	Ammonia	Nitrate plus Nitrite	Organic Phosphorus	Inorganic Phosphorus	Chlorophyll	CBOD	Dissolved Oxygen	Coliform Bacteria
Salinity	x									
Organic Nitrogen		x					x			
Ammonia		x	x				x			
Nitrate plus Nitrite			x	x			x			
Organic Phosphorus					x		x			
Inorganic Phosphorus					x	x	x			
Chlorophyll			x	x		x	x			
CBOD							x	x		
Dissolved Oxygen	x		x				x	x	x	
Coliform Bacteria										x

and a summary of results already have been presented in a previous report (Neilson, 1976). Broad Bay and Little Creek do not have any point sources of pollutants. Loadings were solely the result of runoff from the land. However, Lynnhaven Bay does receive effluent from the Birchwood Gardens Sewage Treatment Plant in addition to surface runoff. Estimates of nonpoint source loadings for each drainage basin for the 30 day period prior to the estuarine sampling program were provided by Malcolm Pirnie Engineers, Inc., which used the model "STORM". This model was calibrated using field observations of the quantity and quality of runoff from a variety of land uses in the 208 Study Area. The field surveys were conducted by VIMS in 1976. The Lynnhaven, Broad Bay and Little Creek models employed no freshwater inflows or loadings above those specified by STORM output, except for the Birchwood Gardens STP discharge.

(a) Calibration and Verification Procedures

The first step of model calibration is to simulate conservative substances such as salt, since the distribution of these substances is solely the result of physical processes. That is, the variations in salinity in the estuary are the result of Bay-derived salty water being transported and mixed with land-derived freshwater. It is assumed that all substances will be transported and dispersed in a similar manner, but that non-conservative substances will experience biochemical transformations during the process. Therefore, the second stage of calibration is to simulate the concentration field

of non-conservative substances. Normally the fecal coliform submodel would be calibrated next since it is simple, having essentially no interactions with other components.

Calibration of the nutrient cycle is complicated and difficult since numerous elements and rate constants are involved. Several rate constants which were not directly measured in the field were determined by successive trials using literature values as guides. The first step in this trial and error approach was to reproduce the observed chlorophyll "a" levels. This process was found to be efficient in the sense that most model components were close to calibration by the time chlorophyll "a" levels were properly adjusted. There remained only some final "tuning" of several rate constants which had minor influence on chlorophyll "a" levels.

The dissolved oxygen (DO) component is the last to be adjusted since the phytoplankton have an effect on DO levels. Changes in the decay rate of oxygen demanding material tend to affect the BOD levels more than DO levels since reaeration plays a dominant role in the DO cycle.

Values for the input constants and transfer rates are given in tabular form: Table 1 enumerates those inputs derived from observation while Table 3 lists those constants which were estimated and literature values for comparison. Nonpoint source loadings from surface runoff were supplied to VIMS by Malcolm Pirnie Engineers, Inc. and were averaged over the 30 day period prior to the intensive survey. The loadings from the Birchwood Gardens STP were obtained from the

TABLE 3. Rate Constants

Broad Bay, Lynnhaven Bay and Little Creek Water Quality Models

Input Constant (Symbol)	Units	Value(s) Used in Models	Literature Values	Reference	Comments
Saturation Light Intensity (RIS)	$\frac{\text{langleys}}{\text{day}}$	340 (B) 340 (Ly) 340 (Lt)	350	Canale, et.al.,1974	From Scavia & Parks, 1976
			230-290	McAllister, et.al., 1961	Habitat-type In-situ experim
			$10\text{-}30 \times 10^{15}$ quanta/sec	Nielsen, 1975	
			340	Parsons, et.al., 1972	Artificial Fertilization Experiment in Freshwater Lake
			2000-3000 ft-cand.	Ryther, 1956	Diatoms & Dinoflagellates
			300	Thomann, et. al., 1974	Tidal Freshwater Ecosystem Model Study
Saturation Phytoplankton Growth Rate (k_{gr})	$day^{-1}{}^{o}C^{-1}$	0.05 (B) 0.048 (Ly) 0.12 (Lt)	1.43	Fuchs, et. al., 1972	From Scavia & Parks, 1976
			.024-.042 mg Carbon/µg chlor. day	McAllister, et.al., 1961	Higher range of values during log phase

Input Constant (Symbol)	Units	Value(s) Used in Models	Literature Values	Reference	Comments
Saturation Phytoplankton Growth Rate (k_{gr}) (con't)			.01-.012mg Carbon/µg Chlor. day	Nielsen, 1975	Planktonic green algae & diatoms
			.025-.10mg Carbon/µg Chlor. day	Parsons, et.al., 1972	Artificial fertilization experiment in Fresh Water Lake
			.05-1.4 mg Carbon/µg Chlor. day	Ryther & Yentsch, 1957	Summary of results from several sources
			1.3-2.7	Sorokin & Krauss, 1962	From Scavia & Parks, 1976
			0.1/day/^{o}C	Thomann, et.al., 1974	Tidal fresh water ecosystem model study
Phosphorus Michaelis Constant (KMP)	$\frac{mg\text{-}P}{\ell}$	0.004 (B) 0.004(Ly) 0.005(Lt)	.053	Fuchs, et. al., 1972	From Scavia & Parks, 1976
			.006-.024	Halmann & Stiller, 1974	Fresh Water
			0	Fhee, 1972	Shortage of extra-cellular P not limiting to growth
			.005	Thomann, et. al., 1974	Tidal fresh water ecosystem model study

Input Constant (Symbol)	Units	Value(s) Used in Models	Literature Values	Reference	Comments
Nitrogen Michaelis Constant (KMN)	$\frac{mg\text{-}N}{\ell}$	0.008 (B) 0.010(Ly) 0.015(Lt)	.014-.018	MacIsaac & Dugdale, 1969	Oligotrophic Syste
			.025	Thomann, et.al., 1974	Tidal fresh water ecosystem model study
Plankton Settling Rate (KCS)	day^{-1}	0.0 (B) 0.0(Ly) 0.0(Lt)	0.1	Penumalli, et.al.,1976	
			$\frac{0.2m}{day}\ \frac{(1+0.008xtemp)}{depth}$	Scavia & Park, 1976	Cleaner model lake ecosystem model study
			$\frac{0.08\text{-}0.67m}{day}$	Titman & Kilham, 1976	Fresh water phytoplankton
Endogenous Respiration Rate (RRESP)	$day^{-1}oC^{-1}$	0.005 (B) 0.0045(Ly) 0.0045(Lt)	8-10% of optimum photosynthetic rate	Nielsen, 1975	
			.005	Thomann, et.al., 1974	Tidal freshwater ecosystem model study
Carbon-Chlorophyll Ratio (AC)	$\frac{mg}{\mu g}$	0.090 (B) 0.12 (Ly) 0.045(Lt)	.015-.02	McAllister, et.al., 1961	Sea water
			.019-.097	Parsons, et.al.,1961	Eleven different species examined
			.027-.049	Parsons & Takahashi, 1972 p. 47	Textbook summary from other sources

Input Constant (Symbol)	Units	Value(s) Used in Models	Literature Values	Reference	Comments
Nitrogen-Chlorophyll Ratio (AN)	$\frac{mg}{\mu g}$	0.015 (B) 0.008(Ly) 0.009(Lt)	$\frac{.08\text{-}.17\ gmN}{gm\ Carbon}$	Collos & Levin, 1976	Ratio tends to increase as growth rate slow
			.0016-.0045	McAllister, et.al., 1961	Log phase growth
			.008-.016	Parsons & Takahashi, 1972, p. 47	Textbook summary from other sources
			.004-.014	Parsons, et.al., 1961	Eleven different species examined
			.01	Thomann, et.al., 1974	Tidal fresh water ecosystem model study
Phosphorus-Chlorophyll	$\frac{mg}{\mu g}$	0.0007(B) 0.0004(Ly) 0.0005(Lt)	.0008	McAllister, et.al., 1961	Log Phase growth
			.0014-.0055	Parsons, et.al., 1961	Eleven different species examined
			.0009-.0023	Parsons & Takahashi, 1972, p. 47	Textbook summary from other sources
			.001	Thomann, et.al.,	Tidal fresh water ecosystem model study

Input Constant (Symbol)	Units	Value(s) Used in Models	Literature Values	Reference	Comments
Organic N-Ammonia Hydrolis rate Constant (KN12)	$day^{-1}{}^{o}C^{-1}$	0.0024 (B) 0.0025(Ly) 0.0030(Lt)	.015/day	Penumalli, Flake & Fruh, 1976	Nitrogen Cycle model
			.007	Thomann, et.al., 1974	Tidal fresh water ecosystem model study
Ammonia Nitrification Rate (KN23)	$day^{-1}{}^{o}C^{-1}$	0.010 (B) 0.010(Ly) 0.005(Lt)	.025/day	Penumalli, Flake & Pruh, 1976	Nitrogen Cycle model
			.01	Thomann, et.al., 1974	Tidal fresh water ecosystem model study
Nitrite + Nitrate Escaping Rate (KN33)	day^{-1}	0.065(B) 0.32(Ly) 0.20(Lt)			
Organic Phosphorus to Inorganic Phosphorus rate Const. (KP12)	$day^{-1}{}^{o}C^{-1}$	0.0008 (B) 0.0012(Ly) 0.0015(Lt)	.007	Thomann, et.al., 1974	Tidal fresh water ecosystem model study
Grazing Constant (KGRAZ)	day^{-1}	0.06 (B) 0.10(Ly) 0.14(Lt)	.85gm/gm/day	Frederive & Sorokin, 1977	These two models have compartment for zooplankton. Grazing rate of phytoplankton per unit zooplankton per unit time.
			0.8 gm/gm/day	Scavia & Park, 1976	

Input Constant (Symbol)	Units	Value(s) Used in Models	Literature Values	Reference	Comments
Photosynthetic Quotient (PQ)		1.1 (B) 1.3 (Ly) 1.4 (Lt)	1.25	Schlieper, 1972, p. 303	Average value for marine phytoplankton
			1.3	McAllister, et.al., 1961	
Respiration Quotient (RQ)		1.1 (B) 1.2 (Ly) 1.2 (Lt)			

NOTE: B = Broad Bay
Ly = Lynnhaven Bay
Lt = Little Creek

State Water Control Board.

The calibration process requires subjective judgements on the accuracy of the simulation. This is especially true when the number of prototype observations is small, as is the case in the Lynnhaven and Little Creek systems. Ultimately the model is calibrated when the scientist judges that values for all input parameters and responses of the various components are reasonable and that the simulation captures the essential characteristics of the ecosystem.

Once the model has been calibrated with intensive survey data, the pollutant loads and other input information for a slack water run are entered into the computer. If the model gives predictions similar to the condition observed, then one says that the model is also verified. Often further fine adjustments are required to get better fit of both intensive survey and slack water run data.

Graphs of observed and predicted values for the intensive survey and a high water slack are given in Appendices A, B and C for Broad Bay, Lynnhaven Bay and Little Creek respectively. The segmentation of these estuaries has been shown as well.

(b) Model Sensitivity

The model components are very sensitive to some of the input rate constants but less so to others. It is important to determine the sensitivity of model components to changes in input rate constants for two reasons: first, to provide a guide for the calibration process; second, to prove the

potential usefulness of the model, since an insensitive model will not be able to discriminate between widely different input conditions.

In some cases, mathematical analysis can be used to predict the sensitivity, but more often model sensitivity is determined by experience gathered in the process of calibration. The data from many computer runs have been used to develop quantitative estimates of sensitivity with continuous pollutant loads. Table 4 indicates maximum sensitivity to changes in the value of particular parameters. These results are not universal; they depend on the range of parameters. Analysis of the field data indicates that nitrogen is the limiting nutrient for Broad Bay under continuous load conditions, so the responses shown in Table 4a are for nitrogen-limited phytoplankton growth. The large sensitivity of nitrite- and nitrate-nitrogen, N3, stems from the smallness of the base. Lynnhaven Bay and Little Creek models indicated that neither nitrogen nor phosphorus was limiting algal growth at the time of field survey. Therefore, the responses shown in Tables 4b and 4c are quite different.

TABLE 4a.

Sensitivity of Broad Bay Water Quality Model with Continuous Pollutant Loads.

Parameter *	Change in Parameter	Component* Response (%) N1	N2	N3	P1	P2	C	CBOD	DO	BACT
KN12	20%	-7.7	13.0	57.1	3.4	-13.3	8.0	3.3	3.1	0
KN23	20%	-1.0	-12.9	7.9	0.9	3.0	-2.4	-0.7	-1.5	0
KP12	20%	0.9	-5.6	-23.8	-6.7	9.9	2.3	6.5	1.0	0
Carbon-C Ratio	20%	0	0	0	0	0	0	9.3	8.0	0
N-C Ratio	20%	5.6	-14.9	-44.6	-4.8	17.1	-9.1	-4.4	-3.7	0
P-C Ratio	20%	-3.0	18.5	71.4	8.1	-23.9	-7.2	-2.1	-3.0	0
KMN	20%	-2.7	40.7	104.8	-1.9	8.7	-5.8	-1.9	-2.6	0
KMP	20%	-2.1	9.3	76.2	-1.5	9.3	-4.3	-1.5	-1.8	0
Sat. Growth Rate	20%	14.2	-44.6	-57.9	10.1	-46.4	30.4	10.7	12.3	0
Grazing Rate	20%	-6.0	22.2	181	-4.3	14.1	-15.7	2.46	-3.6	0
Photosyn. Quotient	20%	0	0	0	0	0	0	0	13.4	0
Resp.Quotient	20%	0	0	0	0	0	0	0	3.94	0
Resp. Rate	20%	-1.9	42.6	376	-1.1	16.0	-19.4	-7.2	-5.7	0
KBAC	20%	0	0	0	0	0	0	0	0	-26

* See Table 4d for definitions.

TABLE 4b.

Sensitivity of Lynnhaven Bay Water Quality Model with Continuous Pollutant Loads.

Parameter*	Change in Parameter	Component* Response (%) N1	N2	N3	P1	P2	C	CBOD	DO	BACT
KN12	50%	-6.75	14.8	7.2	0	0	1.9	0.2	0.5	0
KN23	20%	0	-13.5	+5.0	0	0	-0.6	0.1	-1.3	0
KN33	20%	0	2.0	-14.3	0	0	-1.4	-0.1	-0.2	0
KP12	20%	0	-0.5	-0.2	-5.0	1.6	2.7	0	0	0
Carbon-C Ratio	20%	0	0	0	0	0	0	3.1	2.8	0
N-C Ratio	20%	2.1	-2.0	-11.7	0	0.5	-2.65	-0.3	-0.3	0
P-C Ratio	20%	0	0.7	0.5	2.2	-2.7	-0.5	-0.1	0.1	0
KMN	20%	-0.4	10.2	2.0	-0.5	0.7	-4.2	-0.5	-0.8	0
KMP	20%	-0.4	6.3	3.2	-0.5	0.7	-4.3	-0.5	-0.7	0
Sat.Growth Rate	20%	7.7	-77.6	-72.1	6.6	-12.4	148.1	10.1	16.8	0
Resp. Rate	20%	-0.6	21.5	10.2	-0.5	2.1	-26.5	-2.3	-2.5	0
Grazing Rate	20%	-1.3	22.7	10.9	-0.4	2.3	-28.9	0.4	-2.4	0
Photosyn. Quotient	20%	0	0	0	0	0	0	0	3.3	0
Resp. Quotient	20%	0	0	0	0	0	0	0	0.4	0
KBAC	20%	0	0	0	0	0	0	0	0	-25.3

* See Table 4d for definitions

TABLE 4c.

Sensitivity of Little Creek Water Quality Model with Continuous Pollutant Loads.

Parameter*	Change in Parameter	Component* Response (%) N1	N2	N3	P1	P2	C	CBOD	DO	BACT
KN12	33%	-12.9	12.2	11.9	0.8	-1.2	4.0	2.1	2.4	0
KN23	20%	-0.2	-12.0	3.9	0.3		-0.7	-0.3	-1.4	0
KN33	20%	-1.2	2.1	-11.6	-0.8	0.9	-3.1	-1.7	-2.9	0
KP12	20%	0.4	-0.8	-1.9	-11.8	14.4	0.8	0.5	+0.8	0
Carbon-C Ratio	20%	0	0	0	0	0	0	14.3	17.0	0
N-C Ratio	20%	6.5	-9.3	-25.8	-2.1	3.3	-7.8	-4.2	-5.8	0
P-C Ratio	20%	-0.6	1.6	4.8	+6.8	-8.5	-2.6	-0.9	-1.3	0
KMN	20%	-3.0	12.4	12.5	-2.1	5.4	-9.9	-4.3	-6.9	0
KMP	20%	-2.2	4.9	14.0	-1.7	3.8	-7.0	-3.2	-4.6	0
Sat. Growth Rate	10%	23.2	-33.6	-93.1	16.9	-49.9	92.1	33.1	43.3	0
Grazing Rate	20%	-12.2	23.6	53.5	-8.9	10.9	-32.7	-11.4	-22.4	0
Photosyn. Quotient	20%	0	0	0	0	0	0	0	28.7	0
Resp. Quotient	20%	0	0	0	0	0	0	0	6.0	0
KBAC	20%	0	0	0	0	0	0	0	0	-32.4

* See Table 4d for definitions

TABLE 4d.

Definitions of Parameters and Components
used in Sensitivity Analyses

KN12 is the organic N to NH_3 hydrolysis rate.

KN23 is the NH_3 to NO_3 nitrification rate.

KN33 is the nitrate-nitrogen escaping rate.

KP12 is the organic P to inorganic P conversion rate.

Carbon-C Ratio is the organic carbon to chlorophyll ratio.

N-C Ratio is the organic nitrogen to chlorophyll ratio.

P-C Ratio is the organic phosphorus to chlorophyll ratio.

KMN is the Michaelis nitrogen constant.

KMP is the Michaelis phosphorus constant.

Sat. Growth Rate is the phytoplankton saturation growth rate.

Grazing Rate is the zooplankton grazing rate.

Photosyn. Quotient is the number of oxygen molecule liberated per molecule of carbon dioxide assimilated in the photosynthesis process.

Resp. Quotient is the molecules of carbon dioxide liberated per molecule of oxygen consumed in the respiration process.

Resp. Rate is the phytoplankton endogenous respiration rate.

KBAC is the net fecal coliform die-off rate.

V. RESULTS AND DISCUSSION

Comparison of field measurements and model predictions indicates that, in general, the models are able to reproduce the behavior of the estuaries. A few discrepancies do arise as a result of the limitations inherent in the modelling process. First, the models are one-dimensional and, therefore, cannot reproduce concentration distributions which are two-dimensional in character. The only place where the one-dimensional representation differs significantly from field observations is Broad Bay. Most of the water flowing from Lynnhaven Inlet to Broad Bay enters via the dredged canal. As a result, there tends to be a monotonic gradient from the canal across Broad Bay to the Narrows. However, about a quarter to a third of the water enters via the longer natural channel (Long Creek). Therefore, water conditions near the mouth of the natural channel and the mouth of the canal will be similar, although the mouth of the natural channel is nearly at the midpoint of the Bay. Stated in another way, there will always be some variation in water quality within a model segment. The variation encountered in segment 4 of the Broad Bay model is greater than that normally encountered. The model predictions are for the average conditions within the segment versus field observations which were taken near the mouth of the Long Creek during the intensive survey. Water samples were collected at additional stations during slack water surveys.

The models used are tidal average models and therefore cannot reproduce highly transient phenomena. Rain events or other features which have time scales of the order of minutes or hours cannot be simulated exactly, but events lasting several tidal cycles or several days can be accomodated. The only component of the model which showed appreciable variation between observed and predicted levels was fecal coliforms. Since coliform inputs result primarily from intermittent surface runoff, and since die-off is rapid, it is not unexpected that this component should give less satisfactory simulations.

Chlorophyll "a" concentrations up to 13 µg/l, 14 µg/l and 17 µg/l, a mild algal bloom condition, have been observed in Little Creek, Broad Bay and the Lynnhaven respectively. Analysis of these three water quality models indicates phosphorus to chlorophyll "a" ratios were low, (0.004~0.0007 mg-P/µg-chlorophyll "a"). That is, the amount of phosphorus taken up by the phytoplankton to produce a unit of chlorophyll "a" was less than has been observed in many instances or the phosphorus concentration is merely enough for essential life function, namely growth. The phosphorus inhibition factors (based on field data) were in the range of 0.71 to 0.95, a range with moderate to little inhibition effect. This indicates that phosphorus was not strongly limiting algal growth in these three water bodies at the time of field survey. The ratio of nitrogen to chlorophyll, the amount of nitrogen taken up by the phytoplankton to produce a unit of chlorophyll "a" was 0.008~0.015 mg-N/µg-chlorophyll "a". These values are close

to the average value used by other scientists for other systems. The nitrogen inhibition factors calculated based on field data were in the range of 0.76 to 0.97 for these three estuaries. Again, the availability of nitrogen sources was not strongly limiting algal growth in these three water bodies at the time of field survey. Turbidity and/or depth of water were likely to limit the algal growth in these estuaries. Higher ambient temperature and solar intensity and lower turbidity are likely to trigger algal blooms in these estuaries with concentrations of nitrogen and phosphorus found in field survey. Therefore, waste load allocation studies should focus on potential algal bloom seasons and reducing nutrient levels in these estuaries. It should be noted that nutrient and BOD levels increased slightly with distance up the Western Branch of Lynnhaven Bay, showing the impact of the effluent from the Birchwood Gardens Sewage Treatment Plant.

Dissolved oxygen levels are quite satisfactory under the condition used for calibration and verification. There is only one point source, the Birchwood Gardens Sewage Treatment Plant's effluent, in Lynnhaven Bay. Broad Bay and Little Creek had no point sources of pollutants. The oxygen demand from the decay of phytoplankton has only a small impact on DO levels. Predicted dissolved oxygen levels during field survey were 6.2~7.6 mg/l in the Broad Bay, 6.5~7.0 mg/l in the Lynnhaven Bay, and 5.8~8.5 mg/l in Little Creek. The water quality standard for DO level was not violated. Since there are no large point sources, this was to be expected. However, if the ambient water temperature increases, the DO saturation level

and reaeration will decrease while the rate of BOD and benthic dissolved oxygen demand increase. Thus, a lower DO level can be expected during a prolonged hot summer. If oxygen levels are reduced to 2 mg/l or less, large amounts of nutrients are likely to be released from the sediment exacerbating bloom conditions. Waste load allocation studies should concentrate on the sources of nutrient and the levels which can be assimilated by these estuaries without having eutrophication develop.

Fecal coliform predictions show appreciable deviation from observed levels. Coliform inputs result primarily from intermittent surface runoff which might have time scales of the order of minutes or hours, but the models used are tidal average models and therefore cannot reproduce such highly transient phenomena. Nevertheless, these models did predict higher fecal coliform levels after storm event. In general, predicted fecal coliform levels during dry weather period were less than 10 MPN/100 ml in Broad Bay and Lynnhaven Bay. However, predicted fecal coliform levels immediately after storm event were as high as 86 MPN/100 ml and 500 MPN/100 ml in Broad Bay and Lynnhaven Bay respectively. Fecal coliform up to 960 MPN/100 ml were observed in Little Creek. The predicted bacterial quality of Little Creek was worse than those of Broad Bay and Lynnhaven Bay. The model also predicted high fecal coliform counts in most reaches following rain events. The transport of fecal coliforms in land runoff is apparently the major source and the reason that shellfish closure zones exist in all landward ends of these estuaries. Waste

load allocation studies should demonstrate the effectiveness of nonpoint source abatement on fecal coliform levels in these estuaries.

In summary, use of field observations of estuarine water quality and predictions of stormwater runoff loadings has allowed mathematical models of Broad Bay, Lynnhaven Bay and Little Creek to be calibrated. These models are able to reproduce the physical, chemical and biological processes occuring in these water bodies and are able fo simulate many aspects of water quality. The major water quality problem is high fecal coliform levels found in the landward ends of most reaches. Simulation model studies will allow for delineation of the waste assimilation capacity of these estuaries and examination of problems which might arise. Since these models have been calibrated and verified they are suitable for waste load allocation studies.

VI. REFERENCES

Collos, Y. and J. Lavin, 1976. "Blooms of Surf-zone Diatoms along the Coast of the Olympic Peninsula, Washington. 7. Variations of the Carbon-to-Nitrogen Ratio in Field Samples and Laboratory Cultures of Chaetoceros Armatum", L&O, Vol. 21, No. 2, pp. 219-225, March.

Halmann, M. and M. Stiller, 1974. "Turnover and Uptake of Dissolved Phosphate in Freshwater. A study in Lake Kinnere", L&O Col. 19, No. 5, pp. 774-783. September.

Kuo, A. Y., 1976. "A Model of Tidal Flushing for Small Coastal Basins" in Environmental Modeling and Simulation, USEPA, pp. 543-547.

MacIsaac, J. J. and R. C. Dugdale, 1969. "The Kinetics of Nitrate and Ammonia Uptake by Natural Populations of Marine Phytoplankton", Deep-Sea Res. Vol. 16, No. 1, pp. 45-57. February.

McAllister, C. D., T. R. Parsons, K. Stephens and J. D. H. Strickland, 1961. "Measurement of Primary Production Using a Large-Volume Plastic Sphere", L&O, Vol. 6, pp. 237-258.

Munday, J. C., H. H. Gordon, C. S. Welch, and G. Williams, 1976. Applications of Remote Sensing to Estuarine Management. Annual Report Number 4, Grant NASA-NGL 47-022-005, VIMS.

Neilson, Bruce J., 1976. "Water Quality in the Small Coastal Basins", A Report to the Hampton Roads Water Quality Agency. Virginia Institute of Marine Science.

Nielson, E. S., 1975. Marine Photosynthesis with Special Emphasis on the Ecological Aspects. New York (Elsevier).

Parsons, T. R., K. Stephens and J. D. H. Strickland, 1961. "On the Chemical Composition of Eleven Species of Marine Phytoplankters." J. Fish. Res. Bd. Can. Vol. 18, No. 6, pp. 1001-1016. December.

Parsons, T. R. and M. Takahashi, 1971. Biological Oceanographic Processes. New York (Pergamon).

Parsons, T. R., K. Stephens and M. Takahashi, 1972. "The Fertilization of Great Central Lake. I. Effect on Primary Production." Fish. Bull. Vol. 70, No. 1, pp. 13-27.

Penumalli, B. R., R. H. Flake and E. S. Fruh, 1976. "Large Scale Systems Approach to Estuarine Water Quality Modeling with Multiple Constituents". Ecological Modeling, Vol. 2, pp. 101-115.

Rhee, G. Y., 1972. "Competition Between and Alga and an Aquatic Bacterium for Phosphate". L&O, Vol. 17, No. 4, pp. 505-514. July.

Ryther, J. H., 1956. "Photosynthesis in the Ocean as a Function of Light Intensity". L&O, Vol. 1, No. 1, pp. 61-70. January.

Ryther, J. H. and C. S. Yentsch, 1957. "The Estimation of Phytoplankton Production in the Ocean from Chlorophyll and Light Data". L&O, Vol. 2, No. 3, pp. 281-286. July.

Scavia, D. and R. A. Park, 1976. "Documentation of Selected Constructs and Parameter Values in the Aquatic Model Cleaner." Ecological Modeling, Vol. 2, pp. 33-58.

Schlieper, C., 1972. Research Methods in Marine Biology. Seattle (Univ. of Washington Press).

Sorokin, C. and R. W. Krauss, 1962. "Effect of Temperature and Illuminance on Chlorella Growth Uncoupled from Cell Division". J. Plant Physiol. Vol. 37, No. 1, pp. 37-42. January.

Strickland, J. D. H., 1960. "Measuring the Production of Marine Phytoplankton". Can. Fish. Res. Board Bull. No. 122.

Thomann, R. V., D. M. DiToro, and D. J. O'Connor, 1974. "Preliminary Model of Potomac Estuary Phytoplankton". J. ASCE, Vol. 100, No. EE3, pp. 699-715. June.

Titman, D. and P. Kelham, 1976. "Sinking in Freshwater Phytoplankton: Some Ecological Implications of Cell Nutrient Status and Physical Mixing Processes". L&O, Vol. 21, No. 3, pp. 409-417. May.

APPENDIX A

Observed and Predicted Values of Model Components at High Water Slack for the Broad Bay Subsystem

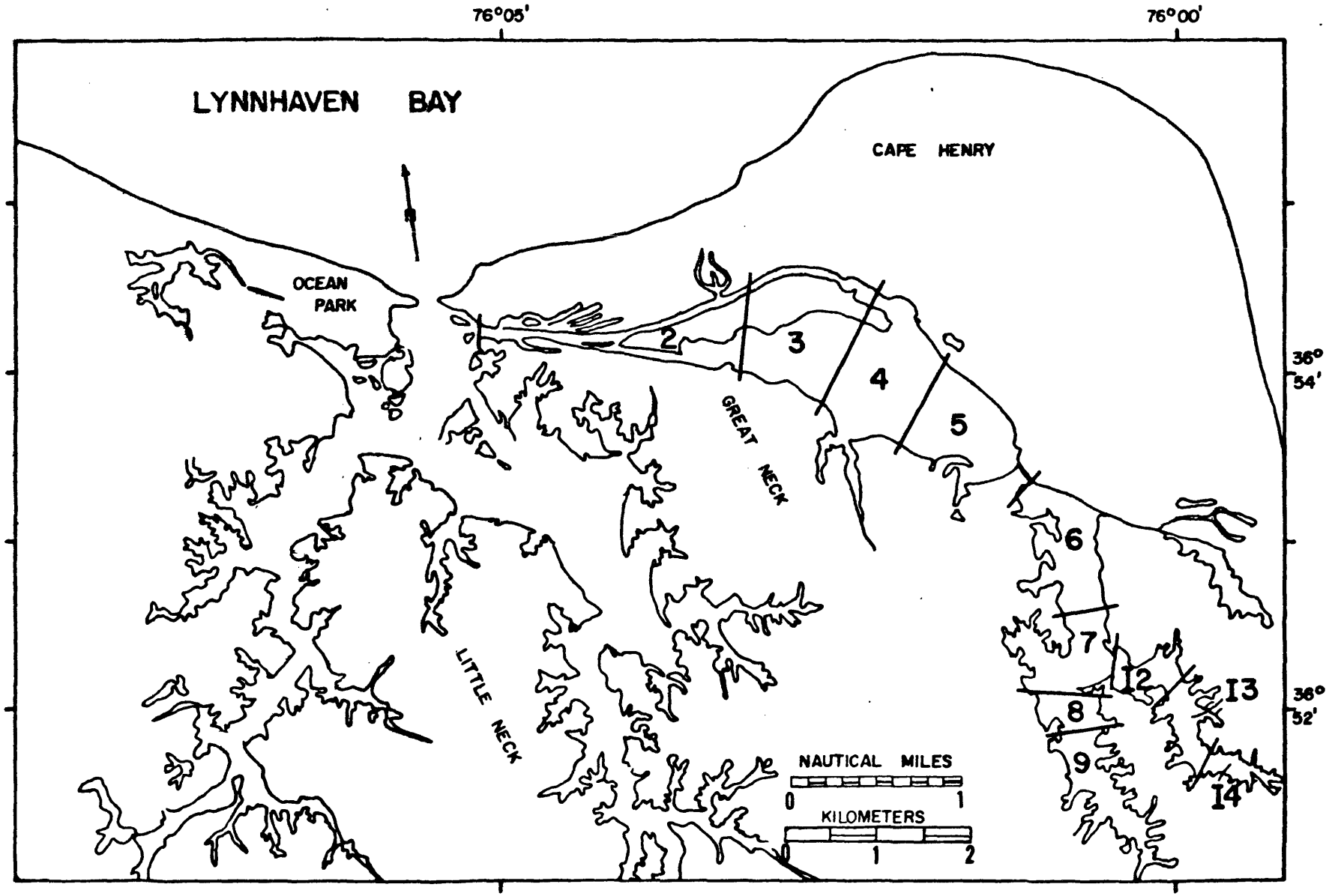

Figure A-1. The Broad Bay showing model segments.

KEY TO THE DRAWINGS

● ○ Field observed.

Model predicted.

●——— Broad Bay and Linkhorn Bay.

○- - - - Little Neck Creek.

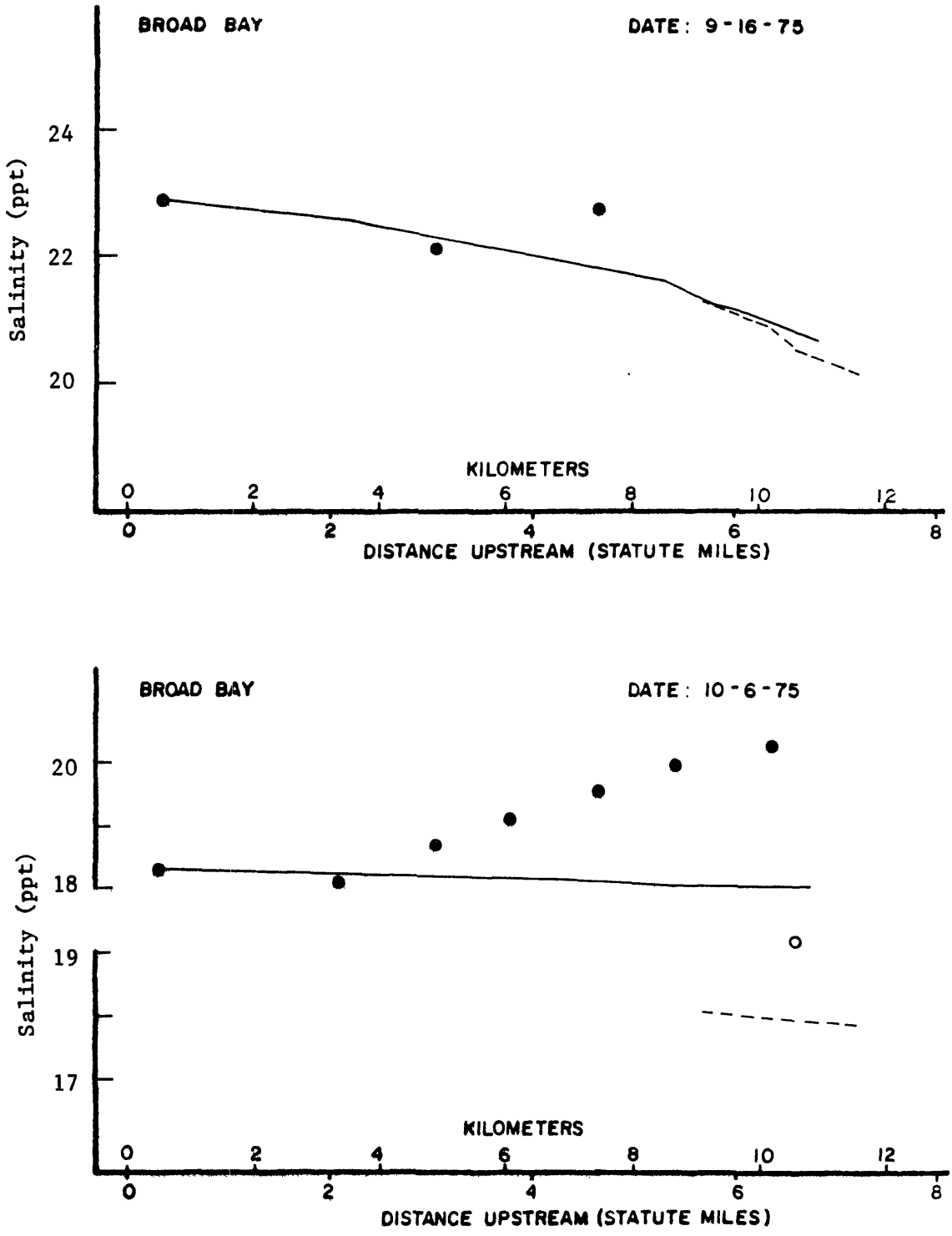

Figure A-2. Longitudinal profiles of salinity.

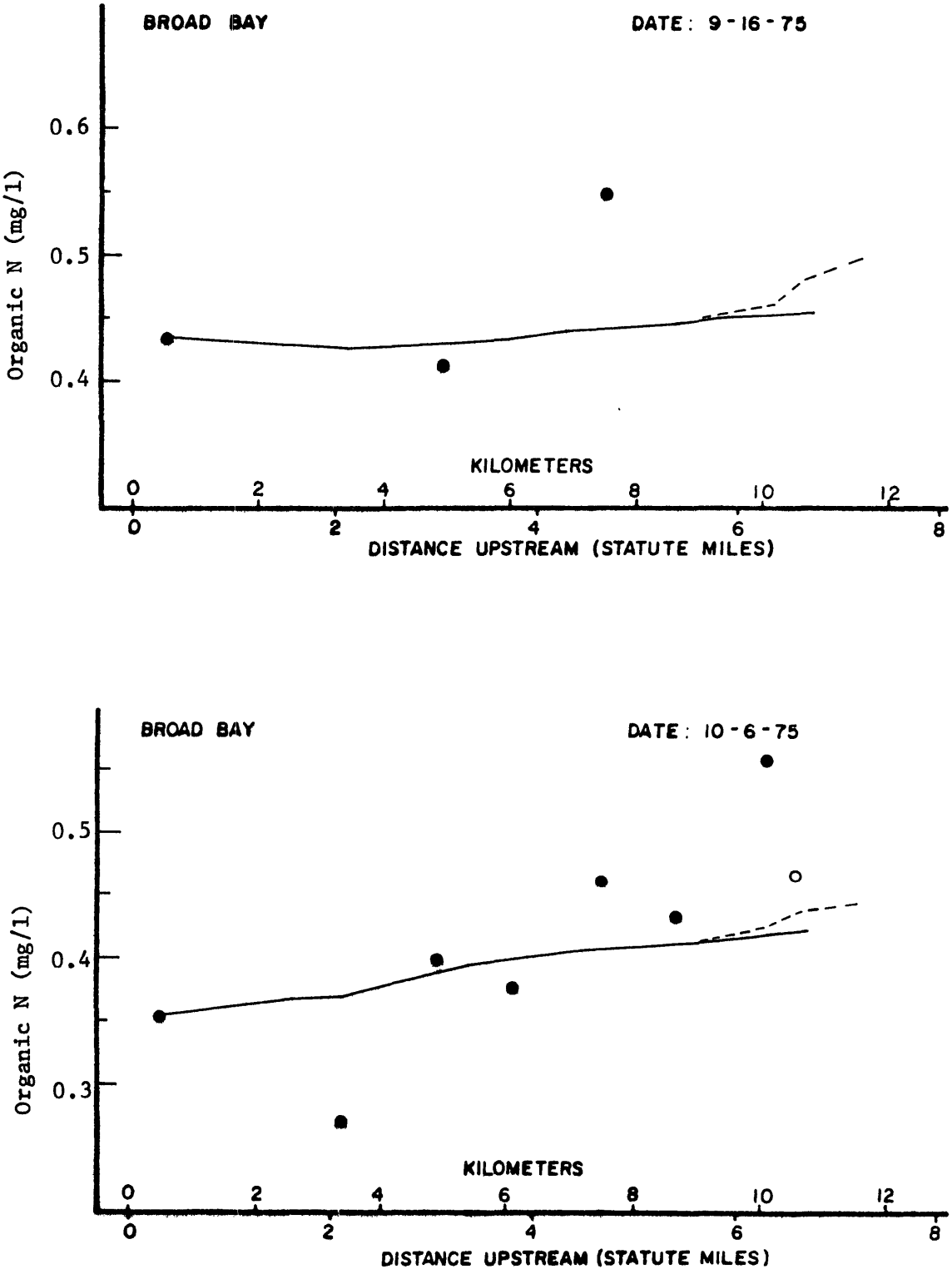

Figure A-3. Longitudinal profiles of organic nitrogen.

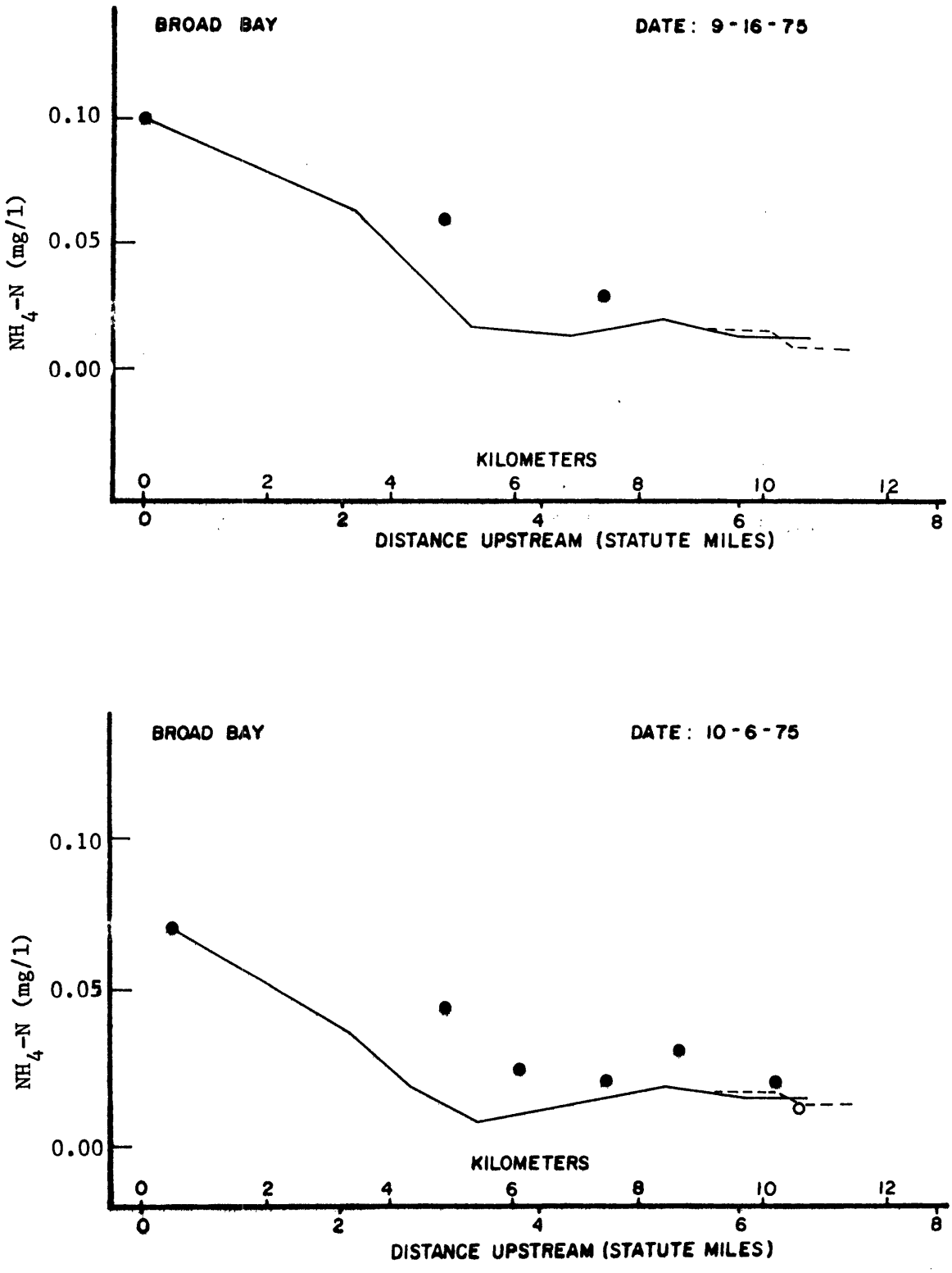

Figure A-4. Longitudinal profiles of ammonium nitrogen.

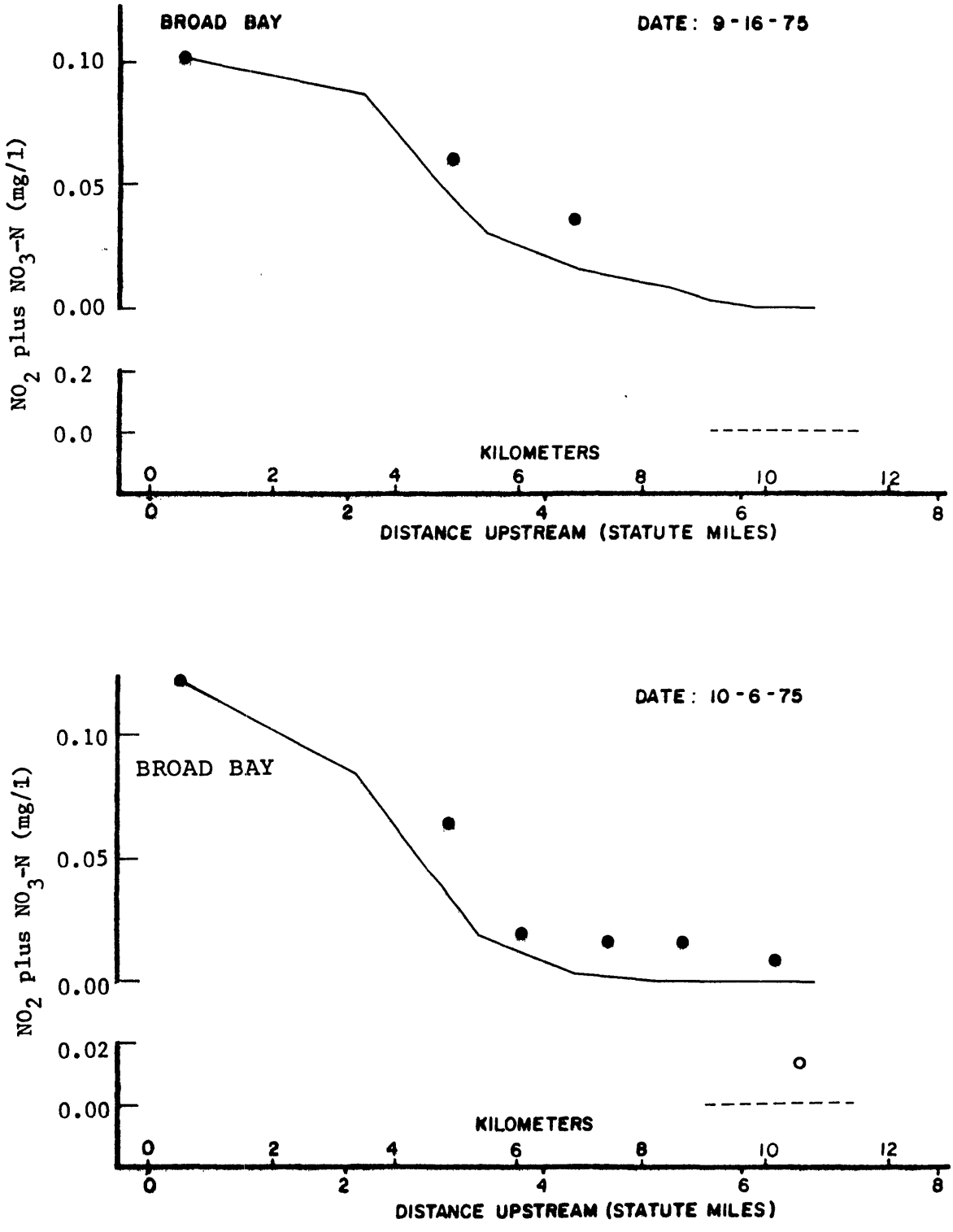

Figure A-5. Longitudinal profiles of nitrite plus nitrate nitrogen.

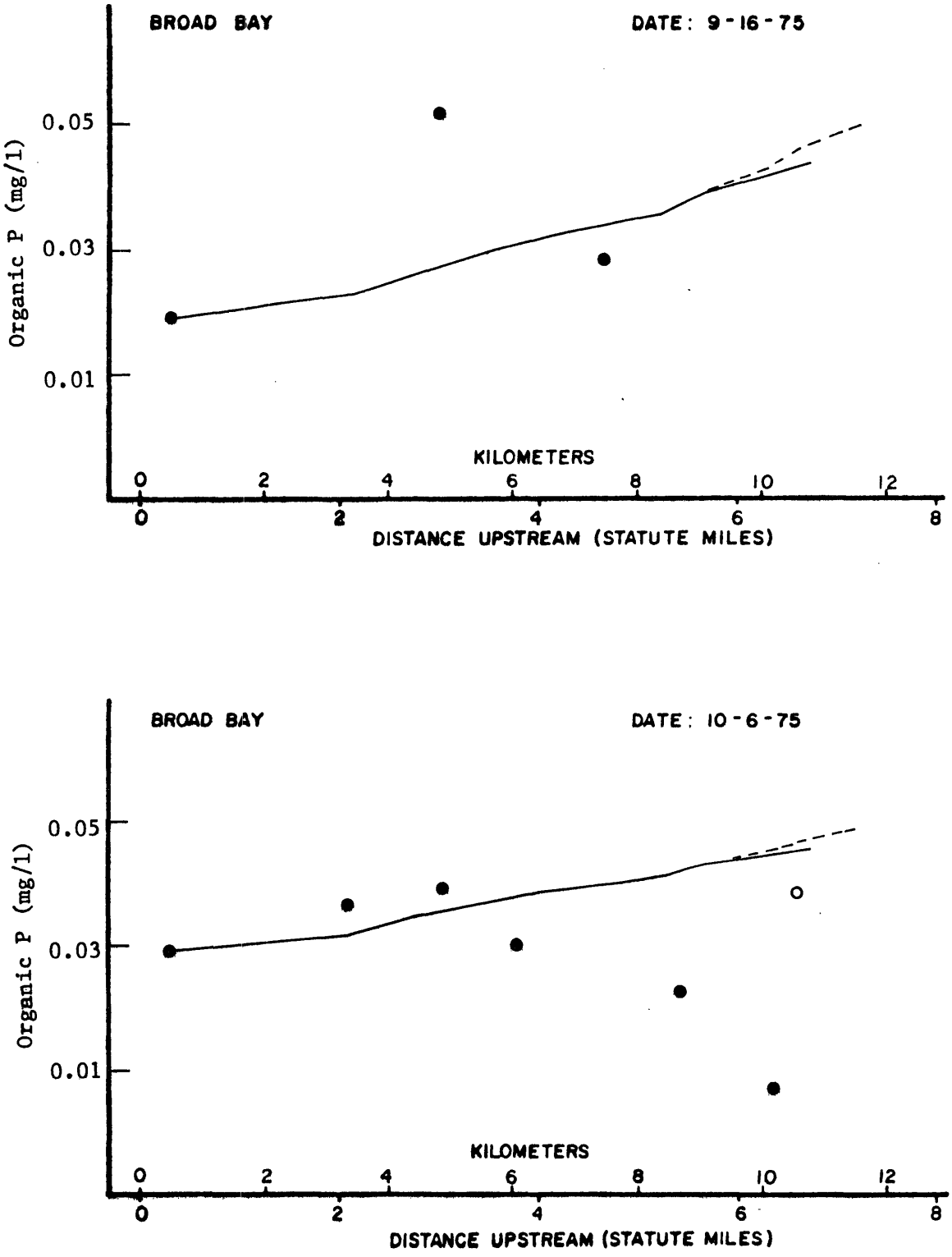

Figure A-6. Longitudinal profiles of organic phosphorus.

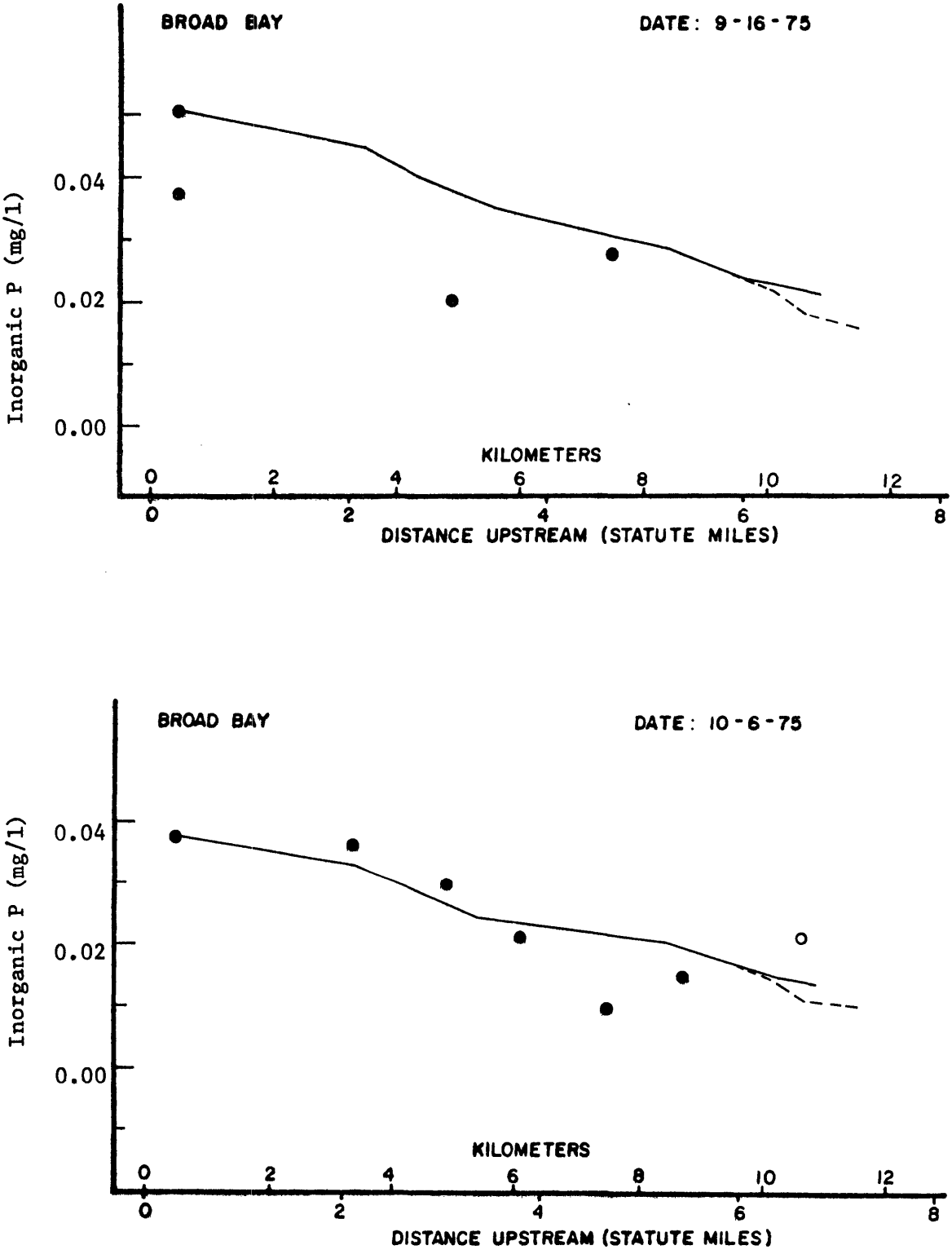

Figure A-7. Longitudinal profiles of inorganic phosphorus.

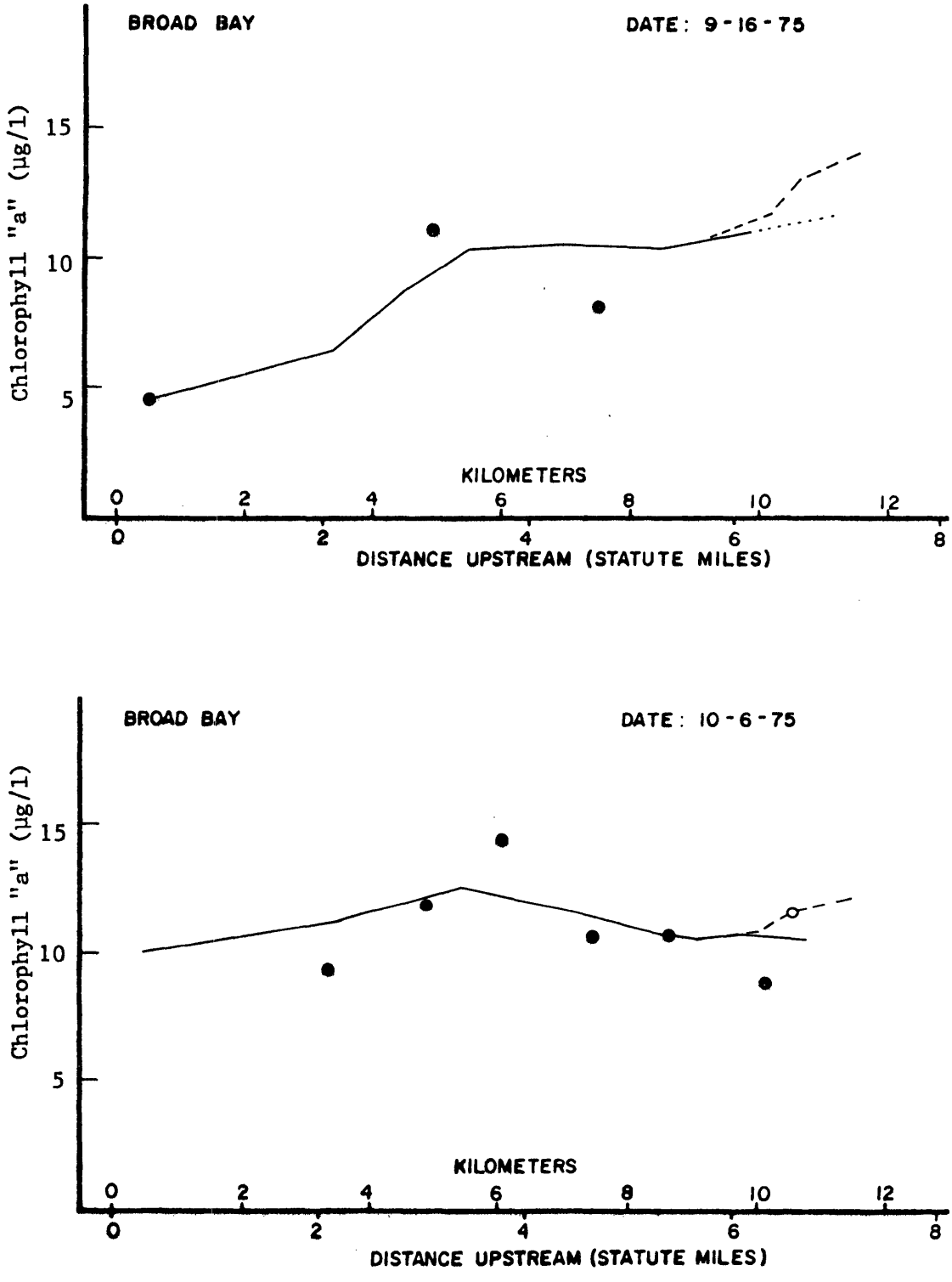

Figure A-8. Longitudinal profiles of chlorophyll "a".

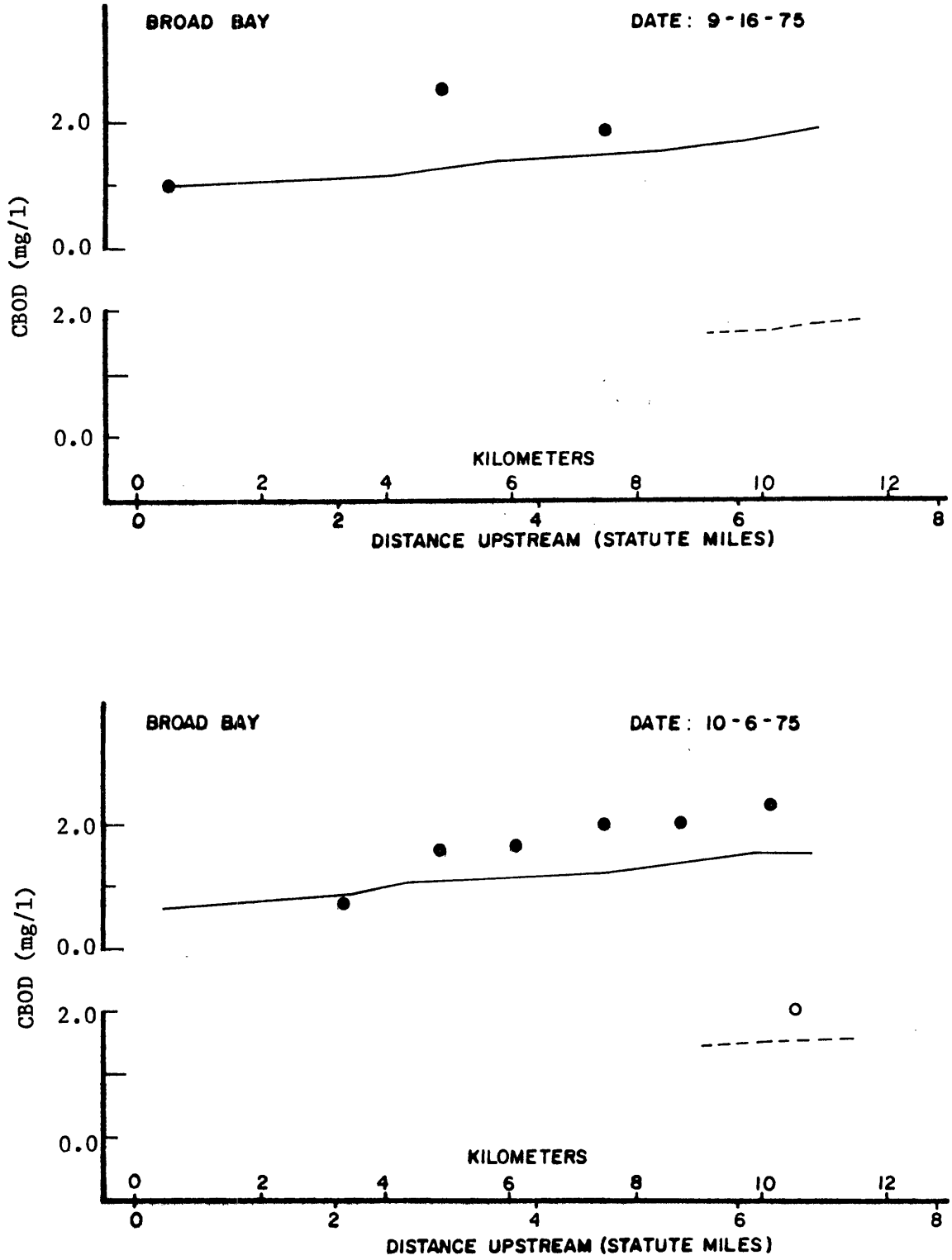

Figure A-9. Longitudinal profiles of CBOD.

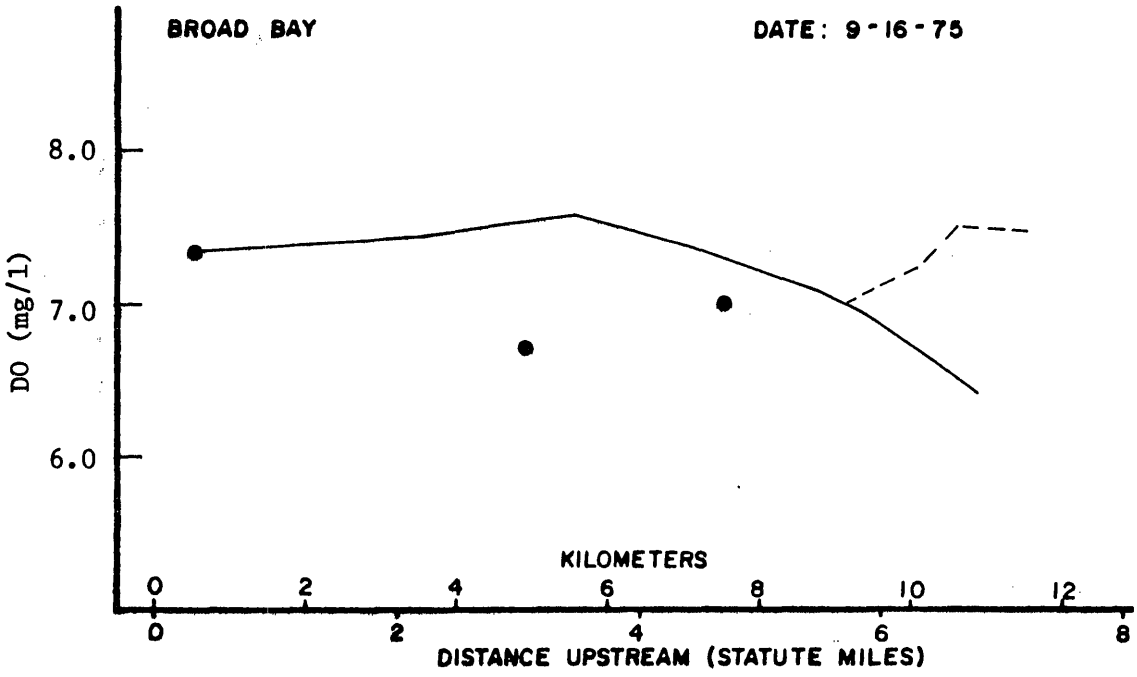

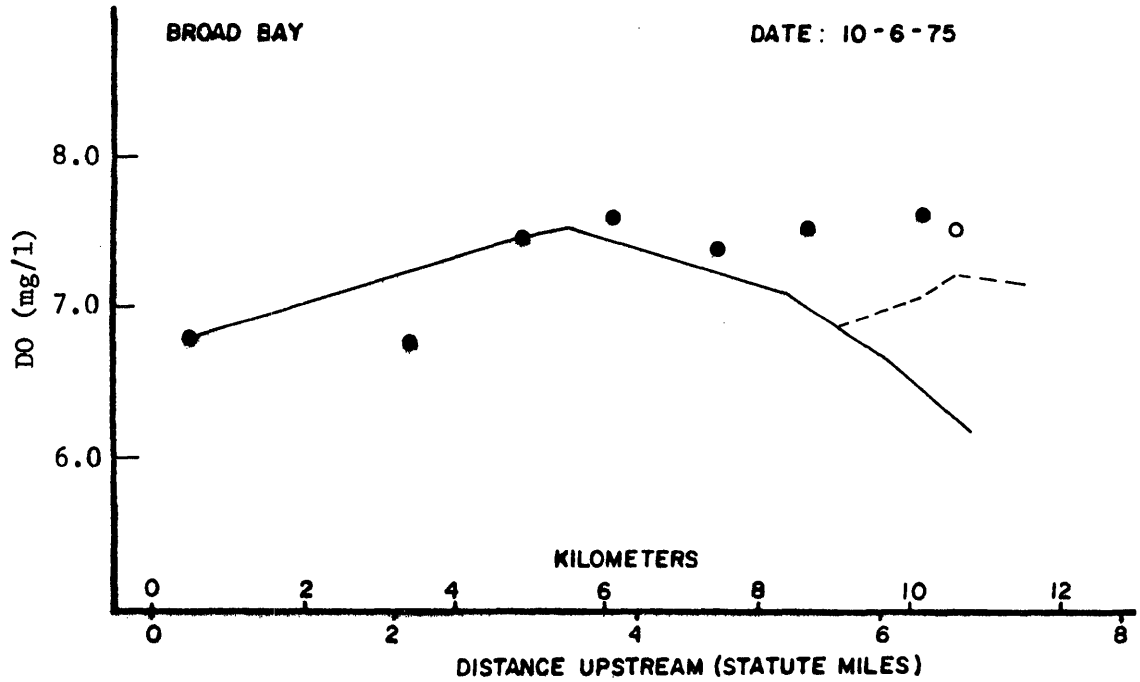

Figure A-10. Longitudinal profiles of dissolved oxygen.

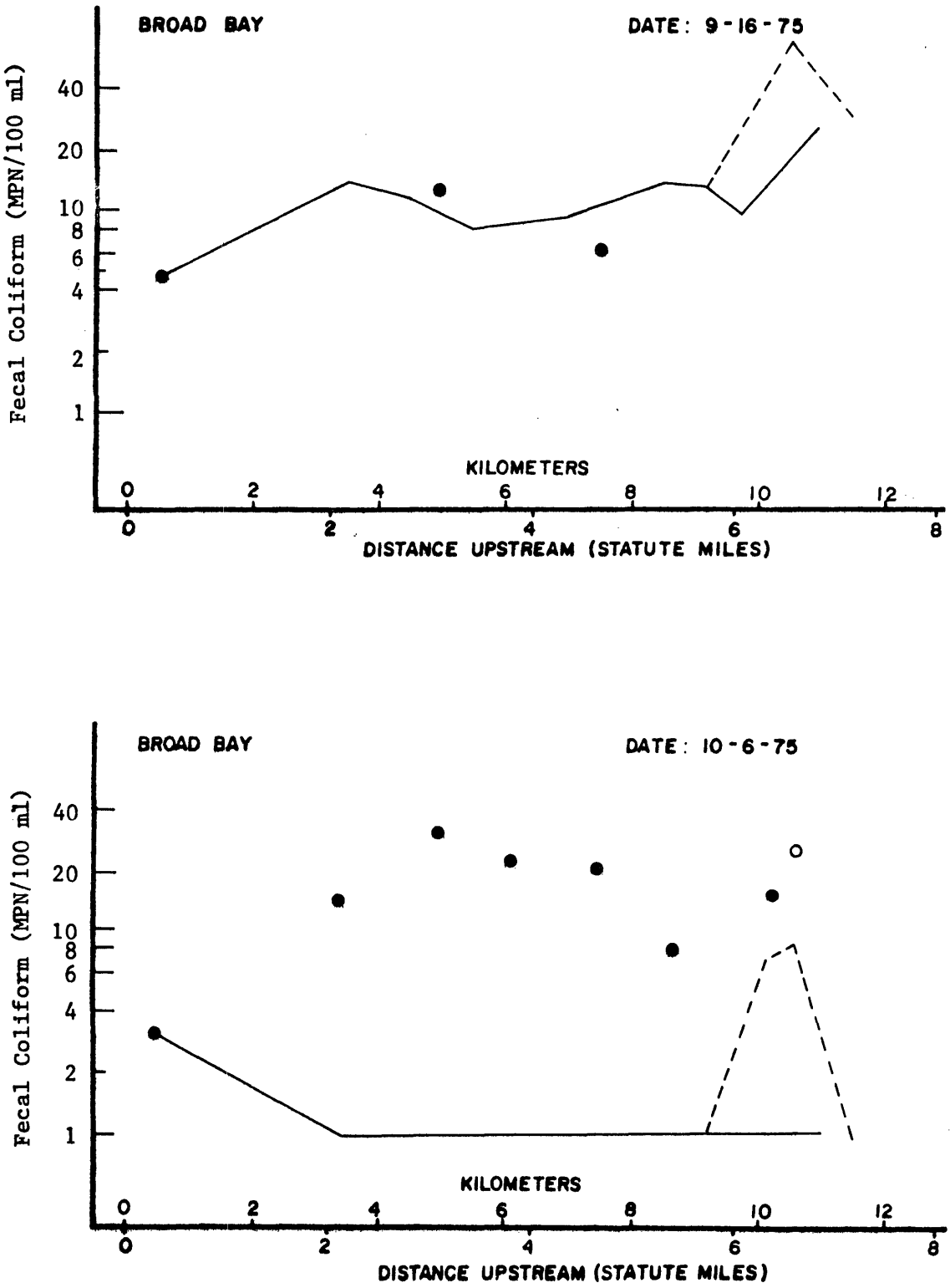

Figure A-11. Longitudinal profiles of fecal coliform concentrations.

APPENDIX B

Observed and Predicted Values of Model Components at High Water Slack for the Lynnhaven Bay Subsystem

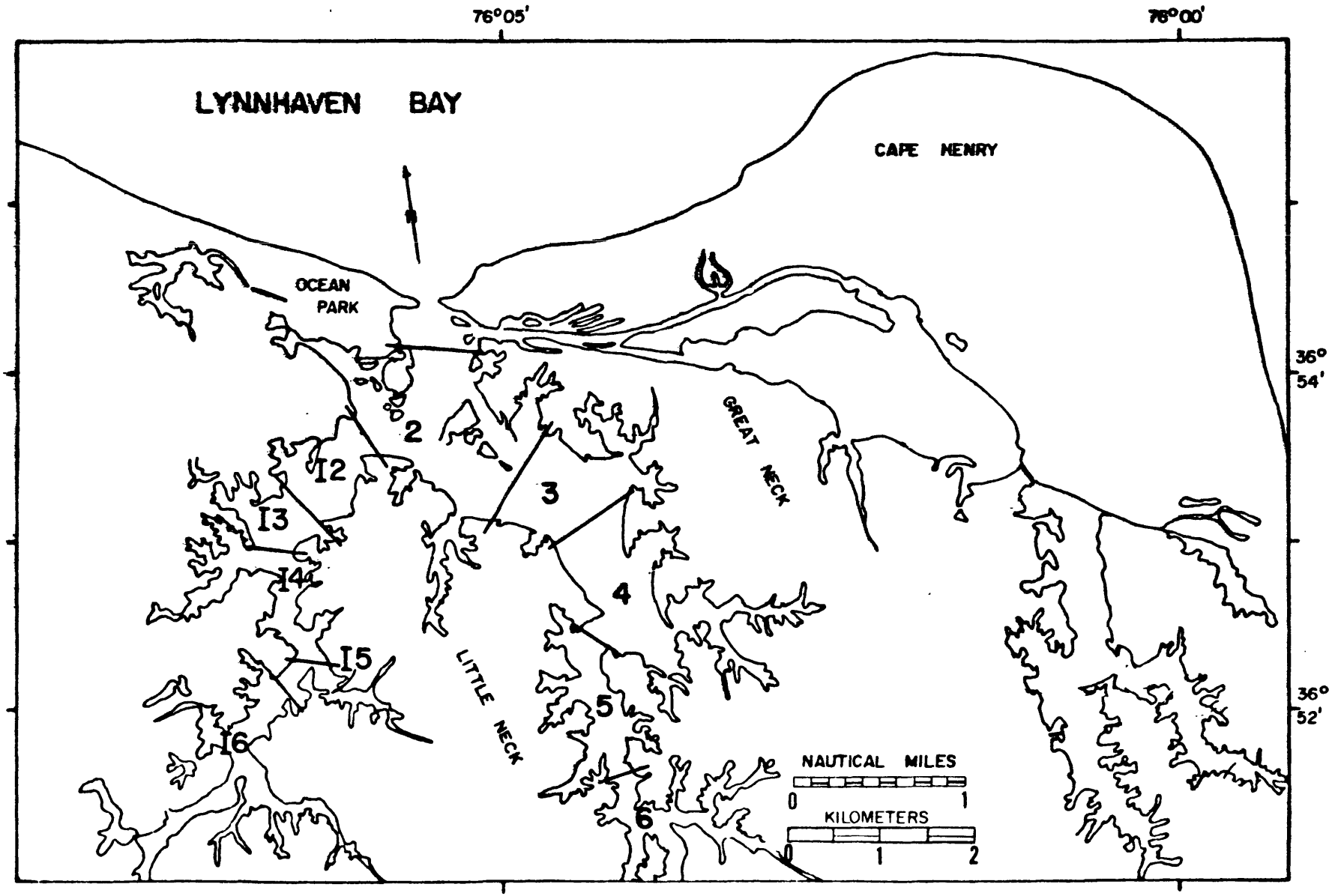

Figure B -1. The Lynnhaven Bay showing model segments.

KEY TO THE DRAWINGS

● o Field observed.

Model predicted.

●——— E. Branch of Lynnhaven Bay.

o- - - - W. Branch of Lynnhaven Bay.

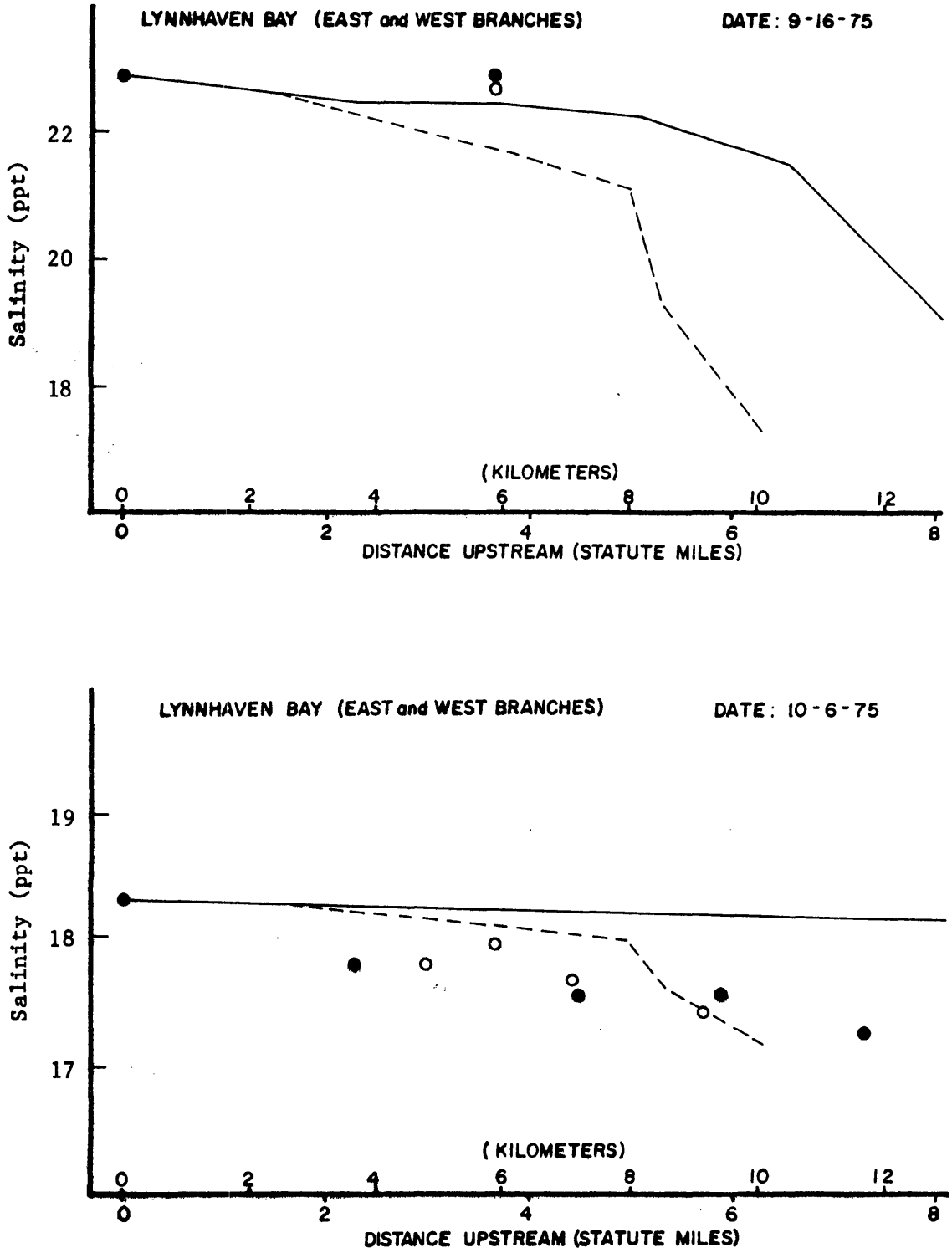

Figure B-2. Longitudinal profiles of salinity.

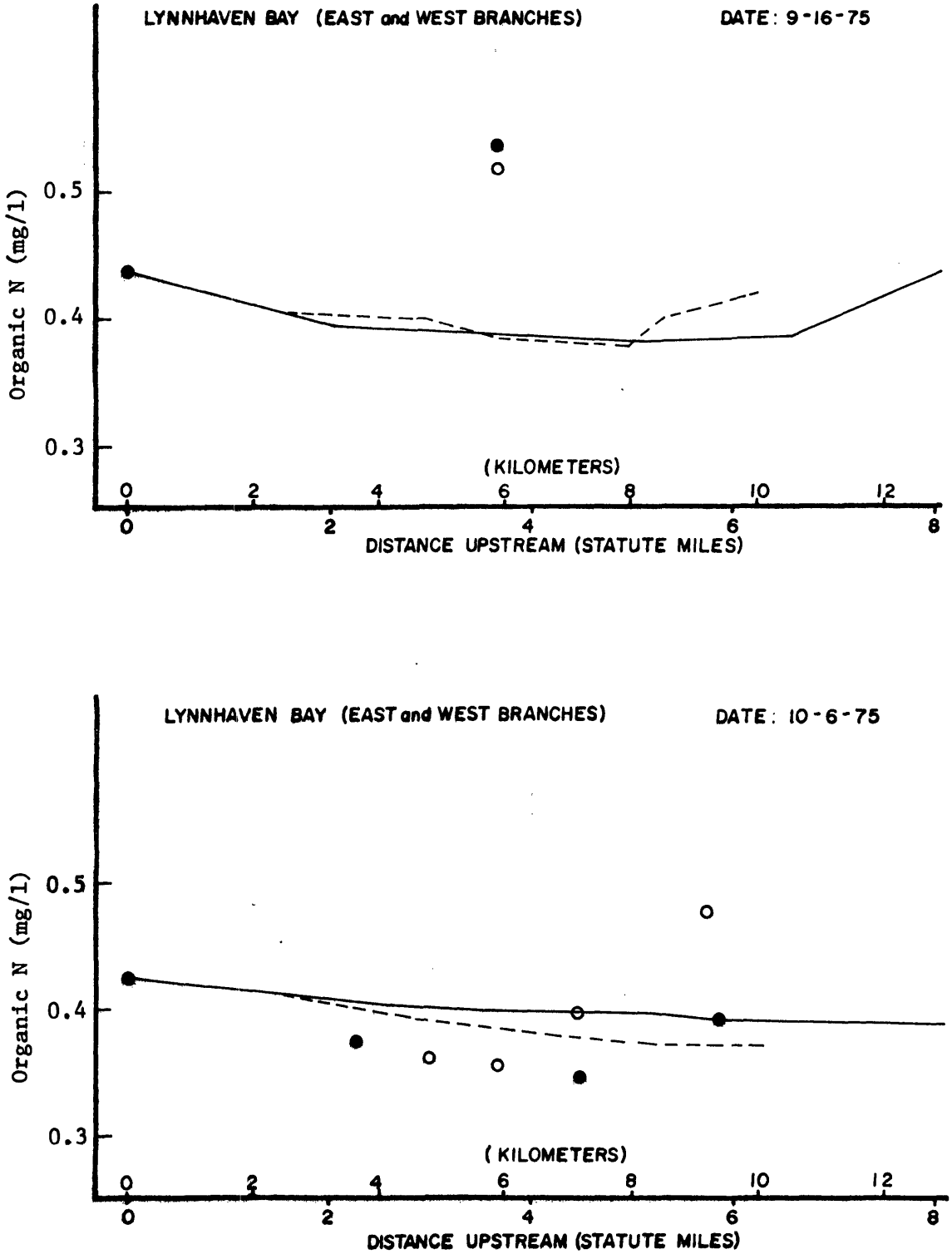

Figure B-3. Longitudinal profiles of organic nitrogen.

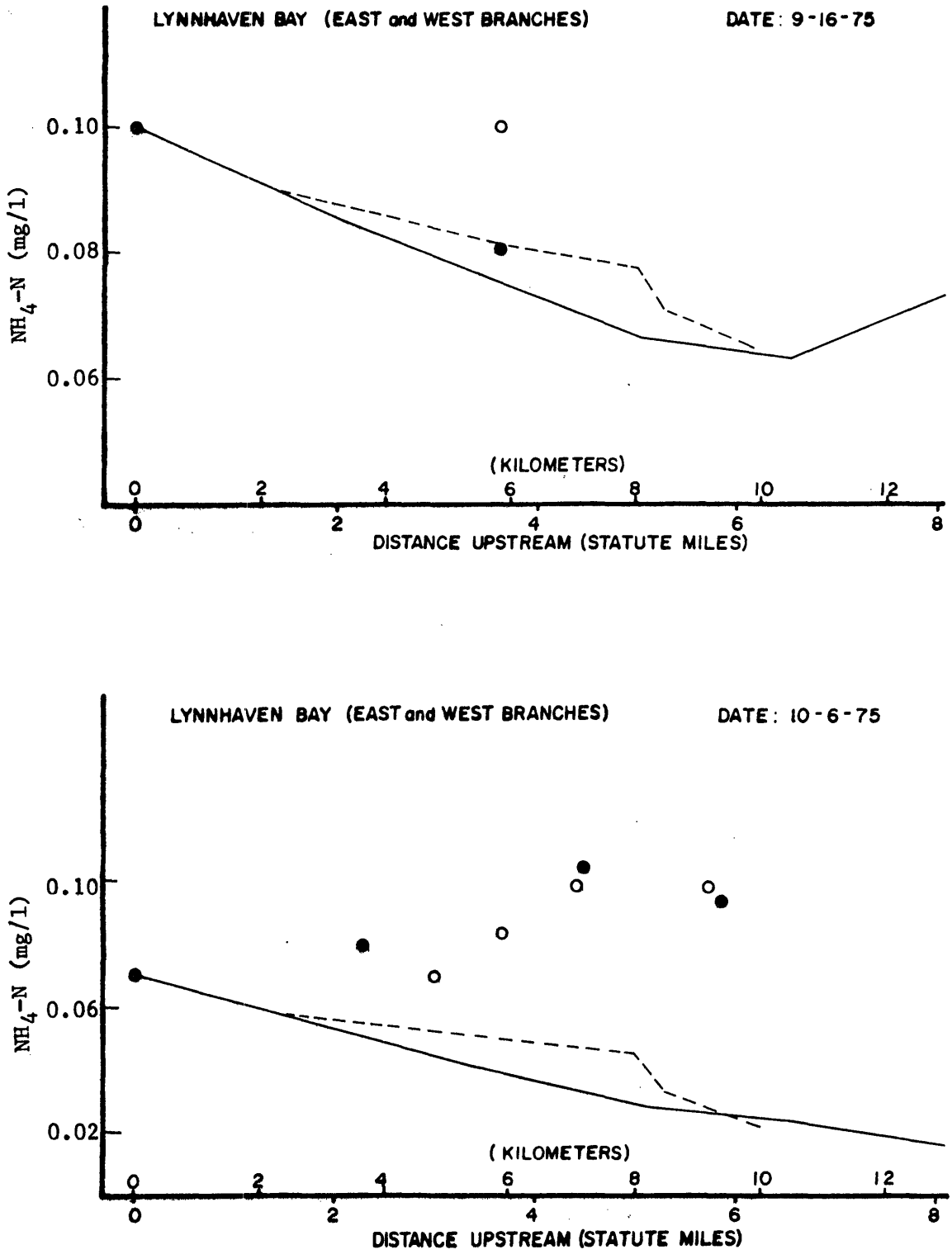

Figure B-4. Longitudinal profiles of ammonium nitrogen.

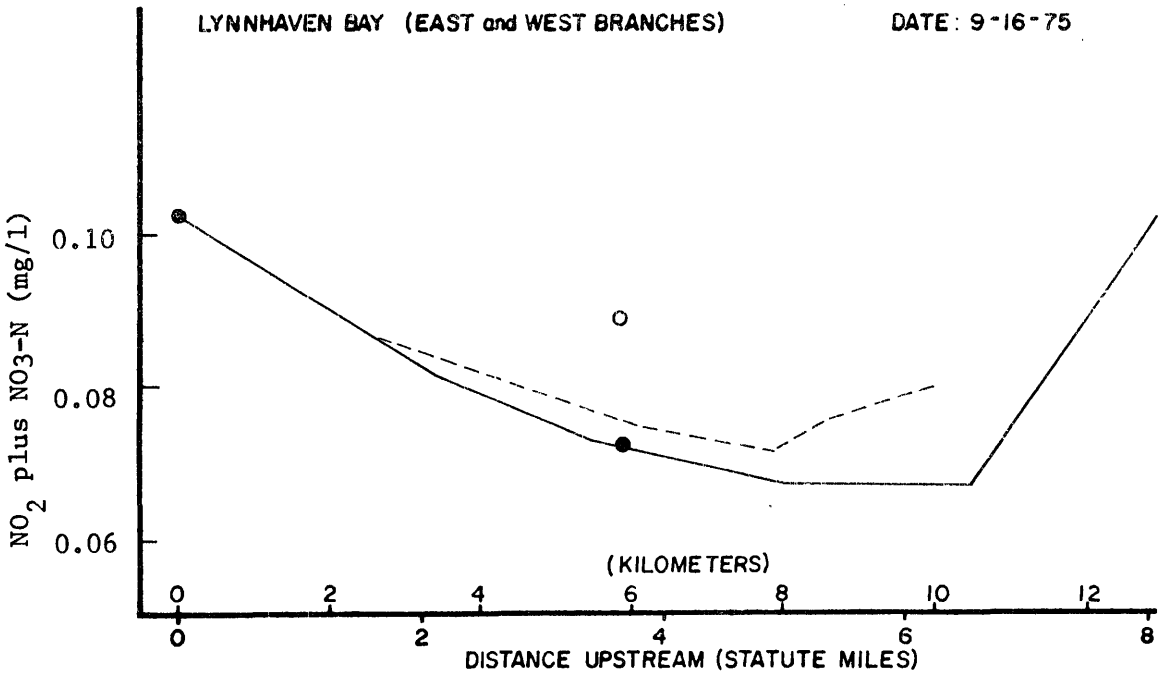

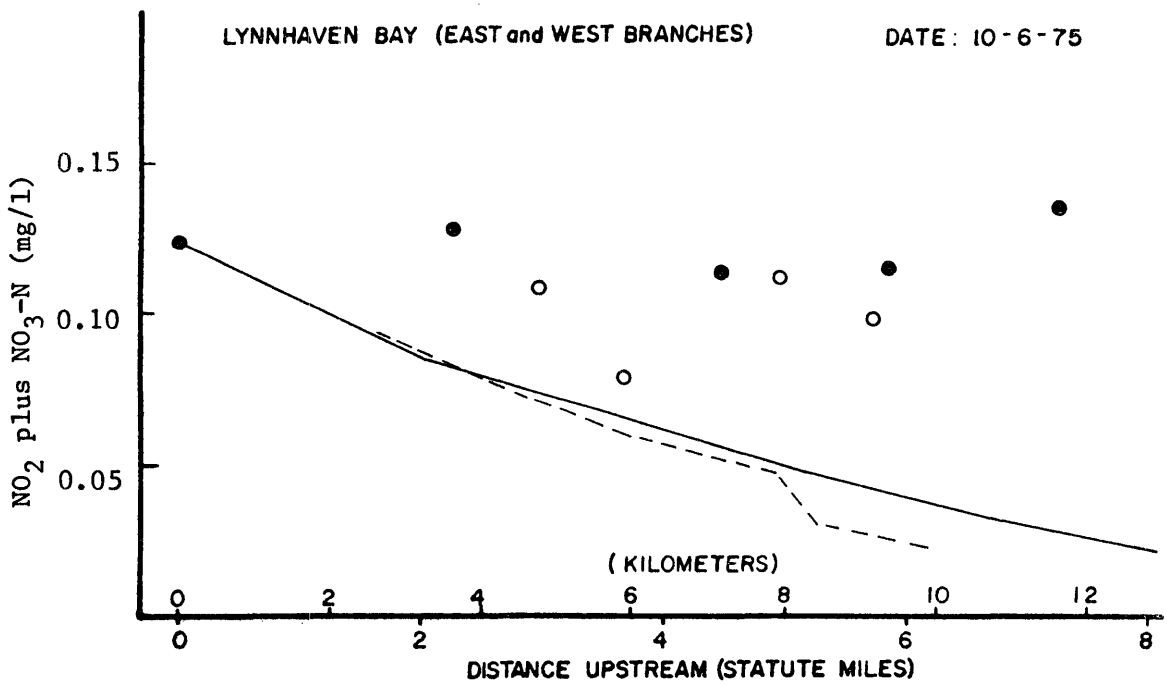

Figure B-5. Longitudinal profiles of nitrite plus nitrate nitrogen.

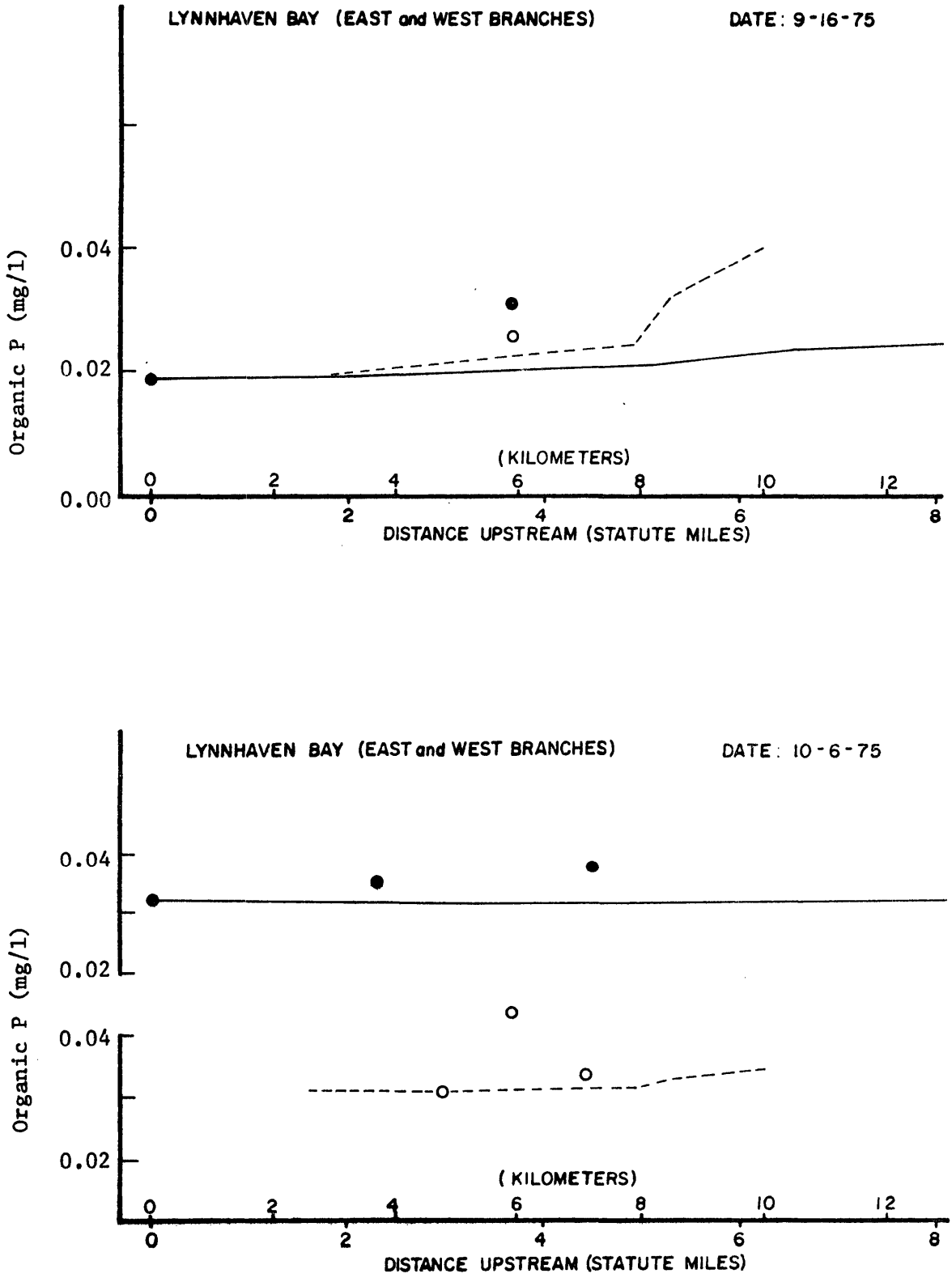

Figure B-6. Longitudinal profiles of organic phosphorus.

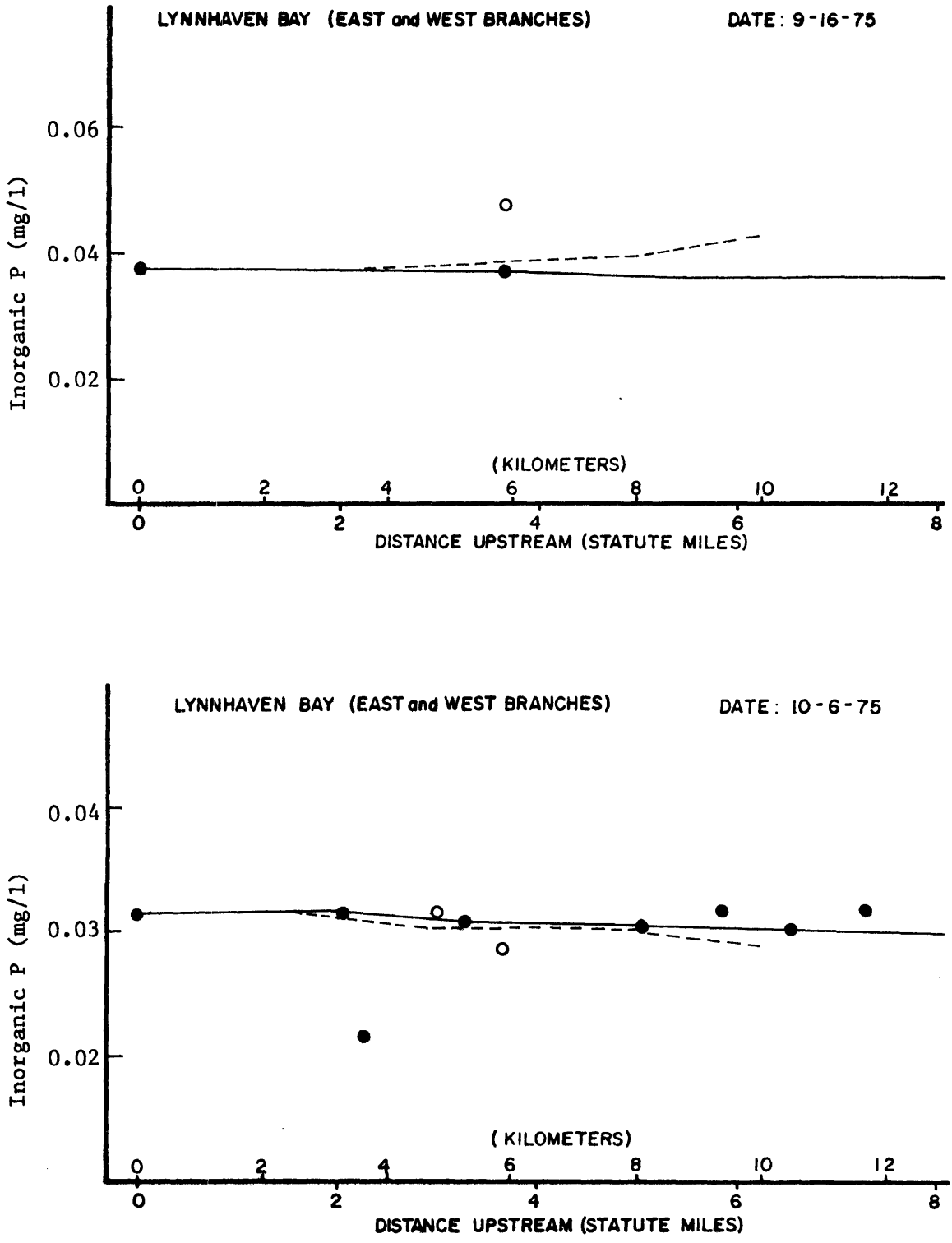

Figure B-7. Longitudinal profiles of inorganic phosphorus.

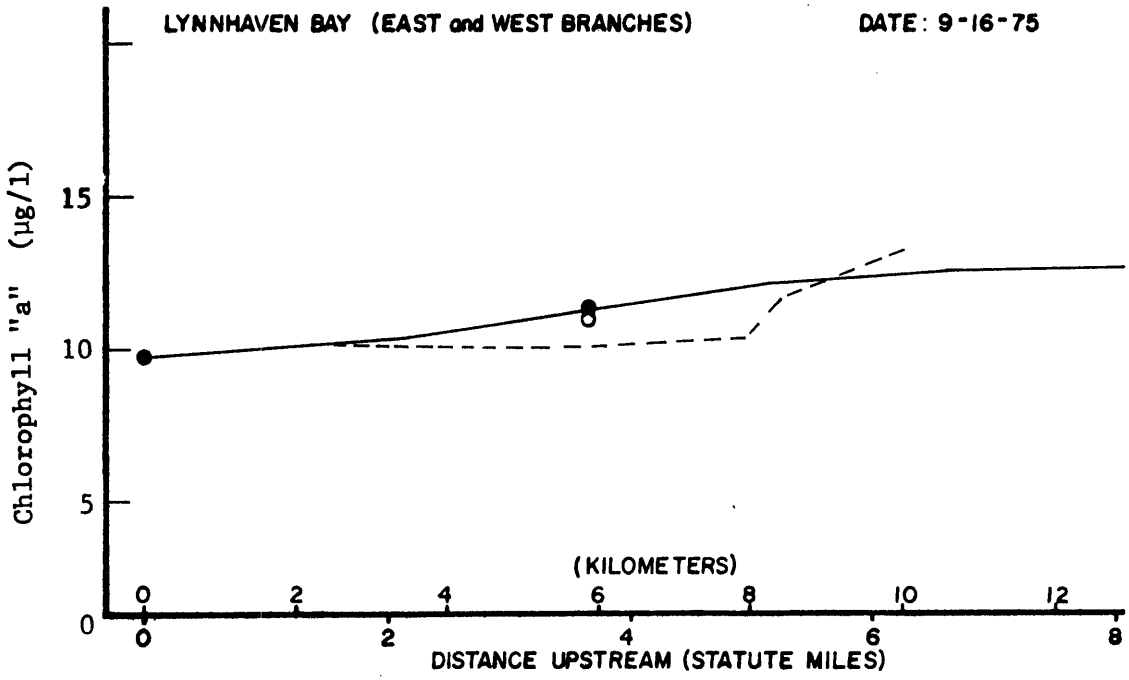

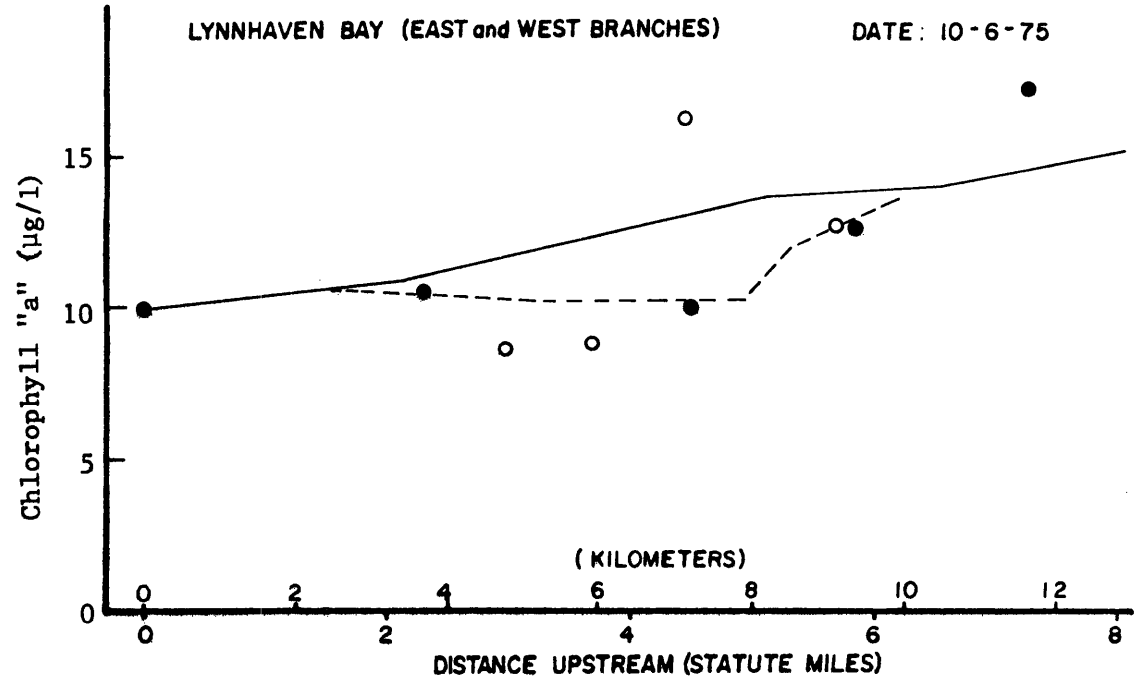

Figure B-8. Longitudinal profiles of chlorophyll "a".

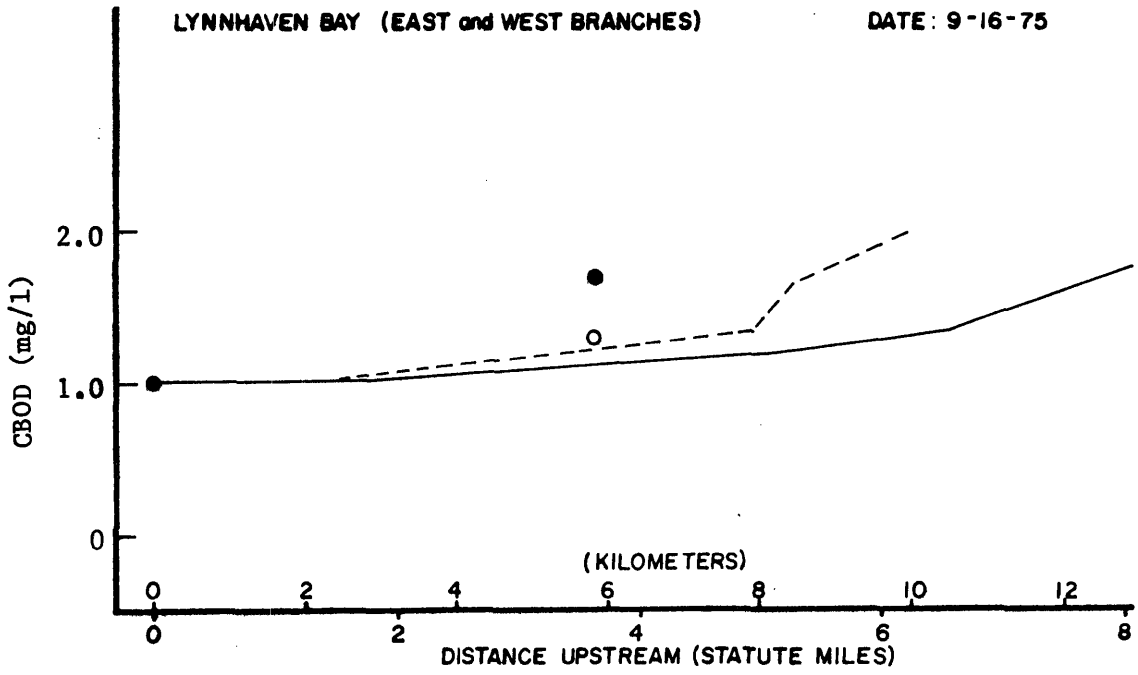

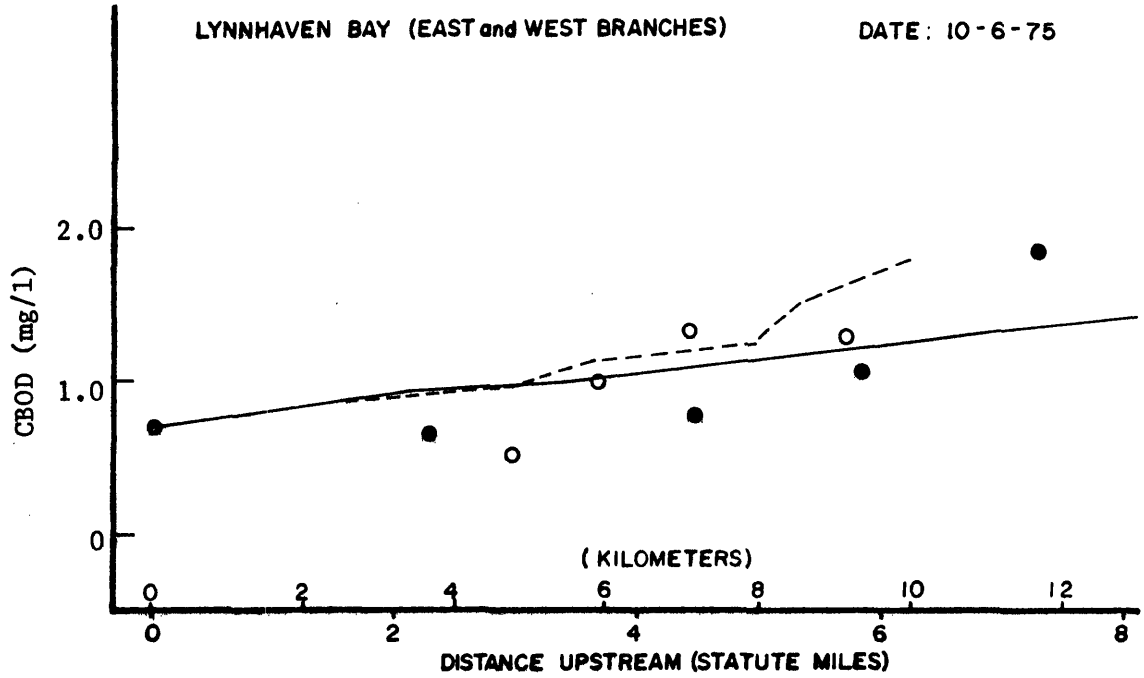

Figure B-9. Longitudinal profiles of CBOD.

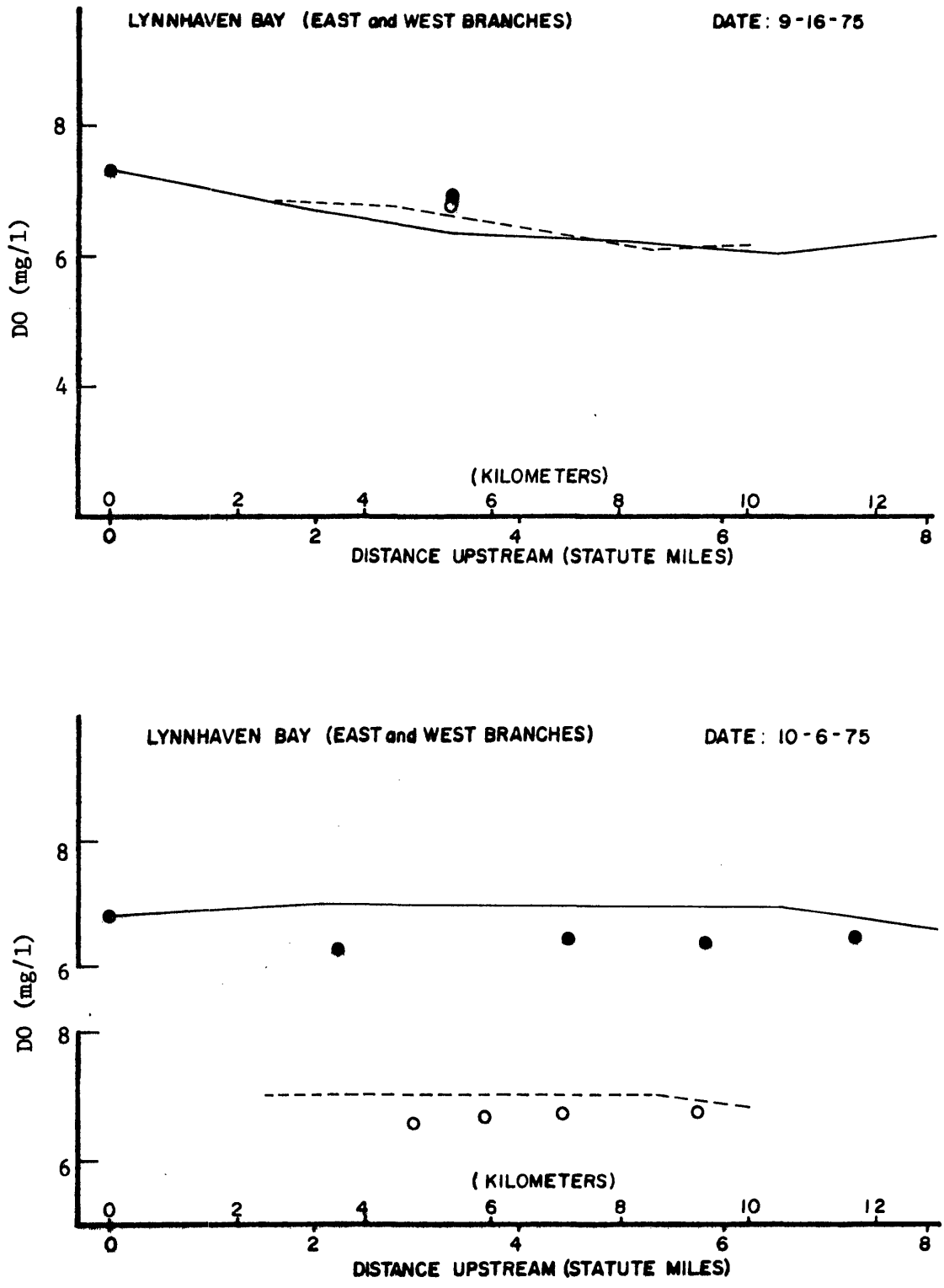

Figure B-10. Longitudinal profiles of dissolved oxygen.

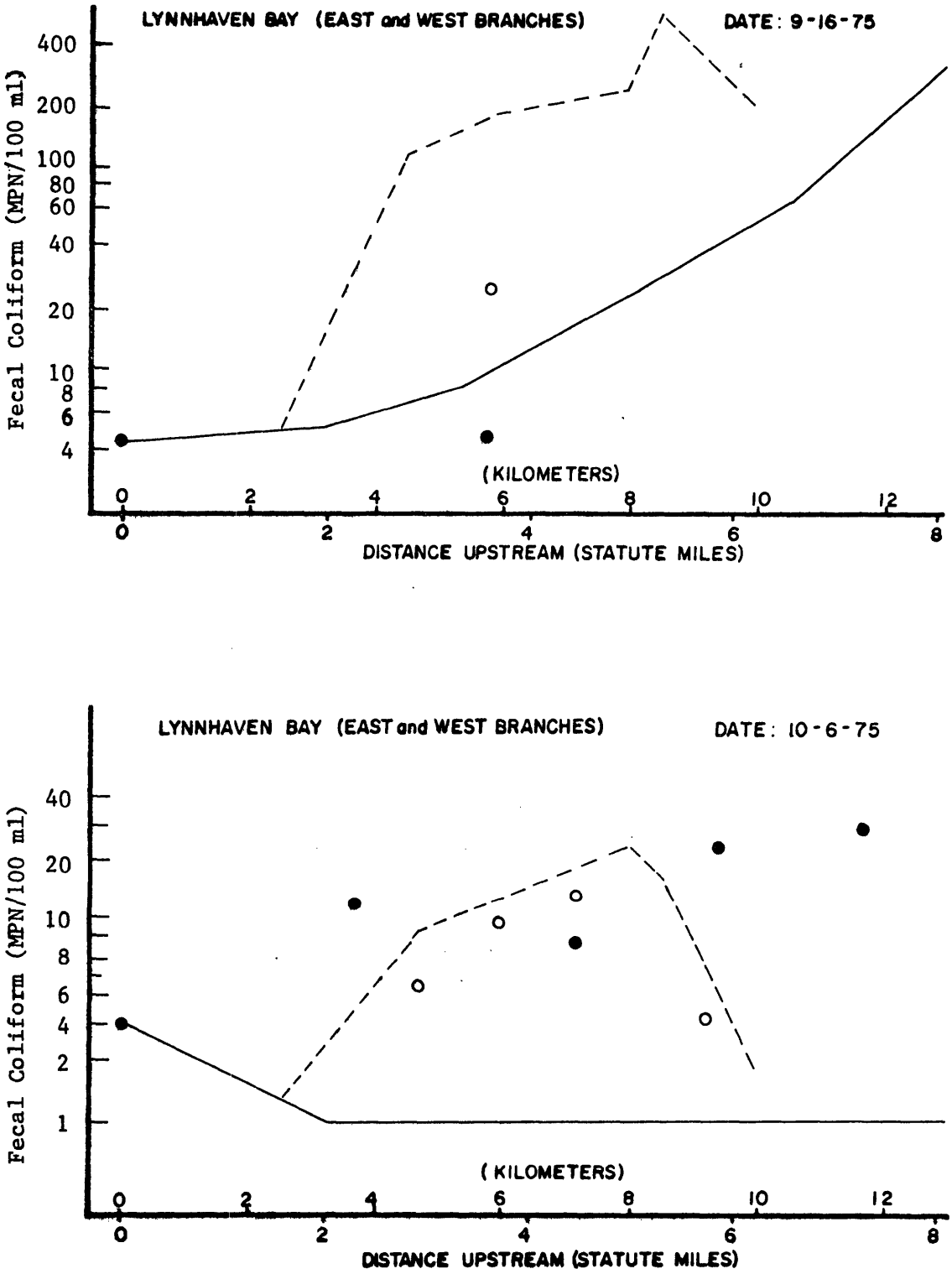

Figure B-11. Longitudinal profiles of fecal coliform concentrations.

APPENDIX C

Observed and Predicted Values of Model Components at High Water Slack for the Little Creek Subsystem

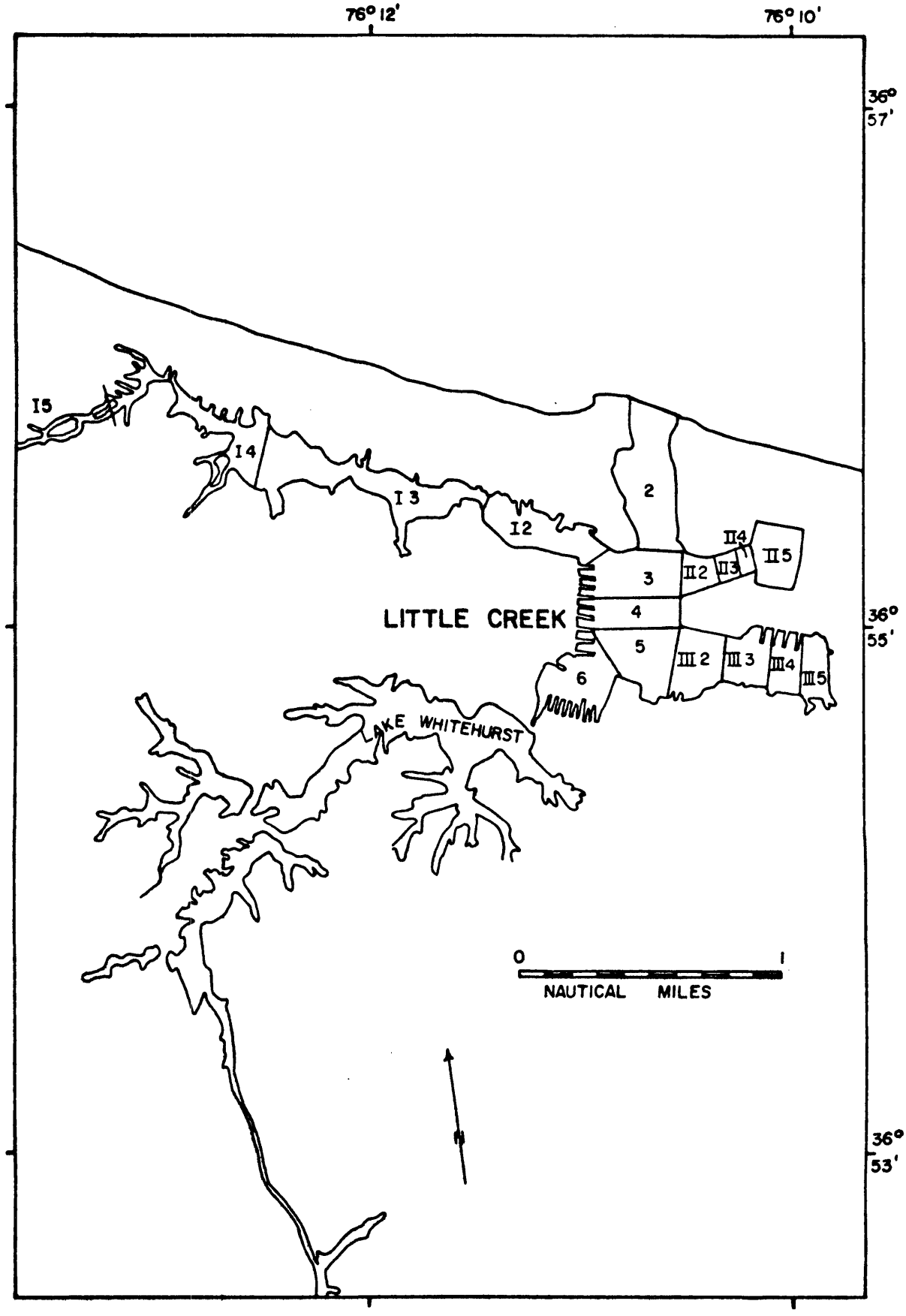

Figure C-1. Little Creek showing model segments.

KEY TO THE DRAWINGS

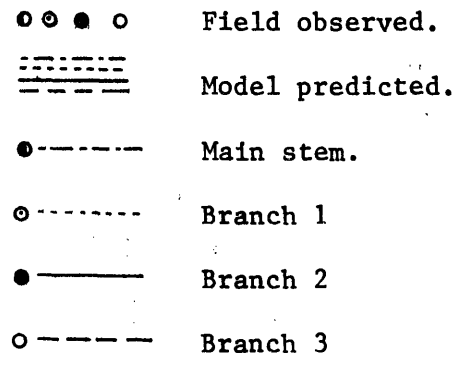

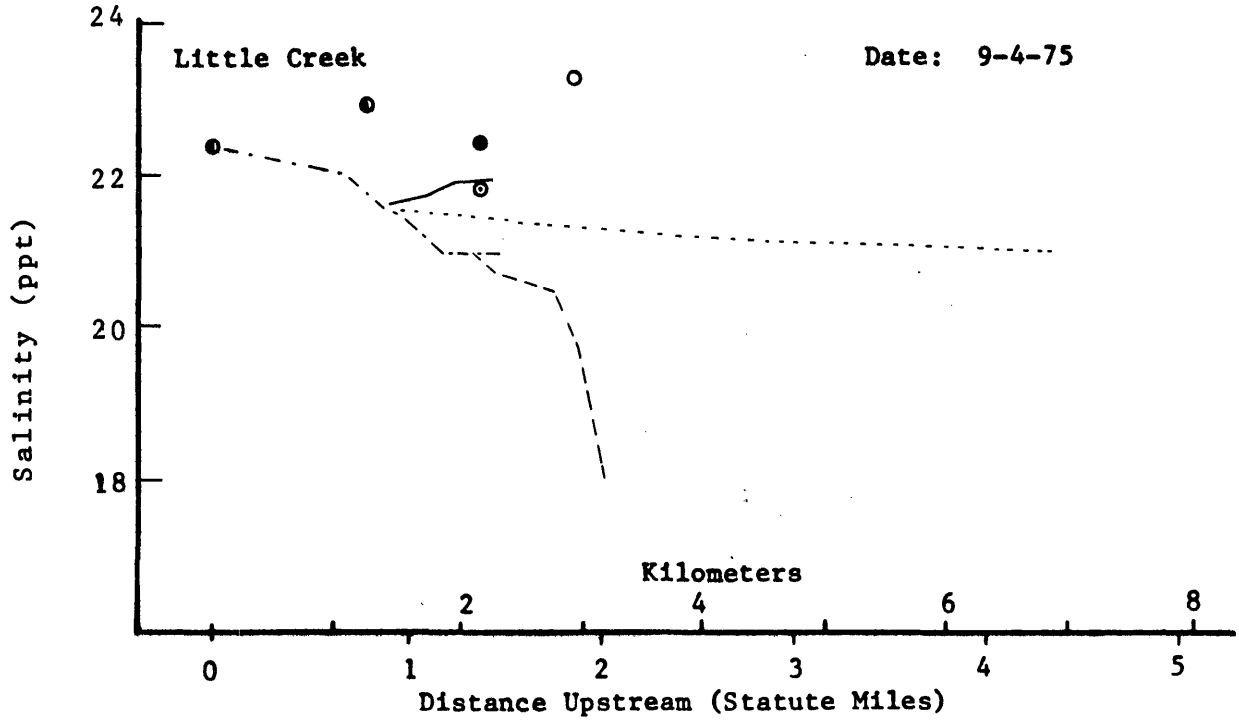

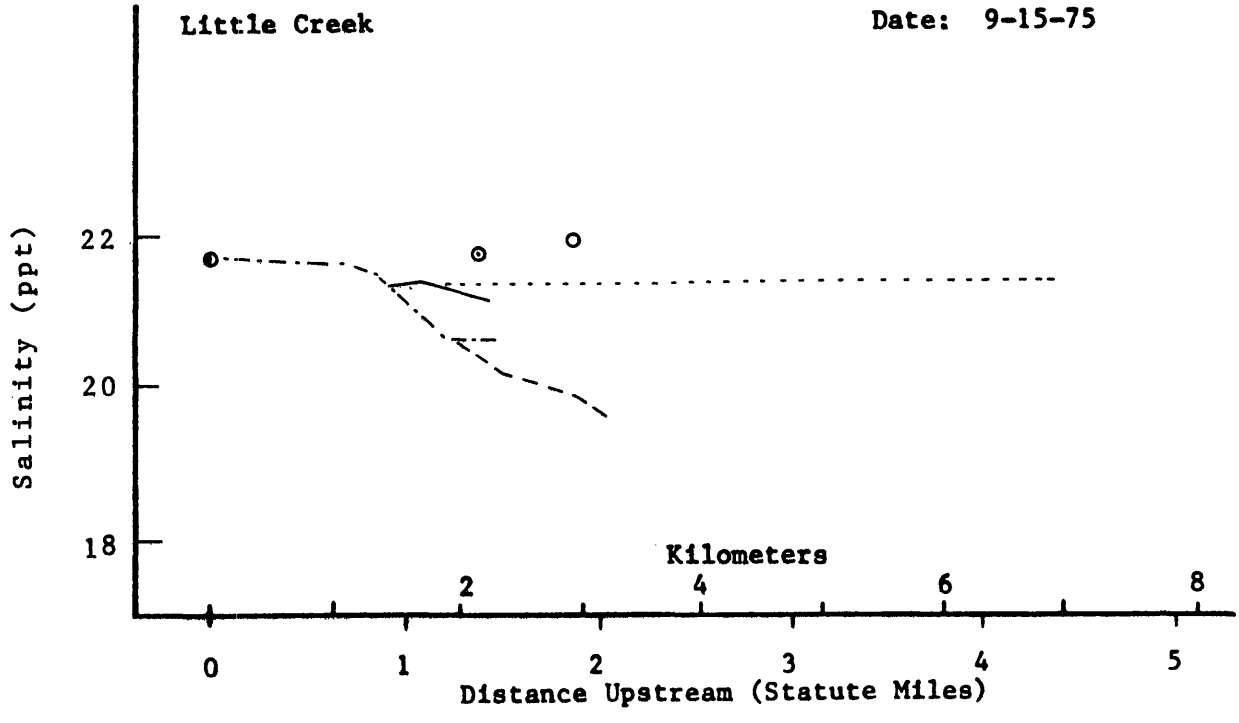

Figure C-2. Longitudinal profiles of salinity.

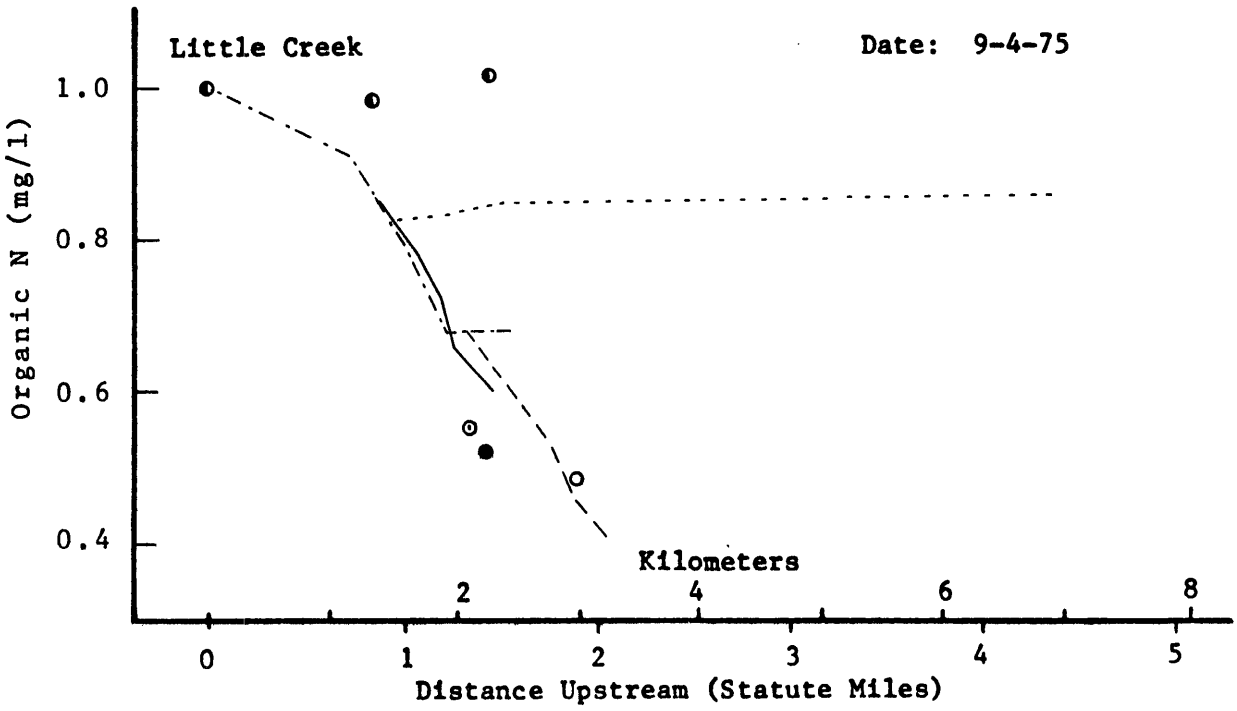

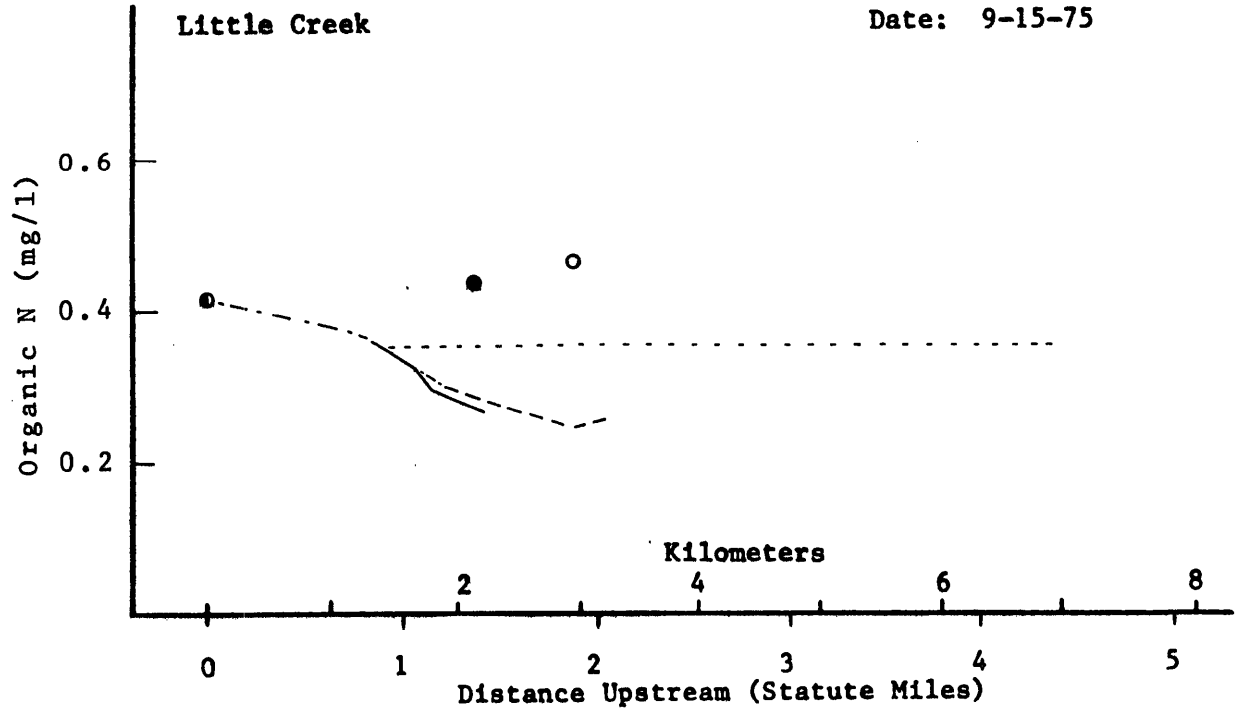

Figure C-3. Longitudinal profiles of organic nitrogen.

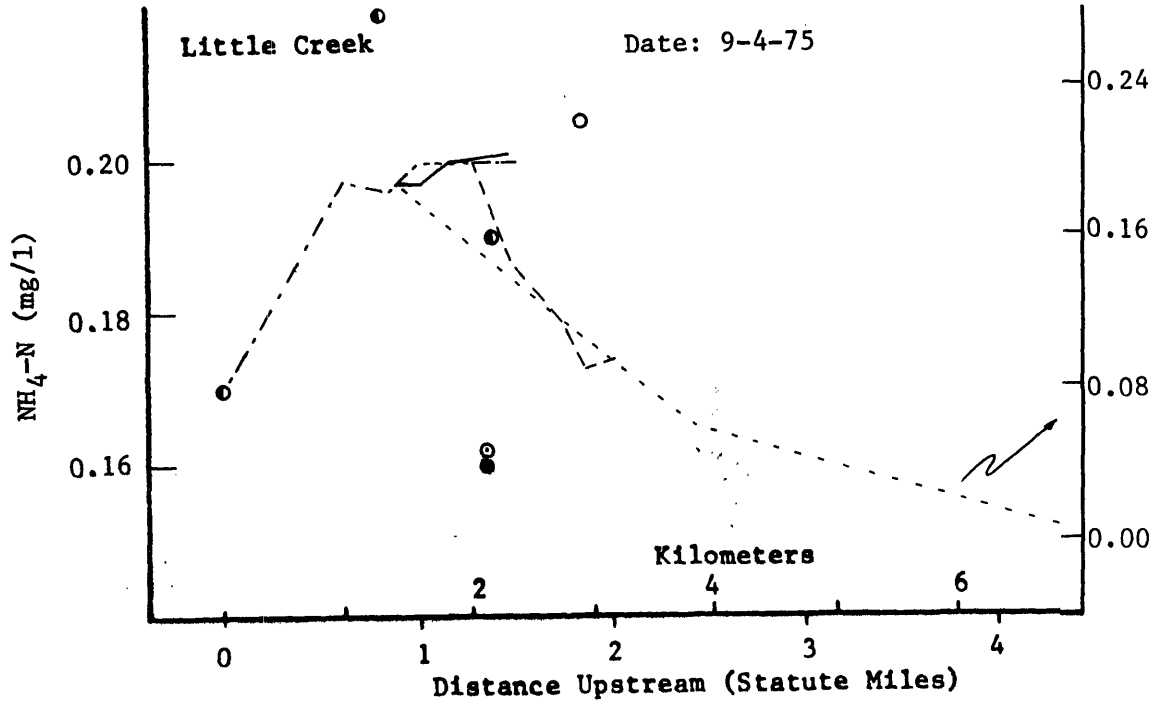

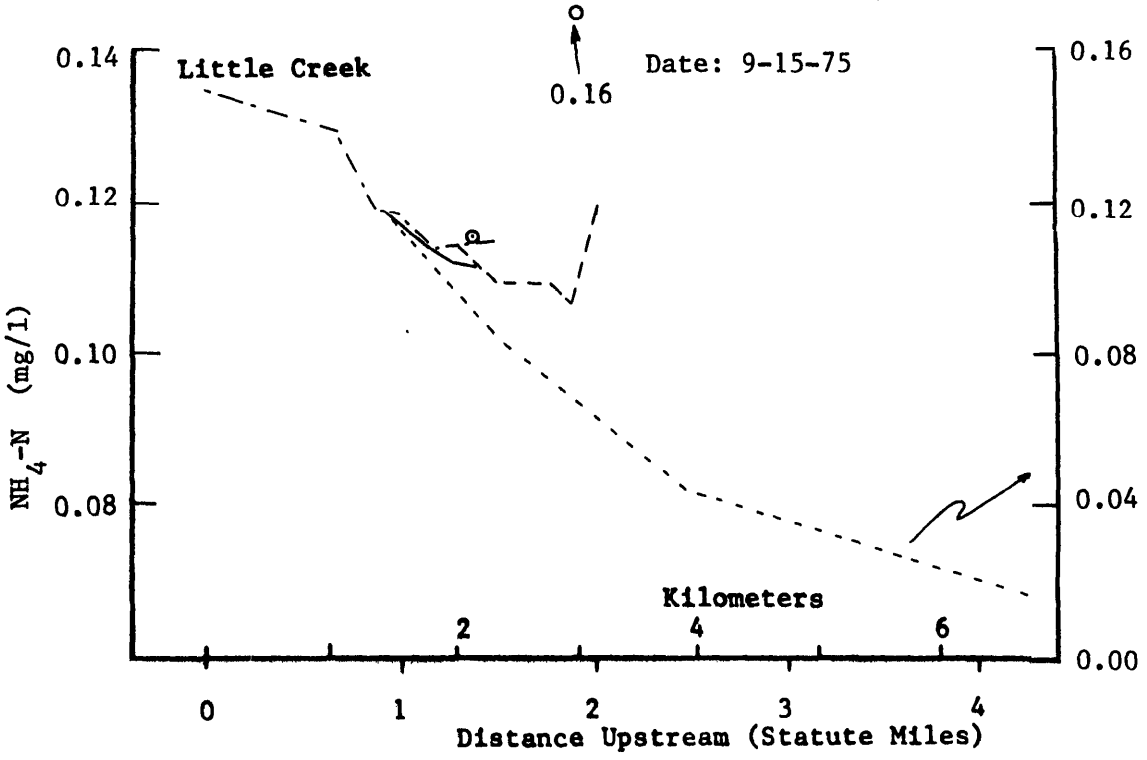

Figure C-4. Longitudinal profiles of ammonium nitrogen.

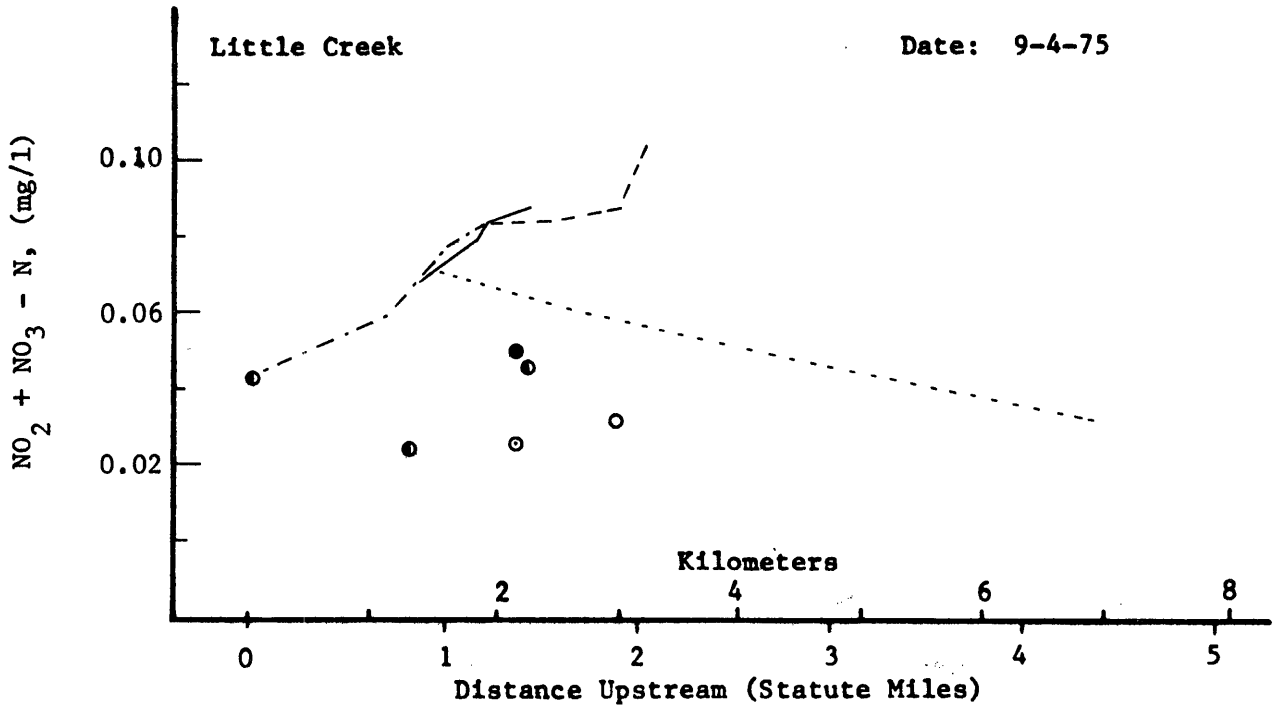

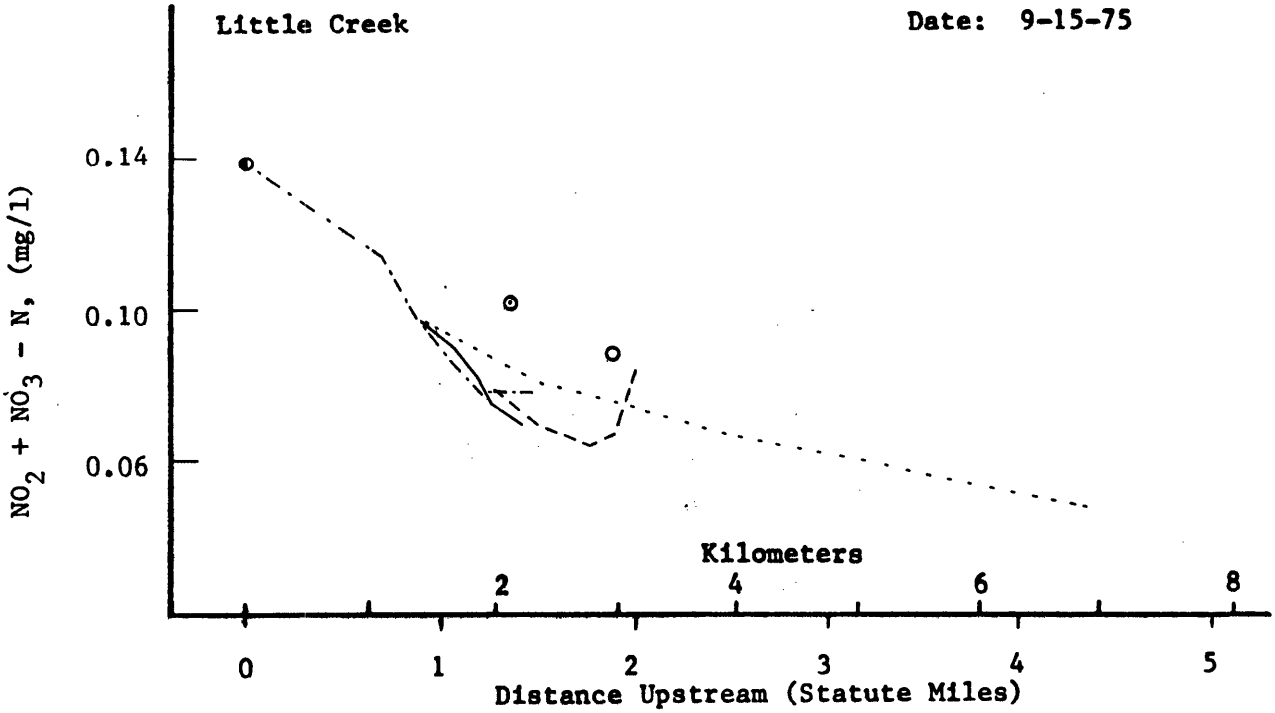

Figure C-5. Longitudinal profiles of nitrite and nitrate nitrogen.

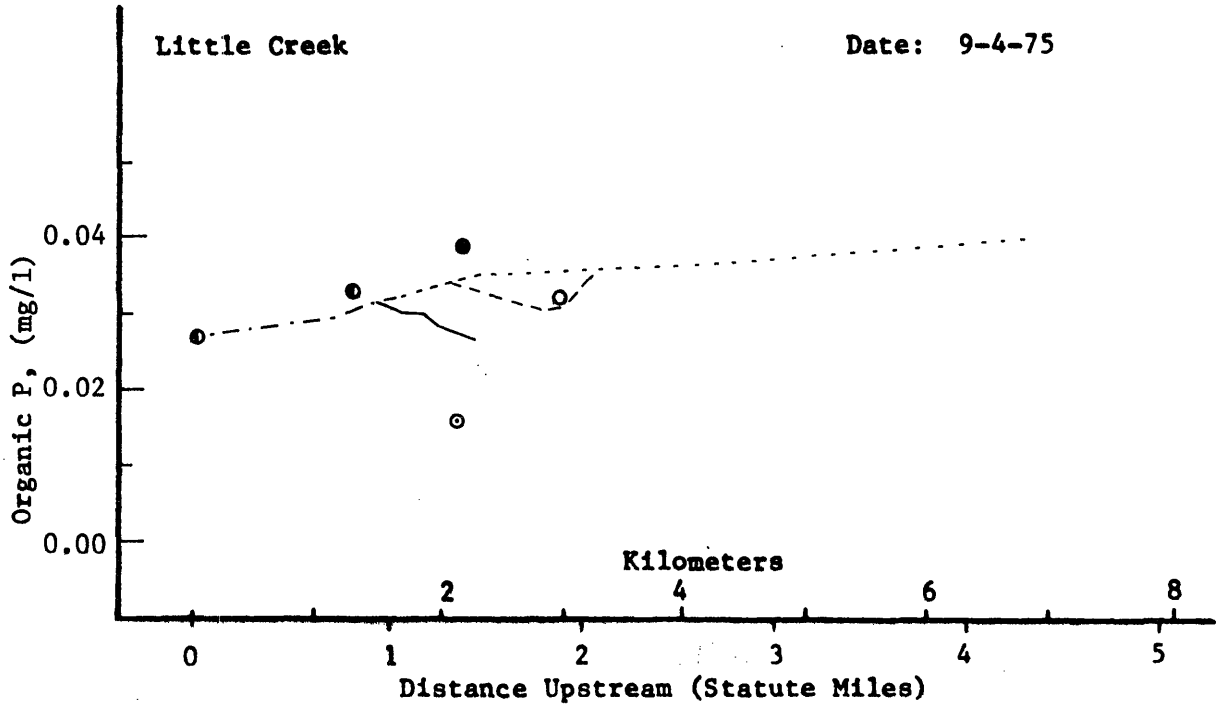

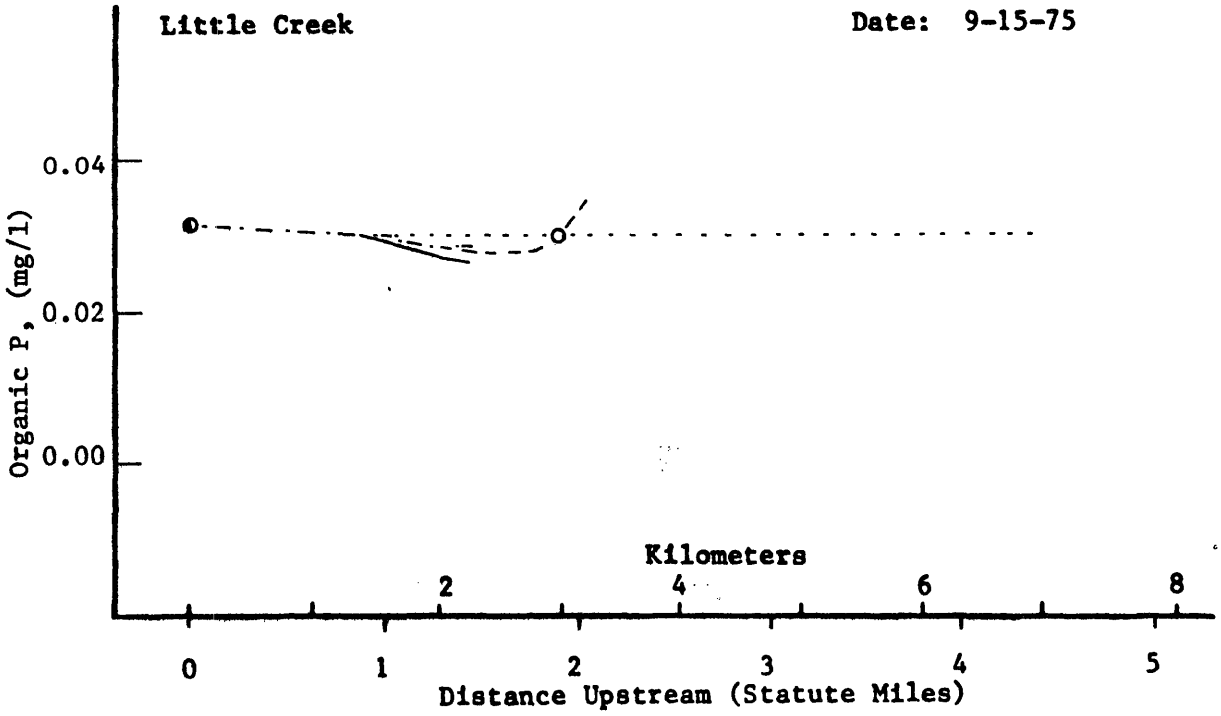

Figure C-6. Longitudinal profiles of organic phosphorus.

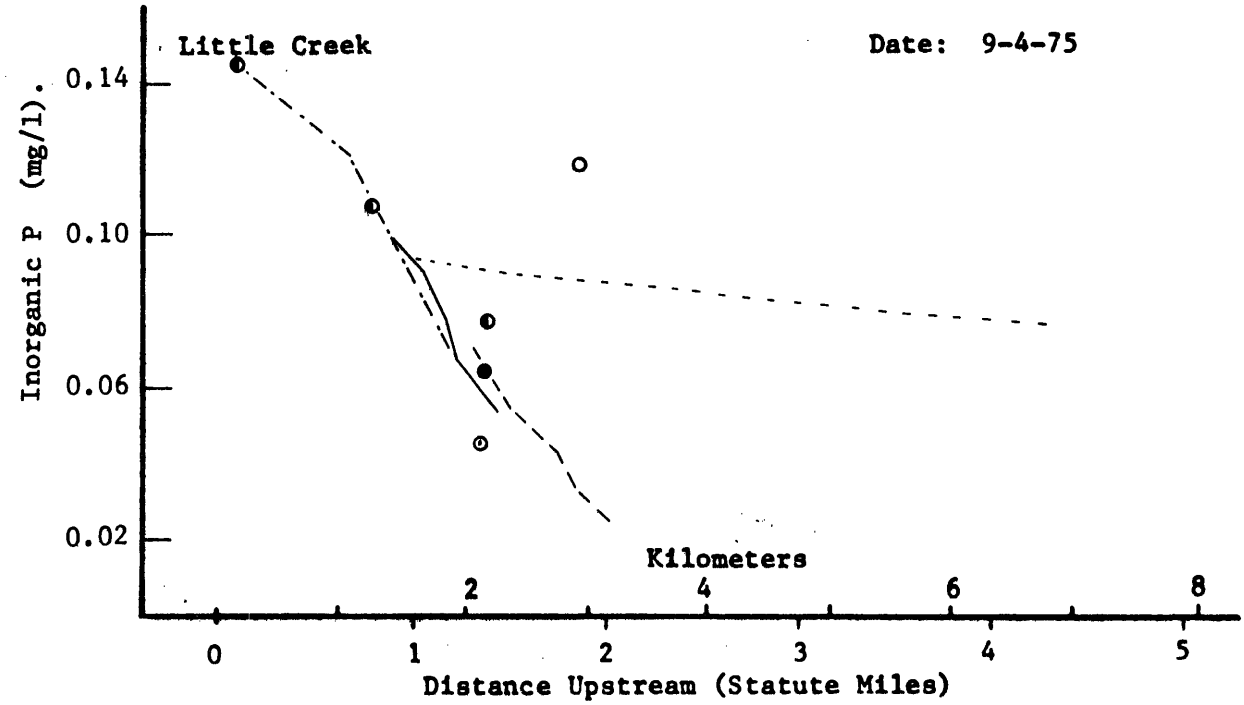

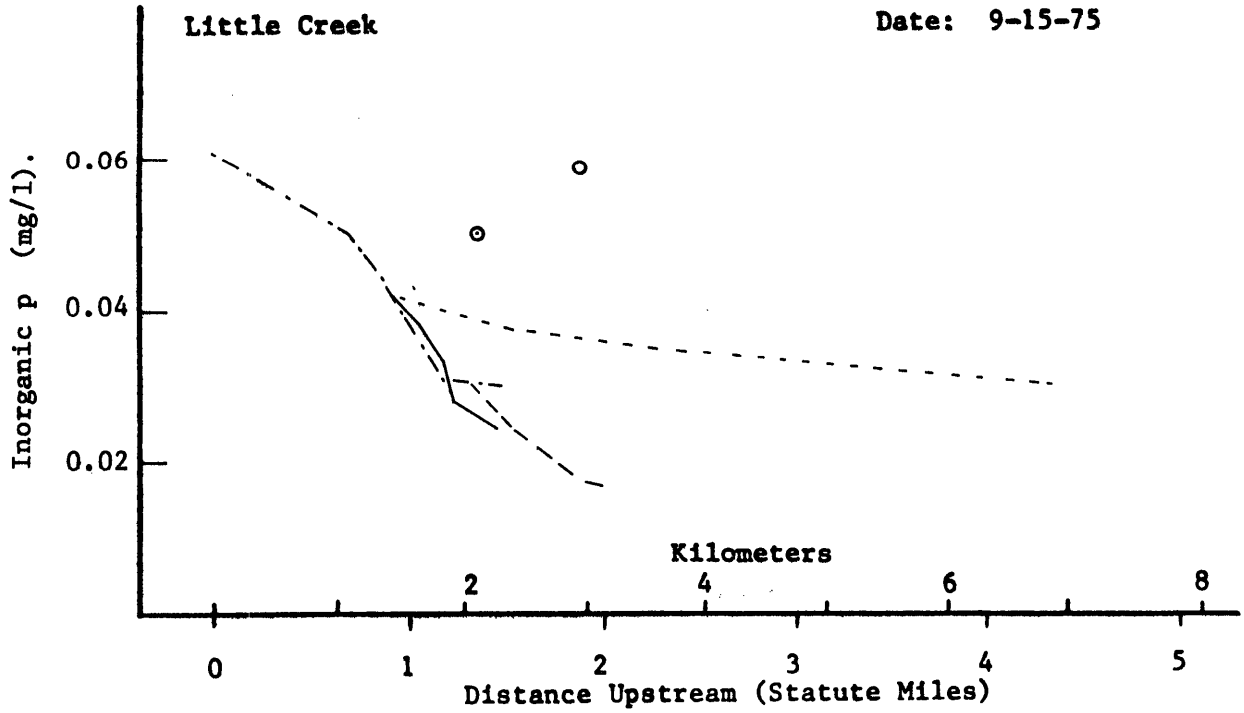

Figure C-7. Longitudinal profiles of inorganic phosphorus.

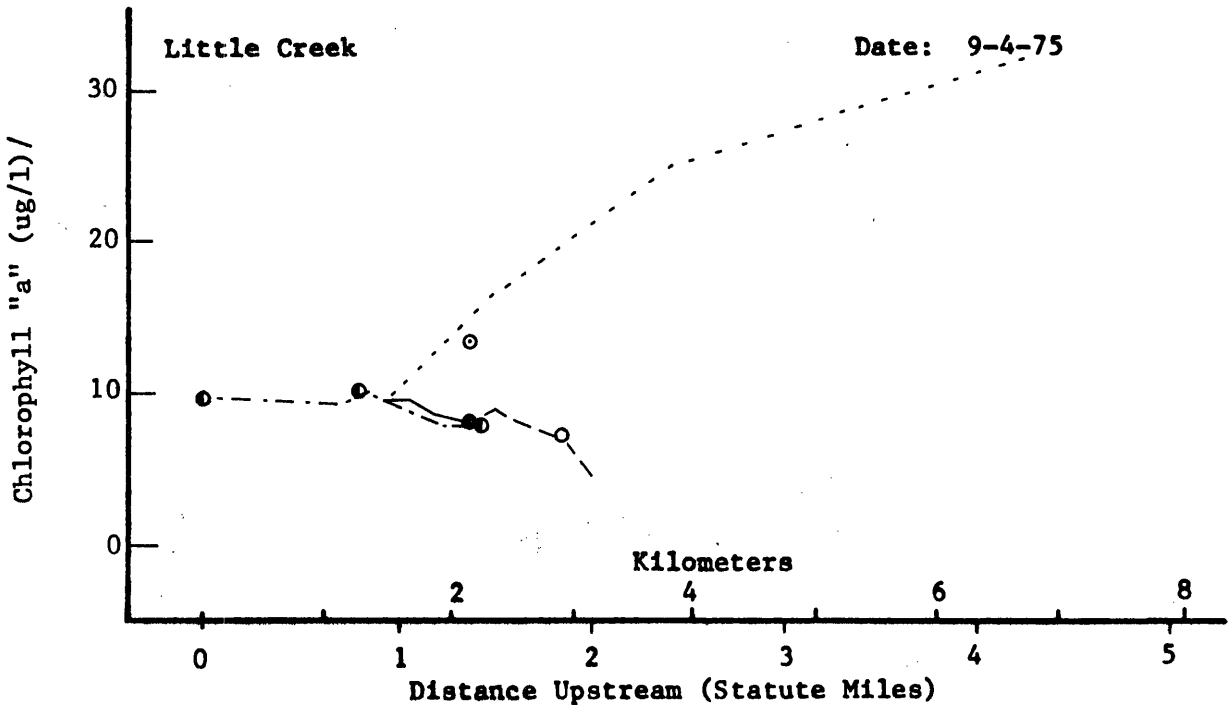

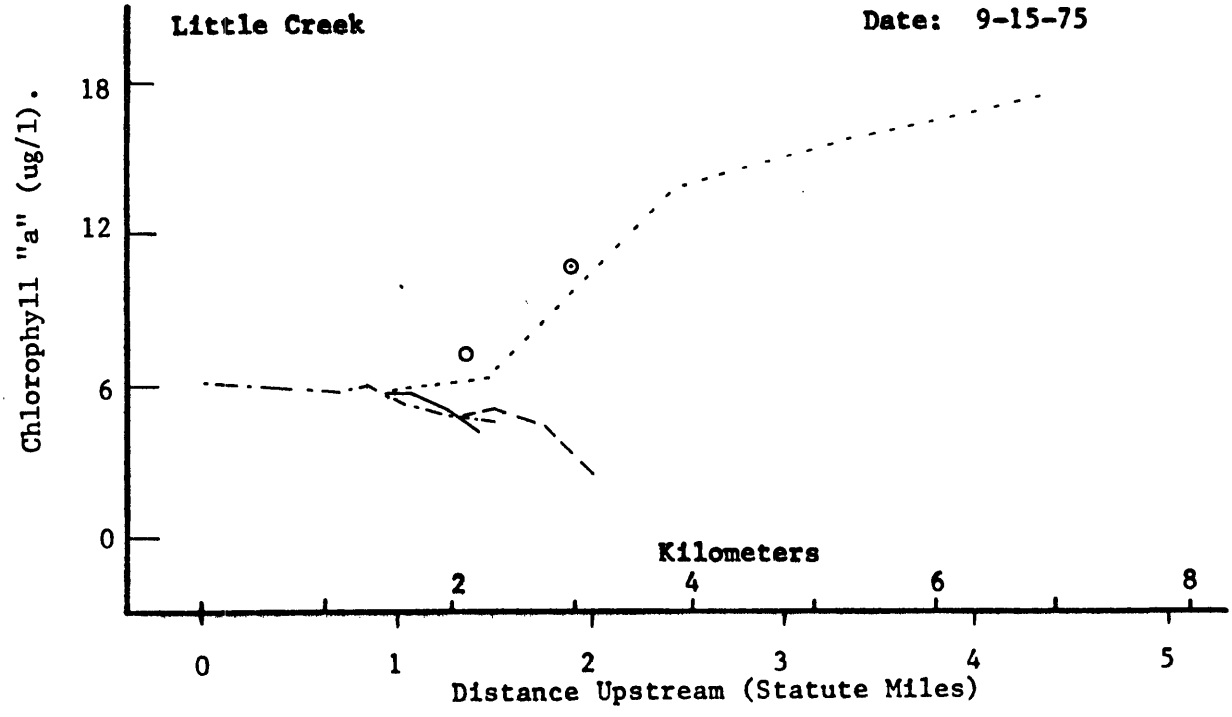

Figure C-8. Longitudinal profiles of chlorophyll "a".

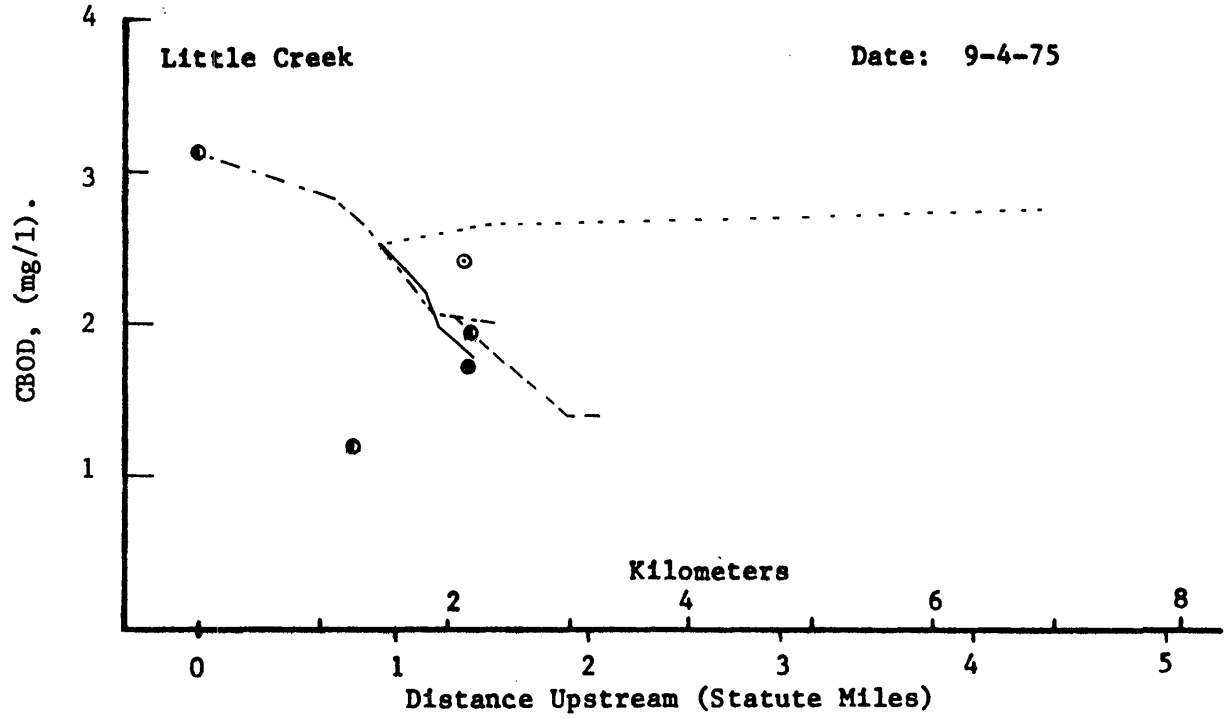

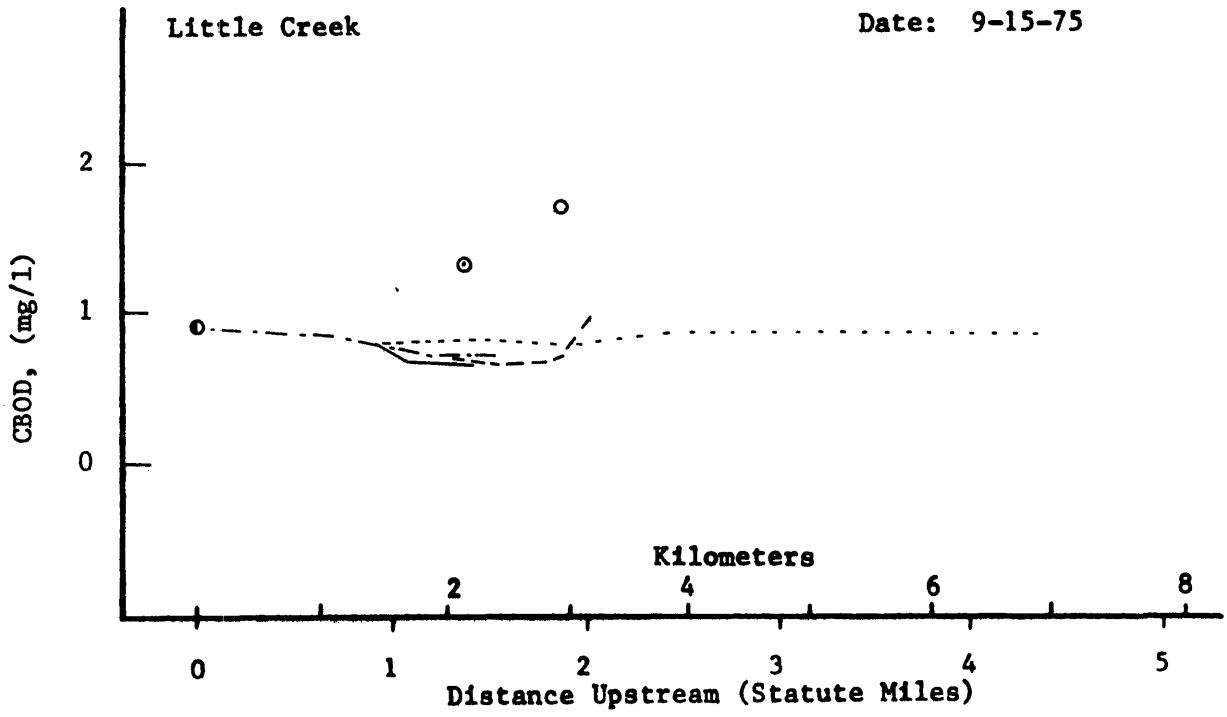

Figure C-9. Longitudinal profiles of CBOD.

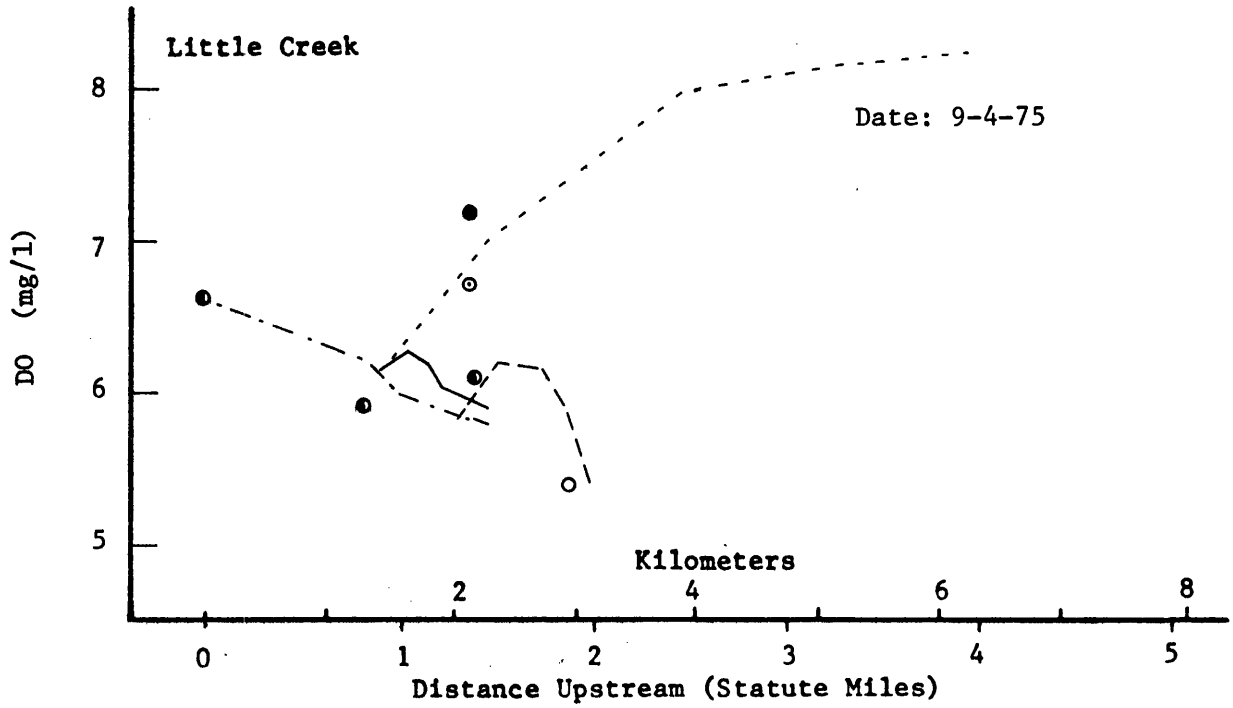

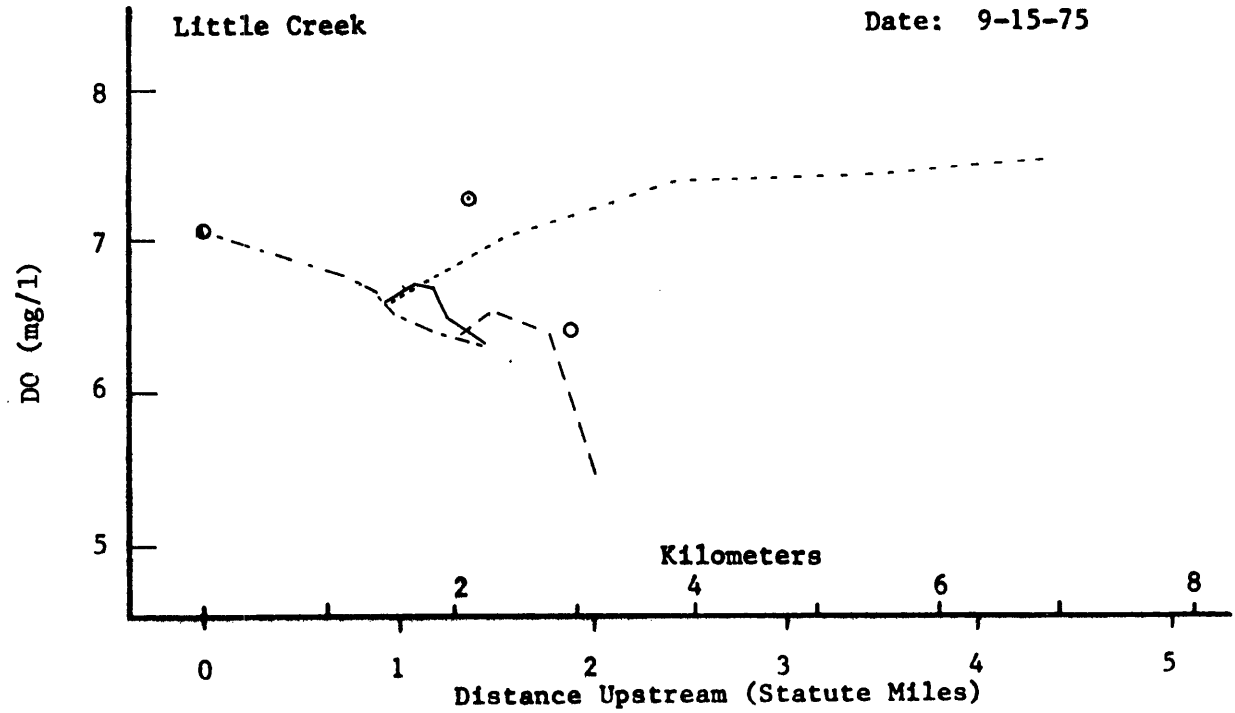

Figure C-10. Longitudinal profiles of dissolved oxygen.

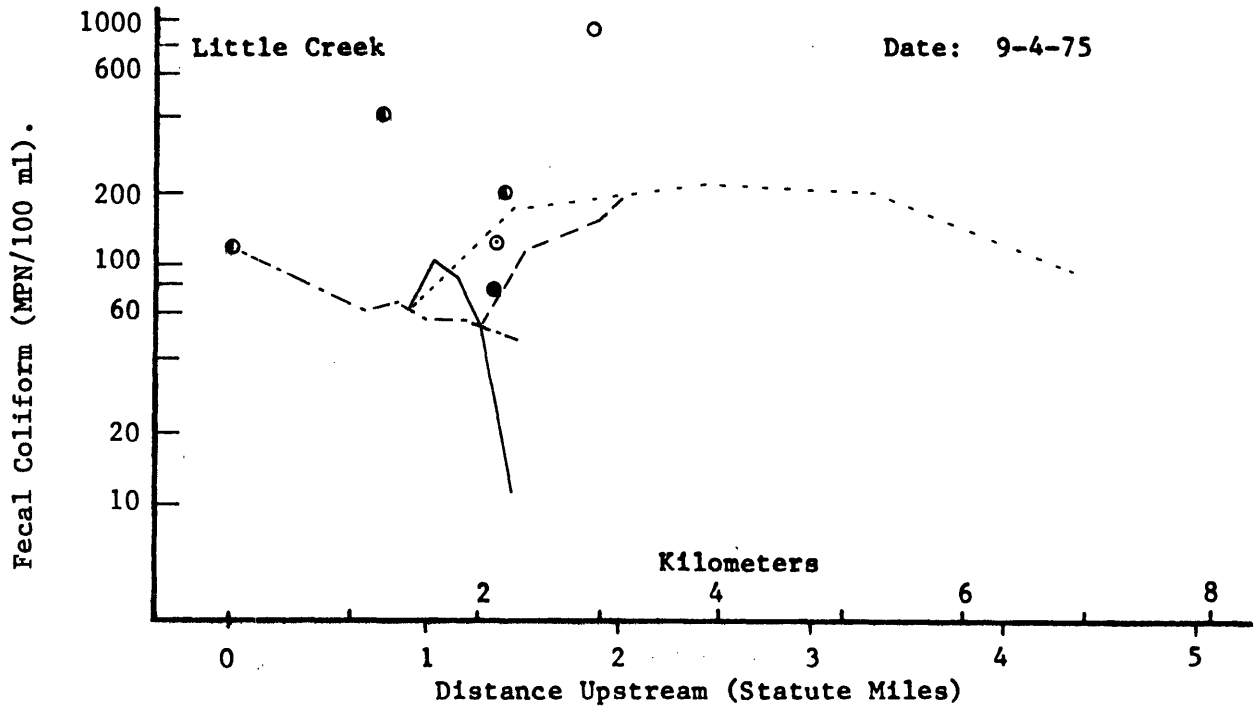

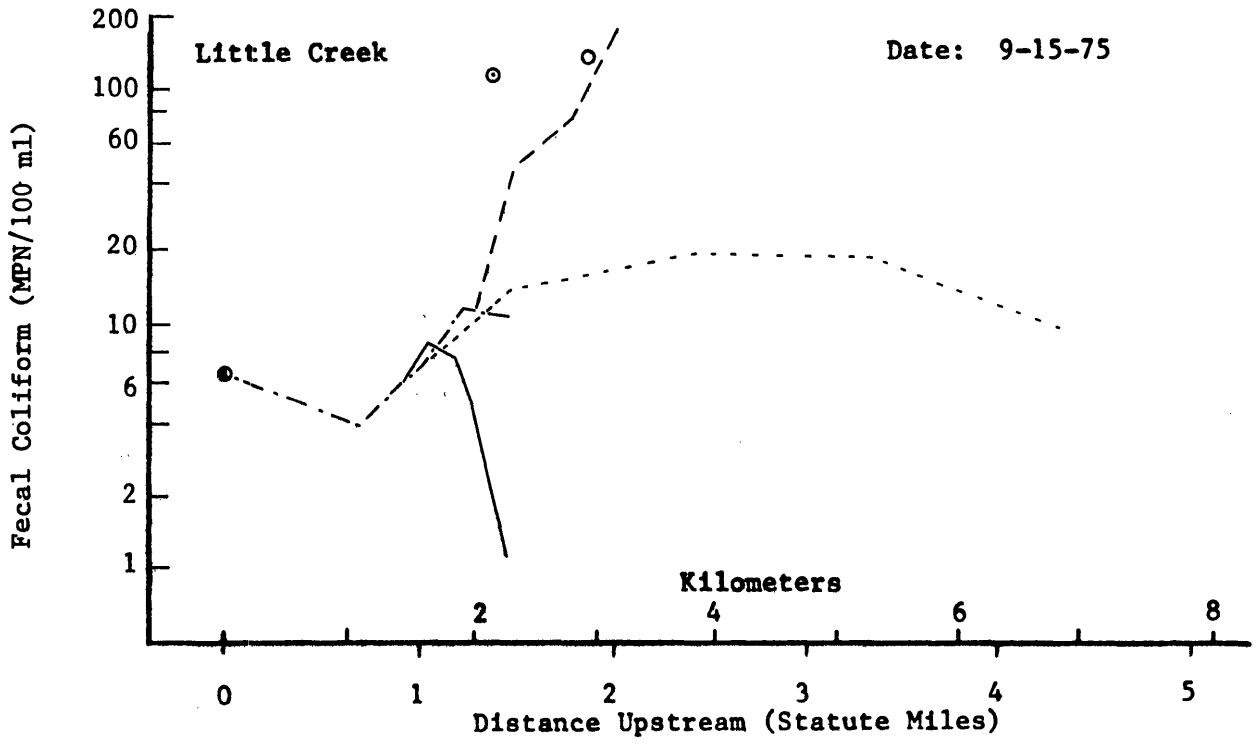

Figure C-11. Longitudinal profiles of fecal coliform concentration.